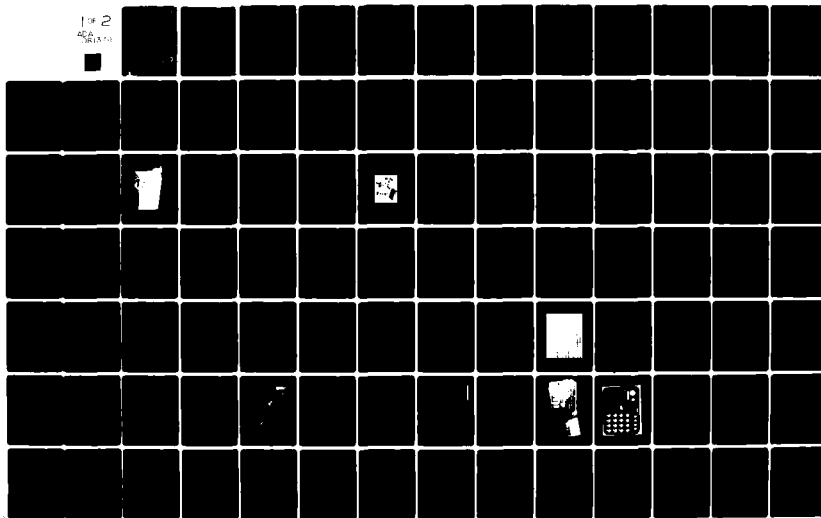PANAMETRICS INC WALTHAM MASS   F/6 22/2
DESIGN OF INSTRUMENTATION SUITABLE FOR THE INVESTIGATION OF CHA--ETC(U)
OCT 79   P R MOREL, F A HANSER, B SELLERS   F19628-74-C-0217
UNCLASSIFIED   AFGL-TR-79-0235   NL

REPORT DOCUMENTATION PAGE		READ INSTRUCTIONS BEFORE COMPLETING FORM
1. REPORT NUMBER AFGL-TR-79-0235	2. GOVT ACCESSION NO.	3. RECIPIENT'S CATALOG NUMBER
4. TITLE (and Subtitle) DESIGN OF INSTRUMENTATION SUITABLE FOR THE INVESTIGATION OF CHARGE BUILD-UP PHENOMENA AT SYNCHRONOUS ORBIT		5. TYPE OF REPORT & PERIOD COVERED Final, 9 Sept. 1974 to 30 Sept., 1979
		6. PERFORMING ORG. REPORT NUMBER
7. AUTHOR(s) Paul R. Morel, Frederick A. Hanser and Bach Sellers		8. CONTRACT OR GRANT NUMBER(s) F19628-74-C-0217
9. PERFORMING ORGANIZATION NAME AND ADDRESS Panametrics, Inc. 221 Crescent St. Waltham, MA 02154		10. PROGRAM ELEMENT, PROJECT, TASK AREA & WORK UNIT NUMBERS 62101F 1L1R4EAA
11. CONTROLLING OFFICE NAME AND ADDRESS Air Force Geophysics Laboratory Hanscom AFB, Bedford, MA 01731 Monitor/Paul L. Rothwell/PHG		12. REPORT DATE Oct. 1979
		13. NUMBER OF PAGES 104
14. MONITORING AGENCY NAME & ADDRESS(if different from Controlling Office)		15. SECURITY CLASS. (of this report) Unclassified
		15a. DECLASSIFICATION/DOWNGRADING SCHEDULE

16. DISTRIBUTION STATEMENT (of this Report)

Approved for public release; distribution unlimited.

17. DISTRIBUTION STATEMENT (of the abstract entered in Block 20, if different from Report)

18. SUPPLEMENTARY NOTES

19. KEY WORDS (Continue on reverse side if necessary and identify by block number)

Electrostatic Analyzers, Solid State Spectrometers, Electron and Proton Detectors, High Time Resolution Spectrum Analysis
Charge Buildup at Synchronous Orbit
SCATHA Satellite Instrumentation

20. ABSTRACT (Continue on reverse side if necessary and identify by block number)

(See reverse side.)

20. ABSTRACT

A satellite-borne Rapid Scan Particle Spectrometer (RSPD) has been designed to measure the charge buildup phenomena at synchronous orbit. Simultaneous measurements along two orthogonal axes are made. Each axis incorporates 4 electrostatic analyzers (ESA) and 2 solid state spectrometers (SSS). Four ESA's (low energy p, low energy e; high energy p, high energy e) and two SSS's (proton, electron) with four and five energy bins, respectively, in each analyzer provide a logical compromise of energy resolution and high time resolution. The low energy ESA's cover the energy range 0.05 to 1.7 keV; the high energy ESA's cover the 1.7 to 60 keV range. The electron SSS's cover the 30 to 1000 keV range and the proton SSS's cover the 70 to 7000 keV range. A complete energy spectrum is generated every 1 second. The digital data output consists of a 9 bit mantissa and a 3 bit exponent, allowing accumulation of > 1.3×10^5 counts. A command control allows the ESA or SSS sweep rate to be decreased, or fixed, enhancing the time resolution of portions of the spectrum. A digital count ratemeter with 250 μsec integration time is included. A multiplexer, controlled by ground command, selects the ratemeter input from one of the 8 ESA's or 8 SSS's. Very high time resolution data can be generated by this circuit. Two instrument's have been fabricated, tested and calibrated. The first of these was launched into near-synchronous orbit on board the SCATHA satellite on 30 January 1979.

FOREWORD

iii

TABLE OF CONTENTS

TABLE OF CONTENTS (Cont'd)

LIST OF ILLUSTRATIONS

LIST OF ILLUSTRATIONS (Cont'd)

LIST OF TABLES

1. INTRODUCTION

As reported by DeForest (Refs. 1.1 and 1.2), it is found that in the presence of magnetospheric substorm particles a satellite may charge to negative potentials as high as ~10 kV, and to several hundred volts while sunlit. Although a number of effects are significant (secondary emission, backscattering), the dominant radiation interaction effects are apparently (1) the collection of substorm electrons by the satellite, which tends to produce a negative potential, (2) the collection of substorm protons, and (3) ejection of photoelectrons by sunlight, both of which tend to produce positive potential. The equilibrium potential achieved by the satellite at any time thus depends on the magnitude of the particle fluxes and on the density of low energy plasmasphere particles in the vicinity of the vehicle. A high plasmasphere particle density tends to suppress the charge buildup, but a large substorm can sweep away these particles. Although the substorm proton flux is normally substantially lower than that of the electrons, the secondary emission coefficient is higher. Hence the effect of protons can be appreciable.

Since this charge buildup can have significant consequences in terms of proper satellite operation, the Air Force, in cooperation with NASA, has instrumented a satellite (SCATHA-Spacecraft Charging At High Altitudes) to investigate this effect (Ref. 1.3). The instrument described herein is one of four (Ref. 1.4) developed by the Air Force Geophysics Laboratory for integration into that satellite.

This instrument is a rapid scan particle spectrometer (RSPD) which makes simultaneous measurements along two orthogonal axes of electrons with energy between 50 eV and 1 MeV and protons in the range of 50 eV to 7 MeV. The design incorporates electrostatic analyzers (ESA) up to about 60 keV and solid state spectrometers (SSS) above 30 keV of particle energy.

The principal advantage of an ESA is that it is capable of high energy resolution (definition of peaks, regions of sharp change with energy, etc.). But because it must be swept in energy, and because its geometrical factor is limited, its time resolution is also limited. Substorm flux intensities can, at times, change very significantly in periods on the order of seconds (e.g., see Refs. 1.2 and 1.5-1.7). Thus, it is desirable to use a pair of semiconductor detector spectrometers for measurement of the more energetic protons and electrons which utilize much larger geometrical factors than the ESAs. A system combining four ESAs (low energy p, low energy e; high energy p, high energy e) and two solid state spectrometers (proton and electron) with four and five energy bins, respectively, in each analyzer, for each of two look angles, represents a logical compromise of energy resolution, while providing the capability to analyze simultaneously at two pitch angles with high time resolution. This approach takes into consideration the fact that the time variation of particle intensities may be such that the satellite spin would probably not be sufficiently rapid (at ≈1 rpm) to allow use of a single

ESA to sweep through the pitch angle distribution with the spin axis <u>normal</u> to the field lines. It also makes it possible to follow changes in the spacecraft potential that occur in periods of a few seconds which result from (essentially) step-function changes in incident particle flux, or the current from on-board particle (electron/ion) guns.

The RSPD uses low energy cylindrical plate electrostatic analyzers (ESAs) with SPIRALTRON Electron Multipliers (SEMs) for particle detection to cover the energy range 50 eV to 1.7 keV, while similar high energy ESA's cover the 1.7 to 60 keV range. Four measurements are made over these ranges, plus a background measurement. Separation of the analysis into low and high energy detectors in this manner allows a choice of different geometrical factors in each region. The electron solid state spectrometers cover the 30 keV to 1 MeV range and the proton solid state spectrometers cover the 70 keV to 7 MeV range. Ten measurements are made over these ranges, in five groups of two (coincidence and anticoincidence).

The intstrument's digital output data is read every 200 ms; thus a complete energy spectrum can be generated every 1 second. A command mechanism is included which allows the ESA or SSS sweep rate to be decreased, or fixed in any particular channel. In this way the readout capability can be used to obtain maximum time resolution for those portions of the spectrum of particular interest at certain times. For example, this could be important for measurement during times when the electron or ion gun (other experiments that are on board) current is varied in such a manner that the vehicle potential changes rapidly relative to the normal ESA scan rate.

A high speed digital count ratemeter ($\sim$250 μsec integrating time) is included within the instrument. A multiplexer, controlled by ground command, selects the ratemeter input signal. Extremely high time resolution data can be generated by this circuitry, the only limitation being the bandwidth of the available satellite PAM telemetry channel.

Details of the basic design of the RSPD have been given in Refs. 1.8-1.10. Also shown in Ref. 1.9 are the results of detailed scans across the aperture of the Spiraltron multipliers used as detectors. In order to provide the desired high time resolution, the energy resolution has been made broad, with the ESA energy channels having about 50% width.

The RSPD was taken to the electron-proton calibration facility at Rice University and calibrated in electron beams of 0.04 to 45 keV, and proton beams of 0.1 to 30 keV. This gave a reasonably precise measurement of the G(E) curves for most of the ESA channels, and sufficient data to allow extrapolation to higher and lower energies. The lowest energy electron SSS channels, where the efficiency is affected by backscattering from the aluminum light and proton shield, also had correction factors measured to allow calculation of the correct G(E) factors. The results of this effort are presented in Ref. 1.11.

2

The SCATHA satellite, with the RSPD on board, was successfully launched on 30 January 1979. The instrument has now been on orbit for more than six months, and detailed output data now available show that the RSPD is functioning properly.

The following sections describe the RSPD in greater detail and describe the instrument's interface requirements and characteristics. This is followed by a discussion of the various tests that the instrument has undergone and then the operating procedures and constraints. The on-orbit performance is discussed in detail. A summary of the RSPD's characteristics is presented in the last section.

2. GENERAL INSTRUMENT DESIGN

The Rapid Scan Particle Detector (RSPD) is designed to measure electrons and protons from 50 eV to a few MeV, in two perpendicular directions, with a minimum one second period for a complete spectrum coverage. The final RSPD design is shown in outline in Fig. 2.1. As mounted on the SCATHA satellite one set of spectrometers measures particles arriving parallel to the spin axis, and the other set measures particles arriving perpendicular to the spin axis. Each spectrometer set measures low energy (0.05 to 60 keV) particles with cylindrical plate ESA s using SEM (Spiraltron Electron Multiplier) detectors, and high energy (60 keV to a few MeV) particles with solid state detector telescopes. To allow the spectra to be measured with good statistical accuracy in a short time period, the energy resolution is about 100%, with no gaps between adjacent channels. The ESA s provide an 8 channel spectral measurement while the solid state spectrometers (SSS s) provide up to 10 energy channels.

The entire RSPD is contained in one housing as shown in Fig. 2.1. The general design characteristics of the individual spectrometers are given in the remainder of this section, while the detailed electronics design is described in Section 3. Final instrument characteristics are given in the summary in Section 7.

2.1 Electrostatic Analyzers

The low energy portion of the electron/proton spectra is measured by four dual ESA s, oriented as shown in Fig. 2.1. Each view direction (perpendicular and parallel to the spacecraft spin axis, $\equiv \perp$ and $||$) uses two ESA s to measure low and high energy particles. Each ESA measures its spectral portion in four steps, with a background measurement comprising a fifth step, all in a minimum time of one second.

The basic design of a dual ESA unit is shown in Fig. 2.2. A positive deflection voltage on the central plate analyzes electrons and protons as shown, with the particles being detected by two SEM s. A -30V grid in front of the SEM s reduces the detection of secondary electrons from particles striking the plates and other surfaces, while the cylindrical plates are serrated and blackened to reduce the detection of scattered solar UV. The SEM s have ± 500V bias on the particle detection ends to accelerate electrons (+500V) and protons (-500V) to at least 500 eV in energy. This is necessary to eliminate problems with poor detection efficiency for low energy particles, as is shown by the efficiency measurements of Channeltrons (similar to the SEM s) for electrons in Refs. 2.1, 2.2 and 2.3, and protons in Ref. 2.4.

4
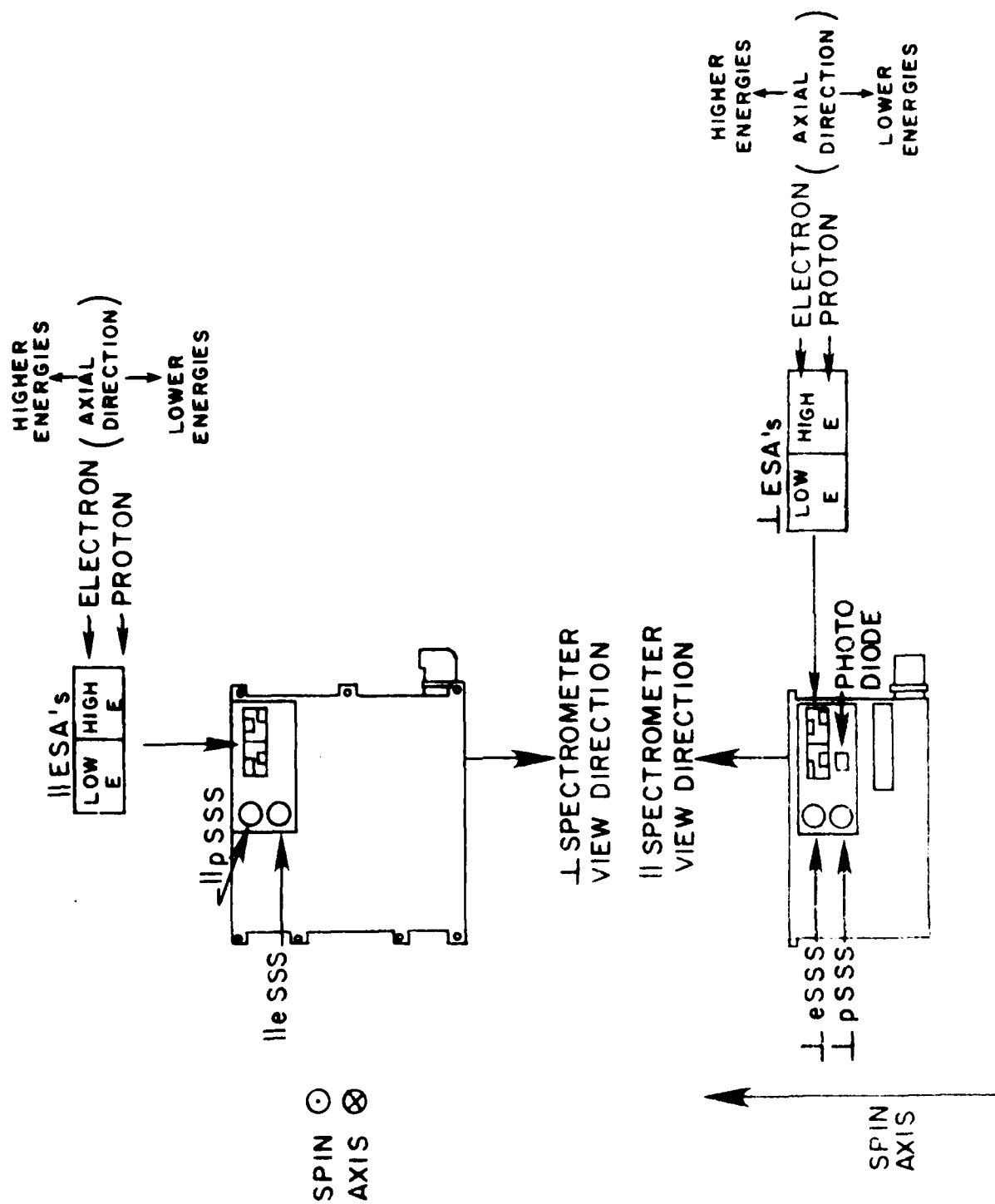
Figure 2.1 Outline of the RSPD Showing the Spectrometer Apertures
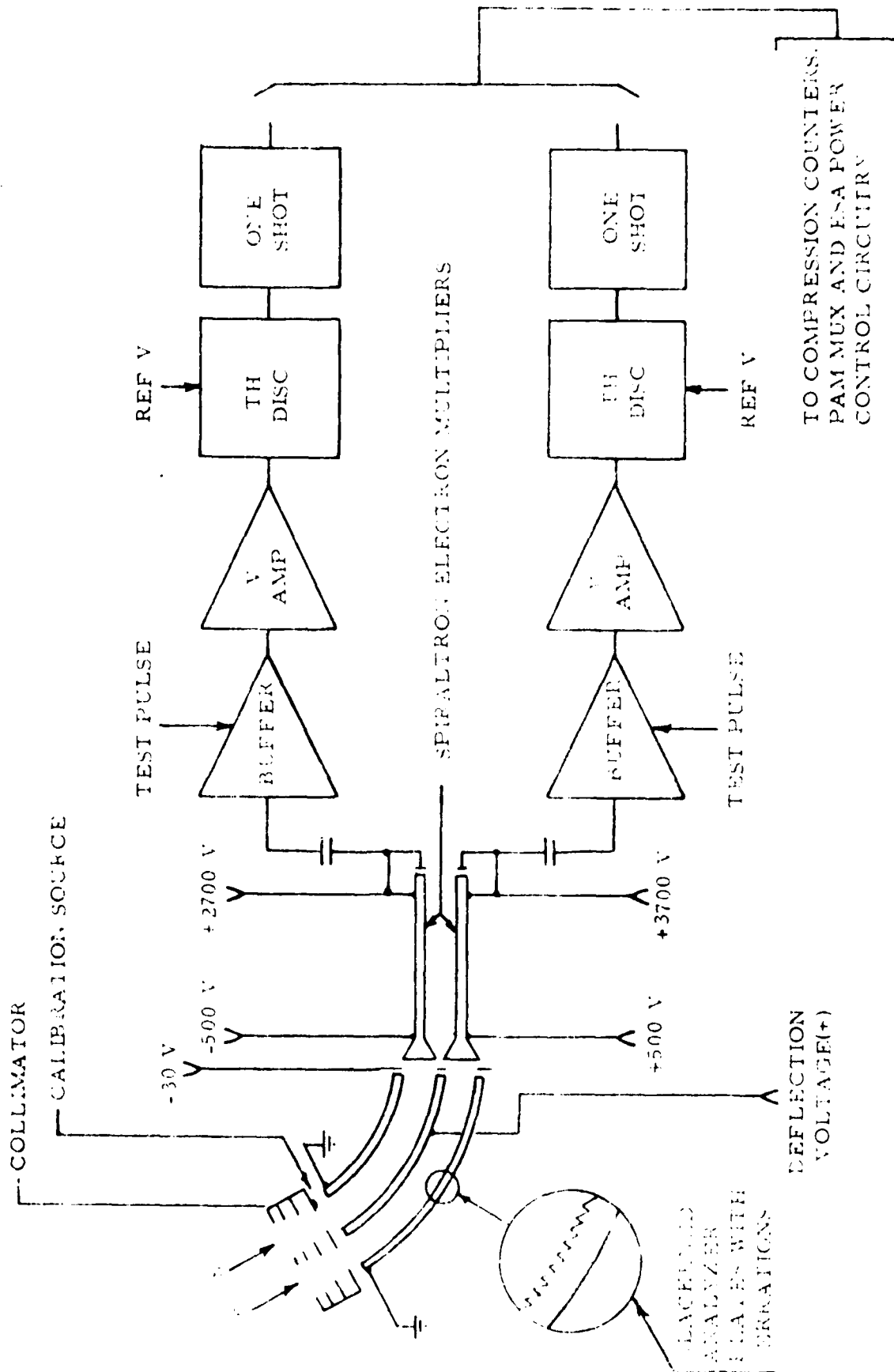
Figure 2.2 Basic Design of a Dual Electrostatic Analyzer Unit.

6

The geometrical dimensions of the ESAs are given in Fig. 2.3. The entrance collimator consists of four rectangular apertures to reduce scattering, and is identical for all ESAs. The positive deflection voltage was chosen since beta source tests indicated that this gave less background. The energy analysis uses a 25° bend, with the radii selected to give the same central energy for protons and electrons and a resolution near 100%. This broad resolution is necessary to allow coverage of the 0.05-60 keV energy range in 8 bins with no gaps. The desired energy bins for the low energy (LE) and high energy (HE) ESAs are given in Table 2.1, along with the channel designations.

The approximate central energies for the design in Fig. 2.3 can be calculated from

$$E_e = \frac{R_3 + R_4}{4(R_4 - R_3)} \quad V = 9.50V \tag{2.1}$$

and

$$E_p = \frac{R_1 + R_2}{4(R_2 - R_1)} \quad V = 9.47V \tag{2.2}$$

where the gaps $R_2 - R_1$ and $R_4 - R_3$ have been assumed to be small compared with the radii R_1 to R_4. Results obtained from Monte Carlo calculations (Ref. 2.5) indicate that the constant in (2.1) and (2.2) is closer to 11, and this value has been used to determine the desired defelection voltage for each channel. Actual calibration data (Ref. 1.11) give an experimental factor nearer 11 than 9.5. The desired voltages using the theoretical factor are given in Table 2.2, along with the final measured values for the flight unit (S/N 1) and the backup unit (S/N 2). The Monte Carlo calculations also gave the full-width-at-half-maximum resolution as 50%, somewhat less than the desired 85% (Table 2.1), but the calculations neglect fringing fields and internal scattering (Ref. 2.5). The neglected effects should broaden the response, so the design in Fig. 2.3 was used with the expectation that the actual response would be closer to the desired 85% FWHM resolution. This was verified by the actual calibrations, which showed the true ESA FWHM to be near 100% (Ref. 1.11).

The peak geometric factor the ESAs can be written approximately as

$$G_o = A_1 A_2 T / d^2 \tag{2.3}$$

where A_1 is the entrance area (aperture 4 in Fig. 2.3), A_2 is the SEM collimator area, d is the distance between A_1 and A_2 taken along the average curved path between the analyzer plates, and T=0.33 is the transmission of the -30V grid over the SEMs. Using Eq. (2.3) and the dimensions in Fig. 2.3 gives

7
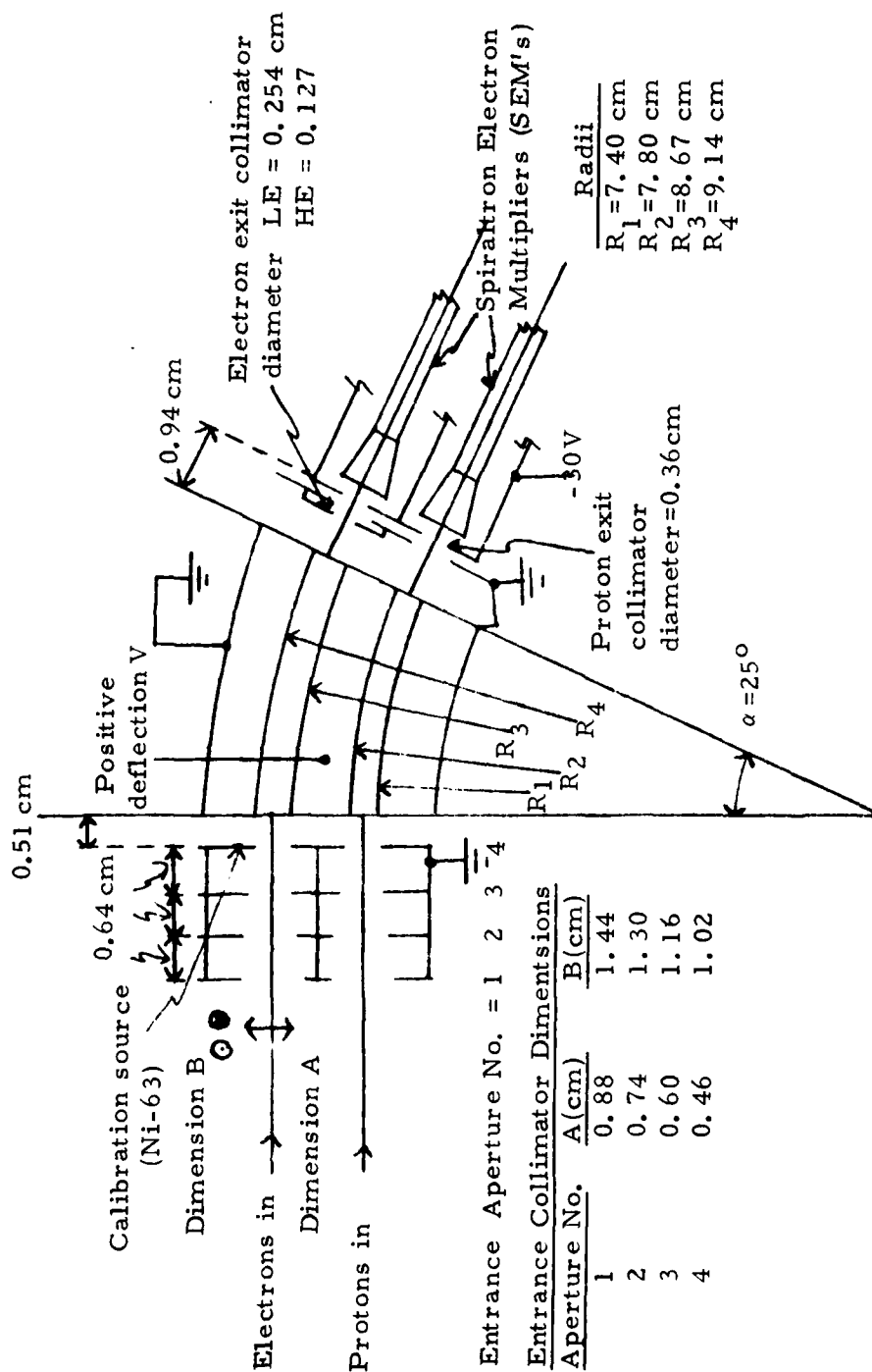
Figure 2.3 Geometrical Dimensions of the ESA s.

The figure contains the following labels and data:

Radii
R₁ = 7.40 cm
R₂ = 7.80 cm
R₃ = 8.67 cm
R₄ = 9.14 cm

Electron exit collimator
diameter LE = 0.254 cm
HE = 0.127

Spiratron Electron
Multipliers (SEM's)

0.94 cm

−30 V

Proton exit
collimator
diameter = 0.36 cm

α = 25°

0.51 cm

Positive
deflection V

0.64 cm

Calibration source
(Ni-63)

Dimension B

Electrons in →
Dimension A

Protons in →

Entrance Aperture No. = 1 2 3 4

Entrance Collimator Dimentsions

Aperture No.	A(cm)	B(cm)
1	0.88	1.44
2	0.74	1.30
3	0.60	1.16
4	0.46	1.02

R₁ R₂ R₃ R₄

8

Table 2.1

Desired ESA Detection Energy Characteristics

ESA Energy Channel Designation	Desired detection energy characteristics (all in keV)			
	(low-high)	Average	(FWHM)	Width Average
LE 0	0	(background)		
" 1	0.05-0.12	0.085	0.070	0.82
" 2	0.12-0.30	0.210	0.180	0.86
" 3	0.3-0.7	0.50	0.40	0.80
" 4	0.7-1.7	1.20	1.00	0.83
HE 0	0	(background)		
" 1	1.7-4.2	2.95	2.50	0.85
" 2	4.2-10.2	7.20	6.00	0.83
" 3	10.2-25	17.6	14.8	0.84
" 4	25-60	42.5	35.0	0.82

Table 2.2

ESA Deflection Volage Characteristics

ESA Energy Channel	Desired Central Energy(keV)	Desired Voltage (V)	Final Measured Voltage (V)	
			Flight Unit (S/N 1)	Backup unit (S/N 2)
LE 0	0	0	0.00	0.056
" 1	0.085	7.7	7.7	7.68
" 2	0.210	19.1	19.2	19.0
" 3	0.50	45.5	45.9	45.2
" 4	1.20	109.	108.8	109.4
HE 0	0	0	0.00	0.18
" 1	2.95	268	266	264
" 2	7.20	655	655	654
" 3	17.6	1600	1614	1597
" 4	42.5	3860	3860	3860

$$G_o(\text{Proton ESA's}) = 7.0 \times 10^{-4} \text{cm}^2\text{-sr} \qquad (2.4)$$

$$G_o(\text{LE Electron ESA}) = 2.8 \times 10^{-4} \text{cm}^2\text{-sr} \qquad (2.5)$$

and

$$G_o(\text{HE Electron ESA}) = 7.0 \times 10^{-5} \text{cm}^2\text{-sr} \qquad (2.6)$$

As discussed in the analysis in Ref. 1.1, the actual ESA count rate for electrons (protons) is

$$C = G_o \, \epsilon(E) \, f E \, dN(E)/dE \qquad (2.7)$$

where $\epsilon(E)$ is the SEM detection efficiency for electrons (protons) of energy E, f (0.50 calculated, 0.85 desired, about 1.0 measured) is the FWHM fractional resolution, and $dN(E)/dE$ is the electron (proton) differential spectrum (particles/$(\text{cm}^2\text{-sec-sr-keV})$). The detailed inversion of (2.7) to obtain $dN(E)/dE$ from C requires the actual shape of $G(E)$, which is obtained from experimental calibration. The ESA calibration is described in detail in Ref. 1.11.

The above approximate G_o values were selected to give the best statistical data for the expected fluxes for the SCATHA satellite. In the case of the proton ESA s, the G_o was set to the maximum possible with the cylindrical plate design, without causing serious UV sensitivity or background problems. Except for the LE proton ESA, which is about an order of magnitude smaller, the values approximate those set out in the early design stage of the ESA (Ref. 1.8).

The ESA s have a number of operating constraints imposed by the SEM characteristics. The typical SEM draws a few μA from the bias supply, and puts out a few pico-coulomb of charge per pulse at typical operating gains. This means that at about 100 kHz count rates the SEM is pathing about 10% of its wall current into the pulse output. Operation at significantly higher count rates will result in a reduction of SEM bias, and hence gain, at the output end, and give increasingly uncertain SEM efficiency. The ESA s thus cannot reliably measure particle fluxes which result in count rates significantly above 100 kHz.

Another SEM characteristic is that they degrade under long-term vacuum operation. This degradation is approximately proportional to total SEM output charge, so a high count rate results in a short lifetime, while a long desired lifetime requires low count rates. Partial SEM recovery can be achieved by raising the bias. SEM lifetime can also be extended by operation at as low a bias as possible to achieve good efficiency, since this reduces the charge/pulse output to the lowest necessary. The $\perp$ ESA s also view the sun once per spin period, and this contributes counts from solar UV, adding further to SEM degradation in those ESA s. The general ESA design thus includes capabilities to vary the SEM bias level, and to turn off the SEM bias during the time period when the ESA s are viewing the sun. The actual use of the capabilities depends on observed degradation characteristics in orbit.

2.2 Solid State Spectrometers

The high energy (60 keV to a few MeV) portion of the particle spectrum is measured by two sets of solid state spectrometers (SSS s), one for ⊥ and one for ‖ arriving particles (see Fig. 2.1). Each set consists of one electron SSS and one proton SSS. The basic design is shown in Fig. 2.4, which also shows the differences between the electron SSS and the proton SSS. While the basic designs are quite similar, there are important differences, so the electron and proton SSS s must be discussed separately.

2.2.1 Electron Spectrometer

The electron SSS has a 0.1 mil aluminum foil light shield and a 300μm thick front detector (Fig. 2.4). The rear (coincidence/anticoincidence) 300μm detector is separated from the front detector by a 1/16 inch aluminum absorber to bring the energy where coincidence detection starts up to about 1 MeV. The details of the electron SSS detector assembly are shown in Fig. 2.5. The maximum angular field-of-view is $\pm 13^\circ$. The Am-241 alpha particle source is degraded in energy to provide in-flight calibration data for the front detector, thus verifying most of the system operation.

The initial design did not have the 1/16 inch Al absorber between the two detectors, and analysis for that condition was given in Ref. 1.8 where the calculated energy losses were given. The energy losses for electrons and protons in the front detector remain the same, while the rear detector will now only detect electrons above about 950 keV. This requires some changes in the coincidence mode configuration to avoid making some meaningless measurements. The revised electron SSS configuration and electron detection energies are given in Table 2.3. Only two channels remain true coincidence measurements, with two channels giving only rear detector measurements and one giving a front detector anticoincidence measurement. Channels EC0 and EC1 are nominally repeated in EC3 and EC4, although the mode type is different. This allows measurement of the effects of penetrating radiation and bremsstrahlung by observing the differences of corresponding channels. EC2 is included to provide a measure of the flux below 950 keV, and so avoid a gap between 550 and 950 keV. The EA3 channel is quite broad, but cannot be narrowed because of the 1/16 inch Al absorber.

The geometric factor for the electron SSS is also given in Fig. 2.5, based on the tungsten collimator dimensions and separation. This value $G_0 = 3.55 \times 10^{-3} cm^2$-sr is for straight line paths of all particles, and requires some correction at low energies for scattering in the 0.1 mil Al foil. This scattering correction is very significant at 30 keV, but becomes negligible above 120 keV (Ref. 1.11). Scattering in the 1/16 inch Al absorber also has some effect on the EC channels (Table 2.3), and some calibration of these channels with high energy electrons is desirable. This has not been done on the flight unit (S/N 1), but is mostly geometry dependent and so should be identical for the backup unit (S/N 2).

11

FRONT SSD: 300μ - e UNITS
6μ - p UNITS

COLLIMATORS

SWEEPING MAGNETS - p UNITS ONLY

THIN FOIL - p UNITS ONLY

CALIBRATION SOURCE

e UNITS ONLY

INTERMEDIATE
ABSORBER
-1/16 In. Al
- p UNITS ONLY

TO PAM MULTIPLEXER AND ESA
POWER CONTROL CIRCUITRY

TO
COMPRESSION
COUNTERS
AND PAM
MULTIPLEXER

COINC

COINC

WINDOW
LOGIC

ONE
SHOT

ONE
SHOT

ONE
SHOT

ONE
SHOT

THRESHOLD DISC

THRESHOLD DISC

THRESHOLD DISC

THRESHOLD DISC

REF

REF

AMP

AMP

CSPA

CSPA

TEST
PULSE

BIAS V

TEST
PULSE

BIAS V

SSD

SSD
300μ

12

Figure 2.4 Basic Design of the Solid State Spectrometers.

Figure 2.5. Details of the Electron SSS Detector Assembly

Front detector
(300μm, 50 mm^2)

1/16 inch Al absorber

Entrance
collimator
(1.00 cm
diameter)

Maximum 13° 13°
entrance
angles

Exit
collimator
(0.021 cm diameter)

0.1 mil Al
foil and cal-
ibration
source (Am-241)

Rear detector
(300μm, 100 mm^2)
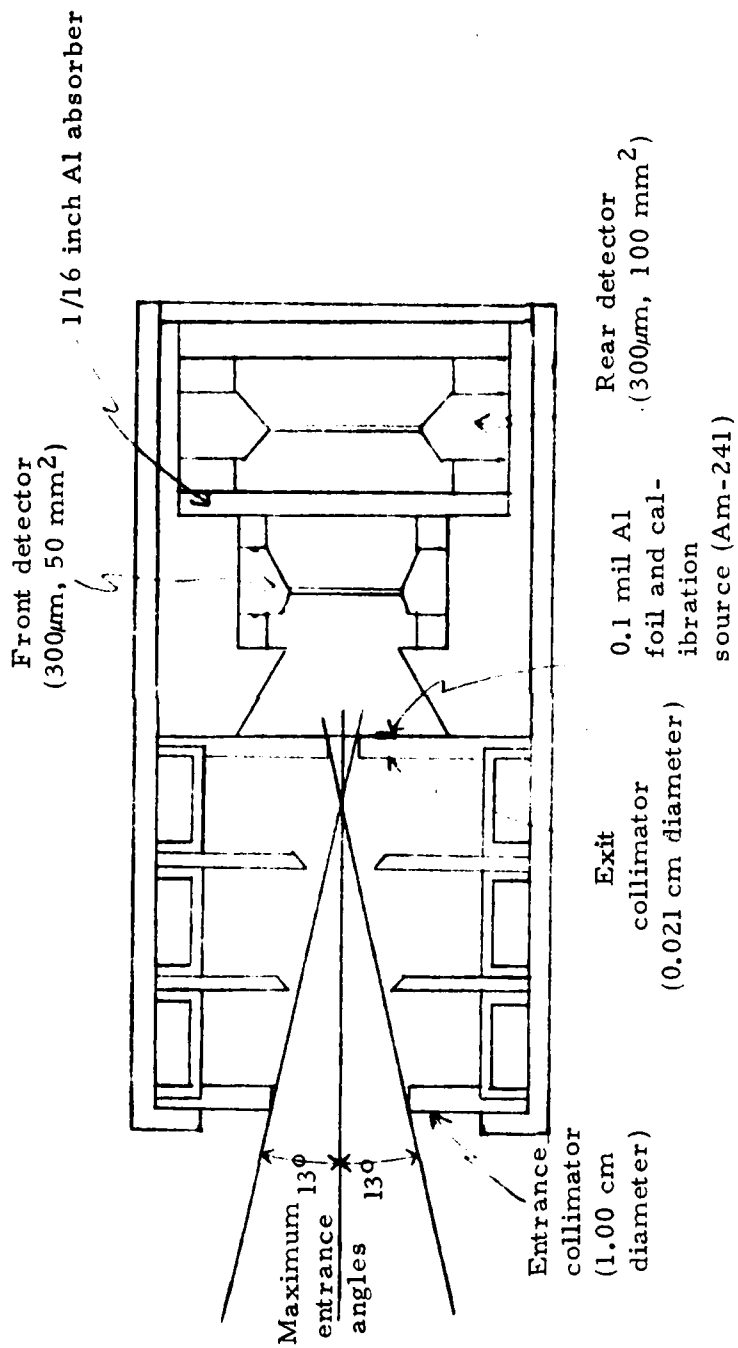
Collimators = tungsten
Baffles and housing = magnesium

Collimator separation = 2.65 cm
$G_o = 3.55 \times 10^{-3}$ cm^2-sr

13

Table 2.3

Revised Electron SSS Energy Channel Characteristics

Note: all energies are in keV.

Channel Designation	Front detector/Rear detector loss range / loss range	Electron detection energy range	Mode type
EA 0	25-41/<50	35-45	Front/anti-rear
EA 1	41-67/<50	45-70	"
EA 2	67-118/<50	70-120	"
EA 3	118-300/<50	120-550	"
EA 4	168-300/<50	170-265	"
EC 0	>25/>50	>950	Front/coinc-rear
EC 1	>41/>150	980-1100	"
EC 2	>67/<50	>0-950	Front/anti-rear
EC 3	-/>50	>950	Rear
EC 4	-/>150	980-1100	"

Table 2.4

Flight Unit Proton SSS Energy Channel Characteristics

Note: All energies are in keV

Channel Designation	Front detector/Rear detector loss range / loss range*	Proton detection energy ranges* p SSS	p SSS	Mode type
PA 0	60-103/<50	101-150		Anticoinc.
PA 1	103-183/<50	150-225		"
PA 2	183-288/<50	225-450		"
PA 3	288-419/<50	325-450		"
PA 4	419-750/<50	450-479	450-547	"
PC 0	60-103/>50	3290-6750	4250-8610	Coinc.
PC 1	103-183/>50	1464-3290	1867-4250	"
PC 2	183-288/>50	733-1464	959-1867	"
PC 3	288-419/>50	491-733	598-959	"
PC 4	419-750/>50	- †	547-598	"

*Flight unit (S/N 1) proton SSS front detector thicknesses are:
⊥ p SSS = 5.3 m; ‖ p SSS = 6.3 m.
†Because of the detector thickness (5.3 m), this channel has no direct detection of protons, but will see a few because of energy loss straggling.

2.2.2 Proton Spectrometer

The proton SSS has a set of sweeping magnets to reduce pileup counts from low energy electrons, and a 5 to 10 μm thick front detector which is rendered light-tight by a 120 μg/cm² layer of aluminum. The rear detector is 300 μm thick, and there is no intervening foil. The details of the proton SSS detector assembly are shown in Fig. 2.6. The maximum angular field-of-view is ±14°. The Am-241 source is degraded in energy to provide in-flight calibration data for the front detector, thus verifying most of the system operation.

The sweeping magnets have a measured field of near 2.5 kG in the gap center, decreasing to about 1 kG opposite the magnet edges. The field at the magnet faces is near 3.5 kG. The effective sweeping field/area is thus a minimum of 2 kG average over about a 1.5 cm wide area. The radius of curvature of an electron with kinetic energy T keV is

$$r = \frac{4.71}{B} \left[T(mc^2 + T/2) \right]^{1/2} \tag{2.8}$$

where mc^2 = 511 keV is the electron rest mass energy, B is in gauss, and r is in cm. This gives complete shielding for electrons below 170 keV (r=0.75 cm), and partial shielding to a few hundred keV.

The proton SSS energy channel characteristics were calculated in Ref. 1.8 for a 10 μm front detector and a selected set of energy loss bins. Because the front detector is quite thin, it is not possible to specify the detector thickness precisely, and a nominally 10 μm detector can actually be anywhere in the range 5 to 10 μm. The detector thicknesses were measured by alpha particle transmission energy loss and by x-ray attenuation, and the actual detector values used to calculate the true response.

The actual flight unit energy bins also depend on the several detector thresholds used, which are partly determined by the lowest level which detector noise allows. The flight unit detectors were measured to be near 5-6 μm thick, and so have slightly higher noise levels than the 10 μm detector for which calculations were made in Ref. 1.8. The flight unit (S/N 1) energy bin characteristics are listed in Table 2.4. The ⊥p SSS front detector was measured to be 5.3 μm thick, the ∥p SSS was 6.3 μm. The resulting energy channels give a negligible width for PC4 on the ⊥p SSS because of the thinness of the front detector. The backup unit (S/N 2) has a 5.4 μm detector for the ⊥p SSS and a 9.7 μm detector for the ∥p SSS. Energy channels are not presented for the backup since the flight unit was the one launched in SCATHA. Should the backup unit be used at some later date it is expected that all solid state detectors would be replaced to improve reliability (to avoid any possible deterioration after some years in storage), and the actual energy channels would depend on the new detector thicknesses.

15

Front Detector
(5-10 µm, 25 mm^2)
(120 µg/cm^2 Al surface toward entrance aperture)

Rear Detector
(300 µm, 100 mm^2)

Sweeping
Magnets

Calibration source
(Am-241)

Exit Collimator
(0.249 cm diameter)
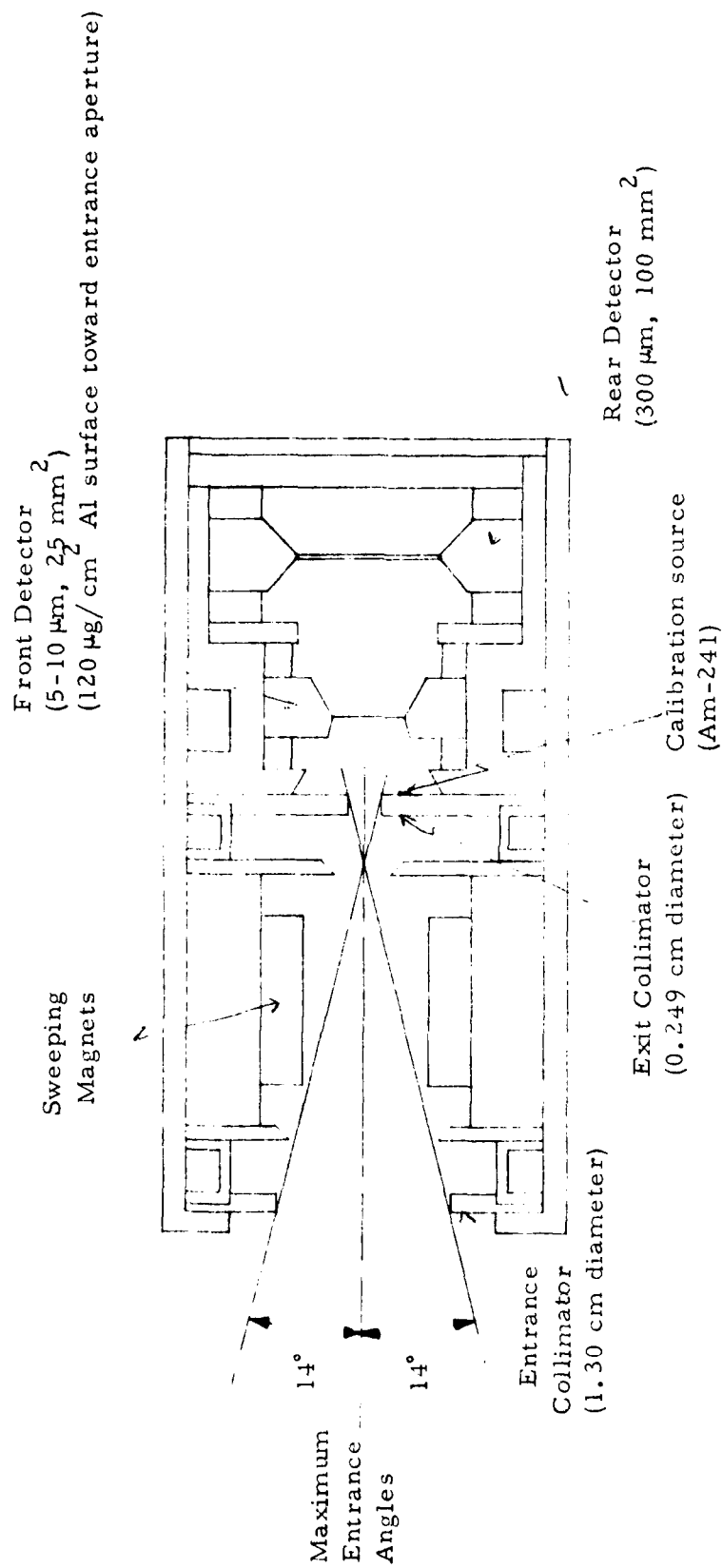
Collimator = tungsten

Housing = magnesium

Entrance
Collimator
(1.30 cm diameter)

Maximum
Entrance
Angles

14°

14°

Collimator separation = 3.11 cm

G_o = 6.68 x 10^{-3} cm^2 - sr

Figure 2.6   Details of the Proton SSS Detector Assembly

16

The geometric factor for the proton SSS s is given in Fig. 2.6, and is $6.68 \times 10^{-3} \text{cm}^2$-sr. This is expected to be quite accurate, since protons do not scatter to the extent that electrons do. The energy bin edges should be quite sharp, except for the rounding introduced by energy loss straggling for protons which penetrate the front detector, and by detector noise. The room temperature measurements of detector noise are given, for the SSS front detectors, in Table 2.5. The proton detectors have 28-50 keV FWHM, which is larger than the 7-8 keV for the electron detectors because of the thinness of the proton SSS front detectors.

Table 2.5

SSS Front Detector Noise Levels

Front Detector of SSS on Flight Unit (S/N 1)	Full Width at Hal Maximum Noise at Room Temperature (keV)
I p SSS	28
I p SSS	50
II e SSS	8
II e SSS	7

3. DETAILED INSTRUMENT DESIGN

The Rapid Scan Particle Detector (RSPD), shown in Figure 3.1, performs a differential energy analysis of 50 eV to >1 MeV electrons and 50 eV to about 7 MeV protons. This is accomplished by using low energy electrostatic analyzers (ESAs) to cover the 50 eV to 1.7 keV range, high energy ESAs to cover the 1.7 to 60 keV range, and solid state spectrometers (SSSs) for measurements above that range. Two complete sets of detectors are used, one of which is oriented perpendicular to the satellite spin axis and the other parallel to the spin axis. A simplified instrument block diagram, shown in Figure 3.2, indicates that the RSPD can be functionally divided into eight (8) major subsystems as follows:

1) Four Electrostatic Analyzers (ESAs) which measure low energy electrons and protons.

2) Four Solid State Spectrometers (SSSs) which measure higher energy electrons and protons.

3) The energy channel control circuitry which allows for completely independent control of ESA and SSS energy channel sweep rate or assignment, via ground command.

4) The digital data circuitry which accumulates the pulses from the ESAs and SSSs, compresses the information so as to minimize the instrument's telemetry requirements, and transfers the information to the spacecraft's data processor.

5) The broadband data multiplexer and signal processor which is assigned to a particular ESA or SSS by ground command and provides a very high time resolution monitor of its activity.

6) The electrostatic analyzer power control circuitry which automatically turns off the ESAs when the flux level exceeds certain predetermined levels which would result in premature Spiraltron Electron Multiplier (SEM) gain degradation.

7) The magnitude command circuitry which receives and decodes a serial command from the spacecraft and provides parallel control lines to various other subsystems.

8) The DC to DC Converter, power control, distribution and analog monitors subsystem which contains all of the required DC to DC Converters and high voltage power supplies, as well as various analog voltage and temperature monitors.

A detailed discussion of these subsystems is contained in the following subsections; their location within the instrument's housing is shown in Figure 3.3.

3.1 Electrostatic Analyzer

A simplified block diagram of the ESA subsystem is shown in Figure 2.2.
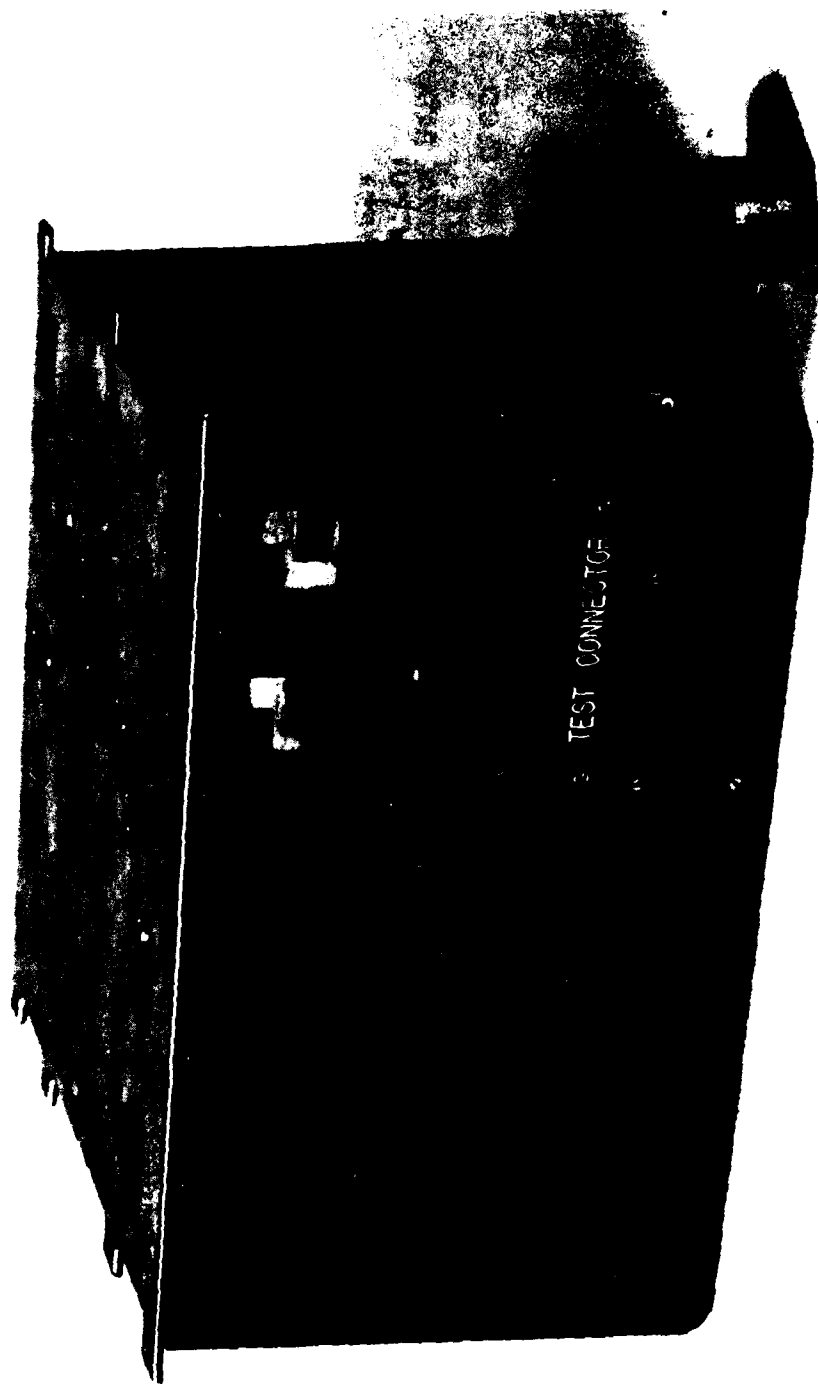
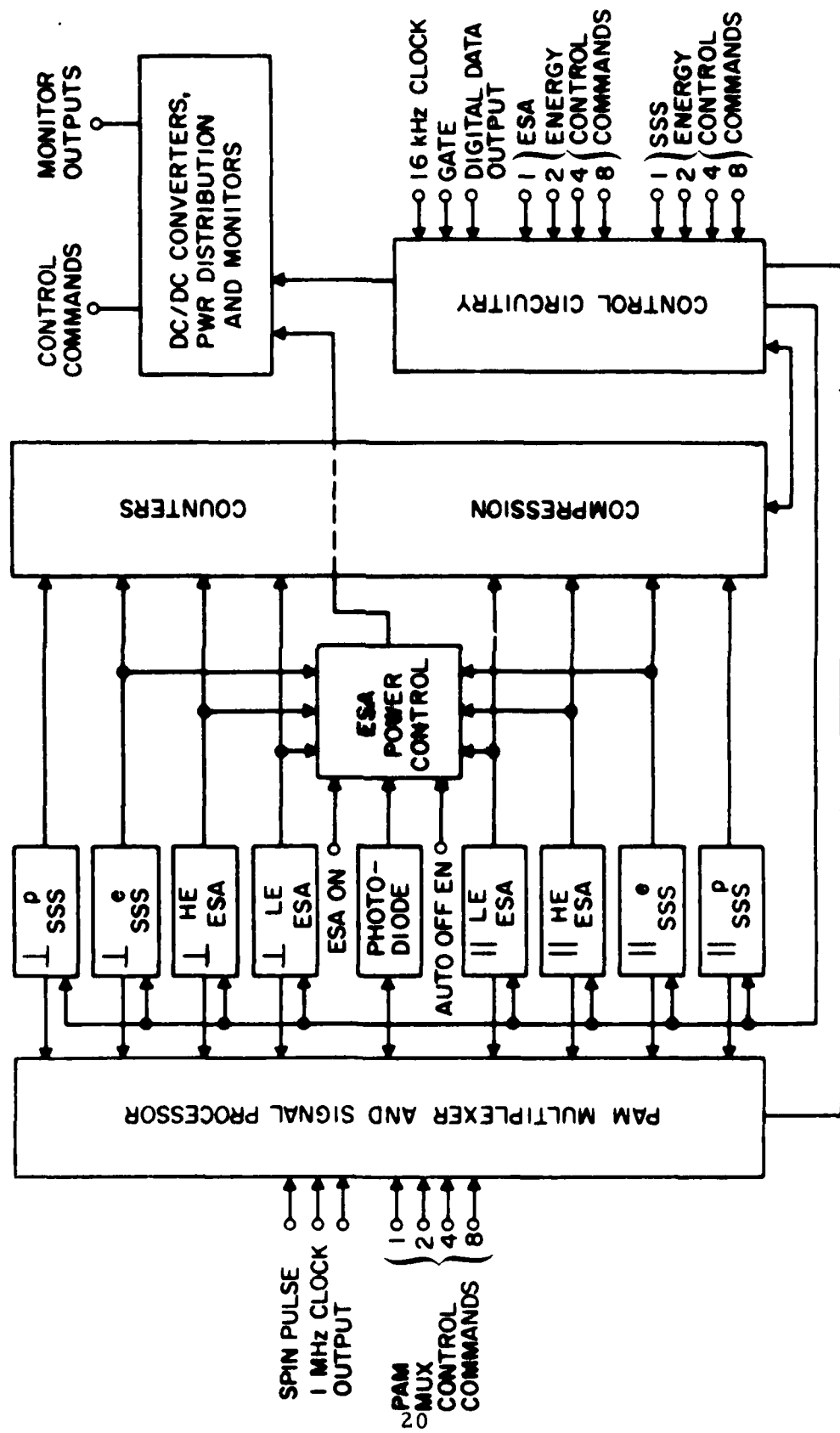Figure 3.1 Rapid Scan Particle Spectrometer (RSPD).

TEST CONNECTOR

Figure 3.2 RSPD Block Diagram

1, 2 p SSS Det Assy
3, 4 e SSS Det Assy
5 DC-DC Converter
6, 8 LE ESA Det Assy
7, 9 HE ESA Det Assy
10 SSS Pc Bd
11 ESA Pc Bd
12 BB Data Pc Bd.
13 Dig Data Pc Bd
14 En Ch/SEM Bias Control Pc Bd
15 ESA PWR Control/Analog Mons Pc Bd
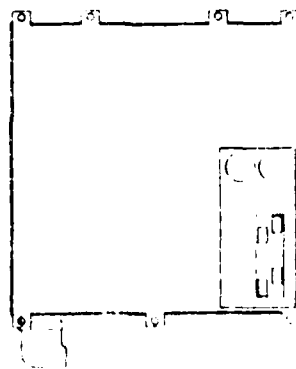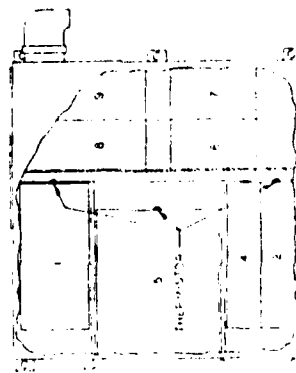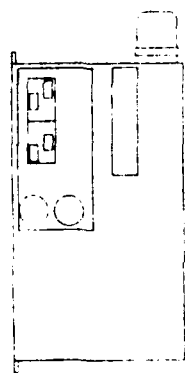
15
14
13
12
11
10
10

Figure 3.3 Sub-System Locations.

21

Energy analysis is accomplished by a three-plate cylindrical electrostatic analyzer with the outer plates grounded, and a programmed, positive deflection voltage applied to the inner plate. Electrons are analyzed by the outer plates while protons are simultaneously analyzed by the inner plates - in both cases selected particles are detected by a Spiraltron Electron Multiplier (SEM).

The front end of the electron SEM is biased at +500V to accelerate low energy electrons, thereby obtaining better detection efficiency. This requires that the output end of the SEM be biased at $\approx$+3700V to obtain a nominal operating voltage of $\approx$3200V. Similarly, the front end of the proton SEM is biased at -500V, requiring its output end to be biased at $\approx$+2700V. These bias voltages are nominal levels; the actual set of bias levels being one of 16 possible sets as selected by ground command. This arrangement allows the SEM's to be biased initially at relatively low voltages (low gain) and to increase the bias voltages (and gains) if gain fatigue is experienced. An additional benefit is that fatigue is delayed, since it is a function of the charge removed from the SEM, not the total accumulated counts. Thus, the total life in terms of accumulated counts is actually extended. A suppression grid biased at -30V is placed between the deflection plates and the electron SEM to inhibit the detection of secondary electrons emitted by the deflection plates.

Each SEM drives a Buffer Amplifier-Voltage Amplifier-Threshold Discriminator-One Shot chain. The input to the high impedance unity gain buffer is protected from damage due to corona or high voltage breakdown in the SEM or deflection plates. The voltage amplifier gain and threshold discriminator firing level are such that nominal SEM gain variations can be tolerated. The threshold discriminator output is fed to a one shot which generates a logic level pulse of fixed duration and drives the compression counter, broadband data multiplexer, and ESA power control circuitry.

A single test pulse is injected into the buffer amplifier input during each data accumulation interval, thus verifying proper operation of the signal processing circuitry. Furthermore, a low intensity Ni-63 conversion electron source is also included in front of the electron analyzer to verify proper system performance. The source intensity is sufficiently low that it will not interfere with spectrum determination during substorms.

The deflection plates, SEMs and buffer amplifiers are contained in the ESA Detector Subassembly, which is shown in the upper portion of Figure 3.4.

Four such subassemblies are included within the instrument. Two low energy (LE) units each cover the 0.05 to 1.7 keV energy range, while two high energy (HE) units simultaneously cover the 1.7 to 60 keV energy range. These are oriented such that two (one LE and one HE) look perpendicular to the satellite spin axis, and the other two look parallel to that axis. The voltage amplifiers, threshold discriminators, and one shots for all of the ESAs are contained on a single plug-in printed circuit board.

22
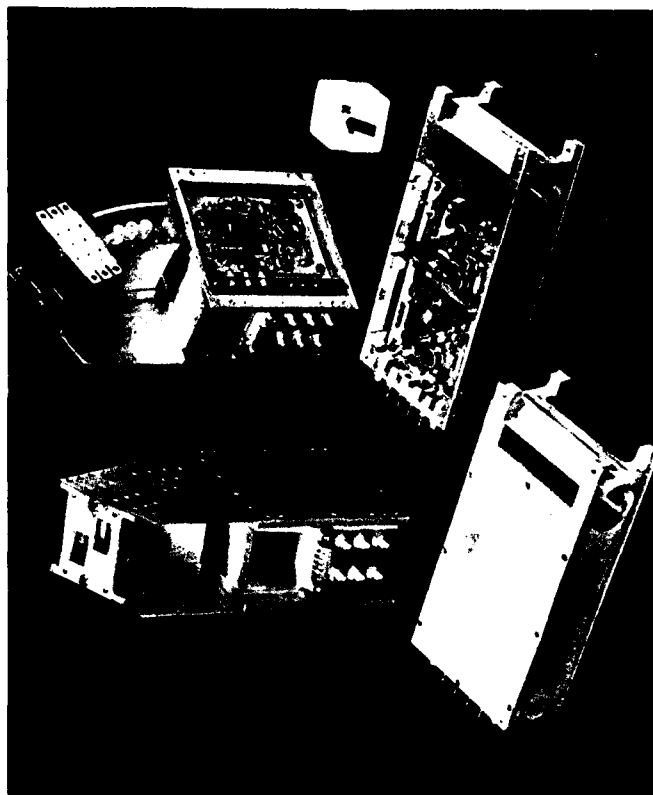
Figure 3.4 Typical ESA (upper) and SSS (lower) Subassemblies.

23

Each ESA's energy range is covered in 4 increments, as shown in Table 2.1. A background measurement is also included yielding a total of 5 ESA energy channels. Data are accumulated and read out in 200-msec blocks; thus, a complete ESA sweep (5 energy channels) can be completed in 1 sec. The ESAs can be commanded to remain in the same energy channel for a number (up to 1024) of 200-msec data blocks, or to be fixed in a particular energy channel.

It should be noted that 8 ESA measurements are made simultaneously: $\perp$ LE e, $\perp$ LE p, $\parallel$ LE e, $\parallel$ LE p, $\perp$ HE e, $\perp$ HE p, $\parallel$ HE e, and $\parallel$ HE p. Any one of these may be assigned to the high time-resolution broadband data signal processor, via ground command.

3.2 Solid State Spectrometer

A block diagram of the SSS subsystem is shown in Figure 2.4. Energy analysis is accomplished by totally depleted silicon surface barrier solid state detectors (SSDs), which produce a charge pulse proportional to the energy deposited by the incident particle. The low noise charge sensitive preamplifier (CSPA) converts this charge pulse into a voltage pulse which is further amplified before being fed to the threshold discriminators. The threshold discriminator outputs drive one shots which generate logic level output pulses of fixed duration. These are combined by the window logic such that an output is obtained if, and only if, the lower level threshold is exceeded, and the upper level threshold is not exceeded. The rear SSD determines whether the incident particle has penetrated the front detector. Simultaneous anti-coincidence ($\overline{\text{COINC}}$) low energy, nonpenetrating, and coincidence (COINC) high energy, penetrating measurements are made and directed to the compression counters and broadband data multiplexer circuitry. A low intensity Am-241 calibration source is positioned in front of the telescope to verify proper system performance. The source intensity is sufficiently low that it will not interfere with spectrum determination during substorms.

The electron and proton SSS subsystems are very similar, the only difference being:

(1) The front solid state detector - the electron SSS front detector is 50 mm^2, 300 μm totally depleted, whereas a 25 mm^2, approximately 5 μm totally depleted detector is used in the proton units. The rear detectors are all 100 mm^2, 300 μm partially depleted.

(2) A thin foil is used in front of the electron units for the elimination of low energy protons.

(3) Sweeping magnets are used in front of the proton units for the elimination of low energy electrons. The use of a very thin detector in this assembly simplifies this problem in that only electrons with energies up to about 40 keV need be eliminated. Higher energy electrons will pass through the detector and not deposit enough energy to cause a false count.

24

(4) The electron SSS contains an additional fixed threshold discriminator and one shot, which is used to activate the automatic ESA power shutdown circuitry during periods of excessively high electron flux levels.

(5) The electron SSS contains an absorber between the two detectors, improving spectral data at high energies by giving a differential flux measurement at 1 MeV and a threshold measurement above 1 MeV. The combinational logic is also modified accordingly.

The solid state detectors and charge sensitive preamplifiers are contained in the SSS Detector Subassembly, which is shown in the lower portion of Figure 3.4. Four such subassemblies are included within the instrument, two electron units each covering the 30 keV to >1 MeV energy range and two proton units each covering the 70 to about 7 MeV energy range. These are oriented the same as the ESAs - two (one electron and one proton) look perpendicular to the satellite spin axis, and the other two look parallel to that axis. The pulse amplifiers, threshold discriminators, one shots, and coincidence logic for all of the SSSs are contained on the two plug-in printed circuit boards. These two boards are essentially identical, each containing the circuitry for one P and one e SSS.

As in the case of the ESAs, there are 5 SSS energy channels. Since two measurements are made simultaneously ($\overline{COINC}$ and COINC) a total of 10 measurements is made over the energy ranges, as shown in Tables 2.3 and 2.4. Since data are accumulated and read out in 200-msec blocks, a complete energy spectrum can be generated in 1 sec. The SSSs can be commanded to remain in the same energy channel for a number of 200-msec data blocks (up to 1024), or to be fixed in a particular energy channel. The command system allows complete independent control of the SSS and ESA energy channels.

It should be noted that 8 SSS measurements are made simultaneously - $\perp$ e $\overline{COINC}$, $\perp$ e COINC, $\perp$ p $\overline{COINC}$, $\perp$ p COINC, $\parallel$ e $\overline{COINC}$, $\parallel$ e COINC, $\parallel$ p $\overline{COINC}$, and $\parallel$ p COINC. Any one of these may be assigned to the high time resolution broadband data processor, via ground command.

3.3 Energy Channel and SEM Bias Voltage Controller

A block diagram of the energy channel control circuitry is shown in Figure 3.5. This subsystem determines the SSS and ESA energy channels and generates the analog reference voltages which actually implement the desired energy channel, as well as that which establishes the desired SEM bias voltage levels.

The INCREMENT ENERGY CHANNEL pulse, generated by the digital data circuitry at the beginning of each 200 msec data accumulation period, is applied to the 10 bit binary counter and both of the 11 channel digital multiplexers. The ENERGY CHANNEL CONTROL BITS, from the magnitude command circuitry, determine which of the multiplexer inputs are applied to the modulo 5 counter inputs. This allows these counters to dwell in a particular state for a selected

Figure 3.5. Energy Channel and SEM Bias Voltage Control Circuitry B.ock Diagram.
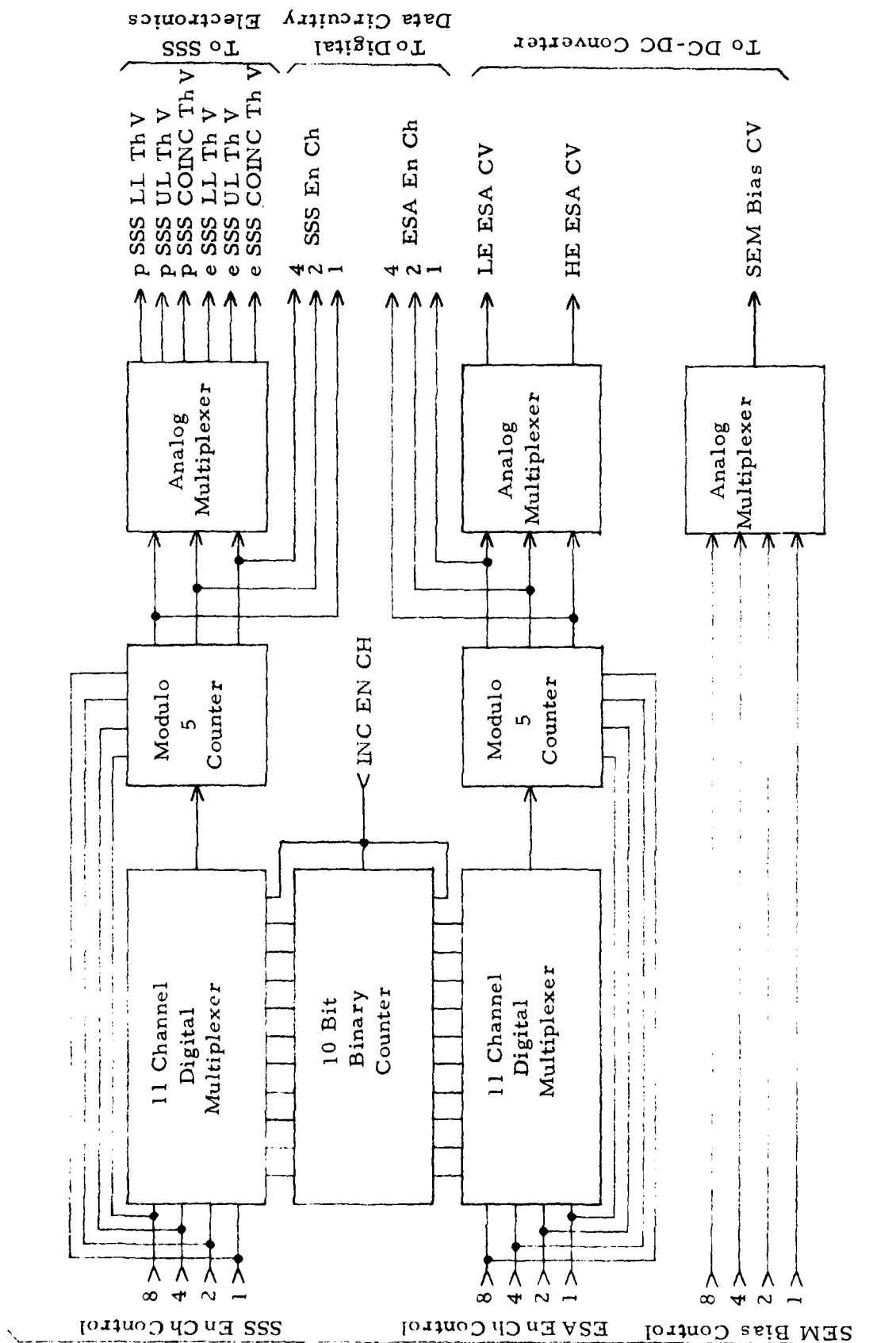
number of data accumulation periods. These counters may also be fixed in any particular state by the energy channel control bits. The three (3) bit parallel outputs of the two modulo 5 counters control the analog multiplexers which select the appropriate analog voltage that actually establish the desired energy channels.

The SSS and ESA energy channels are completely independent - the SSSs may be sweeping at one rate, or fixed in a particular energy channel, while the ESAs are sweeping at the same or any other rate or fixed in the same or any other channel. The actual energy channel dwell time or assignment for each is selected by ground command via 4 magnitude command bits, allowing each to have 16 possible operating modes as shown in Tables 3.1 and 3.2. The designation of the SCATHA satellite commands which establish the various operating modes is also shown.

The SEM bias voltage control circuitry generates a reference voltage which is directed to the DC to DC converter subsystem wherein the desired SEM bias voltage levels are established. This reference level is selected from 16 pre-programmed levels, by ground command, via 4 magnitude command bits, as shown in Table 3.3 - which again gives the associated SCATHA command designations.

The energy channel and SEM bias voltage control circuitry is all contained on a single plug-in printed circuit board.

3.4 Digital Data Processor

A block diagram of the digital data circuitry is shown in Figure 3.6. This subsystem contains all of the electronics associated with the accumulation and transfer of the instrument's digital data.

Sixteen 12 bit compression counters (9 bit mantissa and 3 bit exponent) simultaneously accumulate the pulse outputs from the ESAs and SSSs. Data is accumulated over 200 msec intervals. All counters are reset to zero at the beginning of each data accumulation period; at the end of each data accumulation period, all compression counter data (192 bits) is parallel transferred to the shift register along with 8 status bits (3 - ESA energy channel, 1 - ESA overflow flag, 3 - SSS energy channel and 1 - SSS overflow flag). These 200 bits are serially shifted to the spacecraft data processor over the following 200 msec interval, while the next data set is simultaneously being accumulated.

The spacecraft supplies the CLOCK, GATE, and SYNC signals which control the accumulation and transfer of the digital data. Because the spacecraft's data system runs at 8 main frames per second, achieving 5 RSPD readouts per second becomes reasonably involved. Each main frame consists of 128 words; the RSPD is assigned words 15, 18-20, 44-46, 70-72, 95-97, and 121-123. The enable GATES coinciding with those words are counted, and a gating matrix detects the beginning of the data accumulation intervals, which correspond to the beginning of the following enable gates:

27

Table 3.1

ESA Energy Channel Control Command Assignment

Energy Channel Control Bits				Consecutive Readouts in Each Energy Channel	Complete Energy Sweep Period (sec)	Energy Channel	SCATHA COMMAND DESIGNATION
8	4	2	1				
0	0	0	0	1	1	-	6616
0	0	0	1	2	2	-	6601
0	0	1	0	4	4	-	6602
0	0	1	1	8	8	-	6603
0	1	0	0	16	16	-	6604
0	1	0	1	32	32	-	6605
0	1	1	0	64	64	-	6606
0	1	1	1	128	128	-	6607
1	0	0	0	256	256	-	6608
1	0	0	1	512	512	-	6609
1	0	1	0	1024	1024	-	6610
1	0	1	1	-	-	0	6611
1	1	0	0	-	-	1	6612
1	1	0	1	-	-	2	6613
1	1	1	0	-	-	3	6614
1	1	1	1	-	-	4	6615

Table 3.2

SSS Energy Channel Control Command Assignment

Energy Channel Control Bits				Consecutive Readouts in Each Energy Channel	Complete Energy Sweep Period (sec)	Energy Channel	SCATHA COMMAND DESIGNATION
8	4	2	1				
0	0	0	0	1	1	-	6632
0	0	0	1	2	2	-	6617
0	0	1	0	4	4	-	6618
0	0	1	1	8	8	-	6619
0	1	0	0	16	16	-	6620
0	1	0	1	32	32	-	6621
0	1	1	0	64	64	-	6622
0	1	1	1	128	128	-	6623
1	0	0	0	256	256	-	6624
1	0	0	1	512	512	-	6625
1	0	1	0	1024	1024	-	6626
1	0	1	1	-	-	0	6627
1	1	0	0	-	-	1	6628
1	1	0	1	-	-	2	6629
1	1	1	0	-	-	3	6630
1	1	1	1	-	-	4	6631

Table 3.3

SEM Bias Level Control Command Assignment

Bias	Level	Control	Bits	Bias Level	SCATHA COMMAND DESIGNATION
8	4	2	1		
0	0	0	0	1 (Lowest)	6648
0	0	0	1	2	6633
0	0	1	0	3	6634
0	0	1	1	4	6635
0	1	0	0	5	6636
0	1	0	1	6	6637
0	1	1	0	7	6638
0	1	1	1	8	6639
1	0	0	0	9	6640
1	0	0	1	10	6641
1	0	1	0	11	6642
1	0	1	1	12	6643
1	1	0	0	13	6644
1	1	0	1	14	6645
1	1	1	0	15	6646
1	1	1	1	16 (Highest)	6647
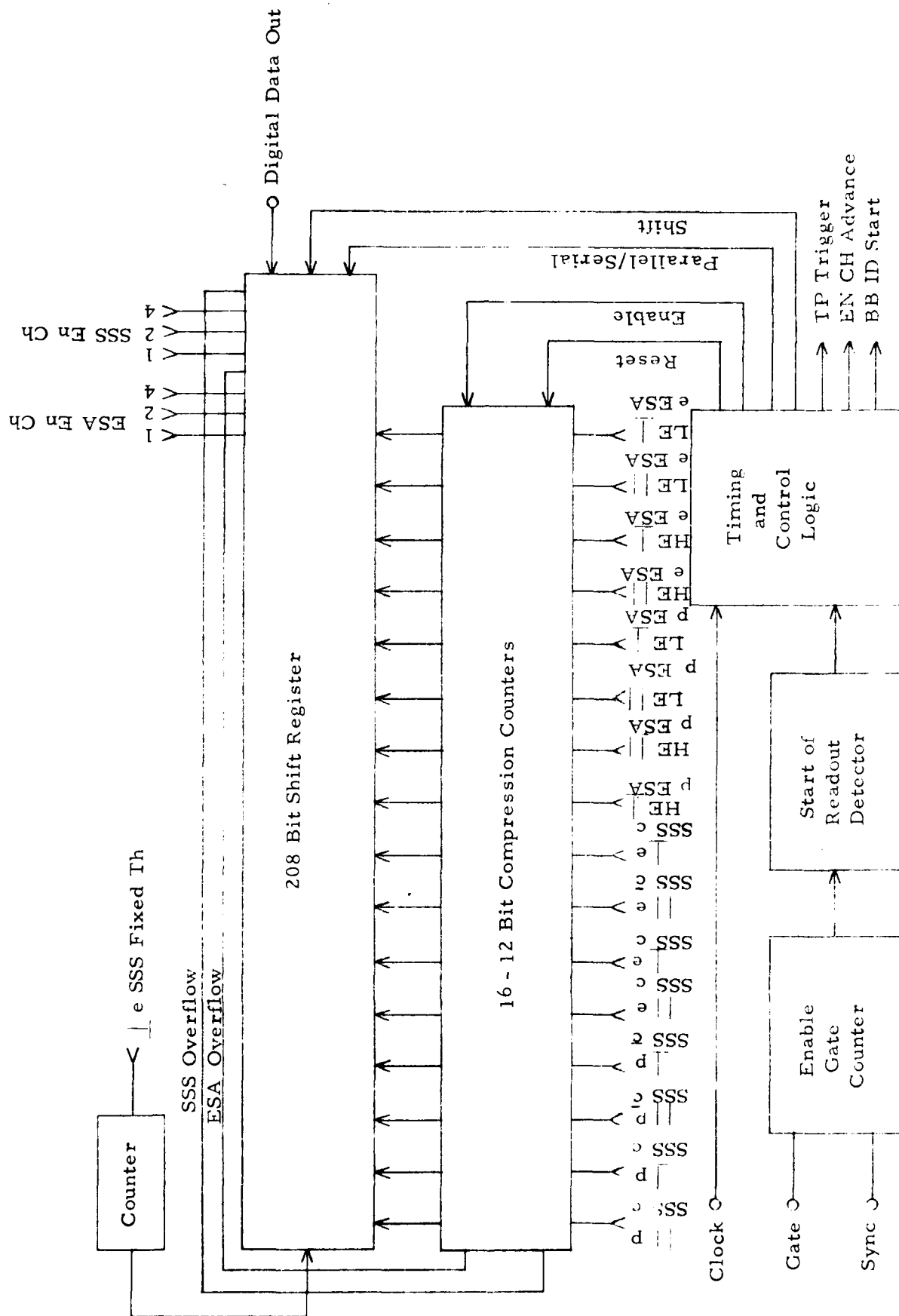
Figure 3.6 Digital Data Circuitry Block Diagram.

31

1)	Main Frame ∅	, Words	18 - 20
2)	Main Frame 1	, Words	95 - 97
3)	Main Frame 3	, Words	44 - 46
4)	Main Frame 4	, Words	121 - 123
5)	Main Frame 6	, Words	70 - 72

The 1 Hz SYNC signal assures that the RSPD's 5 readouts per second are folded into the spacecraft's 8 main frames per second, as shown in Table 3.4. The resulting bit locations for the first 20 bits of the data stream are shown in Table 3.5. Since 3 of the instrument's 5 readouts per second are actually 208 bits long, an additional 8 bits of data, the ⊥ e SSS fixed threshold count, is added onto the end of each 200 bit data set, but these bits are actually read only on those readouts which consist of 208 bits.

Details of the data accumulation and transfer timing are shown in Figure 3.7. Note that the digital data is serially transferred on the rising edges of the clock pulses - data is read by the spacecraft 1/2 bit time later on the falling edges of the clock pulses.

Table 3.4

Digital Data Readout Locations

RSPD Readout #	Main Frame #	Satellite Word #s	Readout # of Words	Length # of Bits
1	0	18-20, 44-46, 70-72, 95-97, 121-123	25	200
	1	15, 18-20, 44-46, 70-72		
2	1	95-97, 121-123	26	208
	2	15, 18-20, 44-46, 70-72, 95-97, 121-123		
	3	15, 18-20		
3	3	44-46, 70-72, 95-97, 121-123	25	200
	4	15, 18-20, 44-46, 70-72, 95-97		
4	4	121-123	26	208
	5	15, 18-20, 44-46, 70-72, 95-97, 121-123		
	6	15, 18-20, 44-46		
5	6	70-72, 95-97, 121-123	26	208
	7	15, 18-20, 44-46, 70-72, 95-97, 121-123		
	0	15		

Table 3.5

Digital Data Bit Assignment and Location (Bits 1-20 Only)

Bit #	Bit Assignment	1st Readout			2nd Readout			3rd Readout			4th Readout			5th Readout		
		Frame #	Word #	Bit #	Frame #	Word #	Bit #	Frame #	Word #	Bit #	Frame #	Word #	Bit #	Frame #	Word #	Bit #
1	SSS Overflow Flag	Ø	18	1	1	95	1	3	44	1	4	121	1	6	70	1
2	SSS Energy Channel 4			2			2			2			2			2
3	2			3			3			3			3			3
4	1			4			4			4			4			4
5	ESA Overflow Flag			5			5			5			5			5
6	ESA Energy Channel 4			6			6			6			6			6
7	2			7			7			7			7			7
8	1			8			8			8			8			8
9	LE ⊥ e ESA - Exponent 8		19	1		96	1		45	1		122	1		71	1
10	4			2			2			2			2			2
11	2			3			3			3			3			3
12	1			4			4			4			4			4
13	- Mantissa 80			5			5			5			5			5
14	40			6			6			6			6			6
15	20			7			7			7			7			7
16	10			8			8			8			8			8
17	8		20	1		97	1		46	1		123	1		72	1
18	4			2			2			2			2			2
19	2			3			3			3			3			3
20	1			4			4			4			4			4

33

Main Frame ∅ Words 18-20
 " " 1 " 95-97
 " " 3 " 44-46
 " " 4 " 121-123
 " " 6 " 70-72

Enable Gates

All Other
Enable Gates

1 Hz Sync
Enable Gate

Gated Clock

Parallel/Serial Control
Counter Enable

Parallel Transfer

Counter Reset
Shift

Reset Enable Gate Counter
Inhibit Counters
Parallel Transfer, Reset Counters
Enable Counters
Serial Shifts

Figure 3.7 Digital Data Timing Diagram

A block diagram of a single compression counter and its associated shift register is shown in Figure 3.8. Since all counters are initially reset to zero, the prescaler divides by 1. After 512 (2^9) input counts the mantissa overflows, and the exponent becomes 1, causing the prescaler to divide by 2. An additional prescaling stage is inserted each time the exponent is incremented. This yields an output of:

$$ n = \left[512(2^E - 1) + 2^E m \right]_{-0}^{+2^E - 1} $$

where n is the number of input counts, m is the mantissa, and E is the exponent. A 9 bit mantissa combined with a 3 bit exponent allows the accumulation of more than 1.3×10^5 counts. A flag bit is set if the counter should overflow - all ESA overflow flags are ORed as are all SSS overflow flags for inclusion in the 8 bit status word at the beginning of each readout.

The digital data circuitry and the magnitude command circuitry discussed in Section 3.7 are contained on the same plug-in printed circuit board.

3.5 Broadband Data Multiplexer and Signal Processor

A block diagram of this subsystem is shown in Figure 3.9. The 8 pulse outputs from the ESAs, the 8 pulse outputs from the SSSs, and the 2 fixed threshold pulse outputs from the e SSSs are applied to the inputs of a digital multiplexer. One of these inputs, as selected by the timing and control logic, is directed to the input of the signal processor.

The signal processor is a high time resolution digital count ratemeter, controlled by an internal clock (≈ 125 kHz), as shown in Figure 3.10 - the processor timing diagram. The selected input counts are accumulated in a 5 bit compression counter (3 bit mantissa plus 2 bit exponent) while the EN-ABLE line is high (≈ 242 μsec). The counter contents are then strobed into a 5 bit latch; the counter is reset, and the next accumulation interval started. The contents of the 5 bit latch are applied to a D to A converter yielding the output voltage versus input count characteristic shown in Table 3.6. This arrangement assures the resolution of single counts at low rates while still providing adequate accuracy at higher count rates. The use of a 5 bit compression counter and a ≈ 242 μsec accumulation time provides for satisfactory operation up to count rates of 500 kHz.

The output of the signal processor along with the UV photodiode signal and the ID generator output are fed to an analog multiplexer. One of these inputs, again selected by the timing and control logic, is fed through a unity gain buffer amplifier to the satellite PAM signal processing circuitry.

The Broadband Data channel assignment is controlled by 6 bits from the magnitude command circuitry. These 6 bits are applied to the timing and control logic allowing 64 possible assignment modes of which 45 are subcommutated. The 64 assignments modes are shown in Table 3.7, along with the designation of the SCATHA satellite commands which establish the various
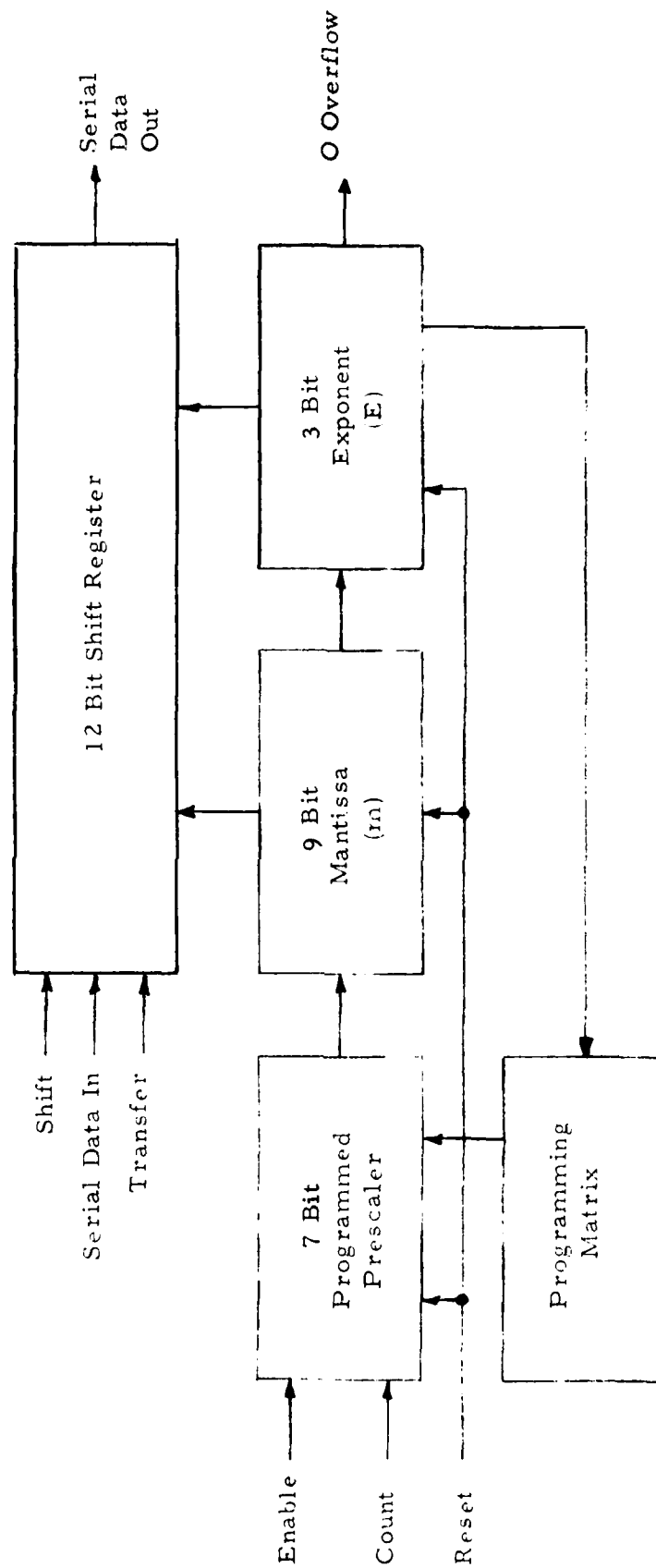
Figure 3.8 Compression Counter Block Diagram
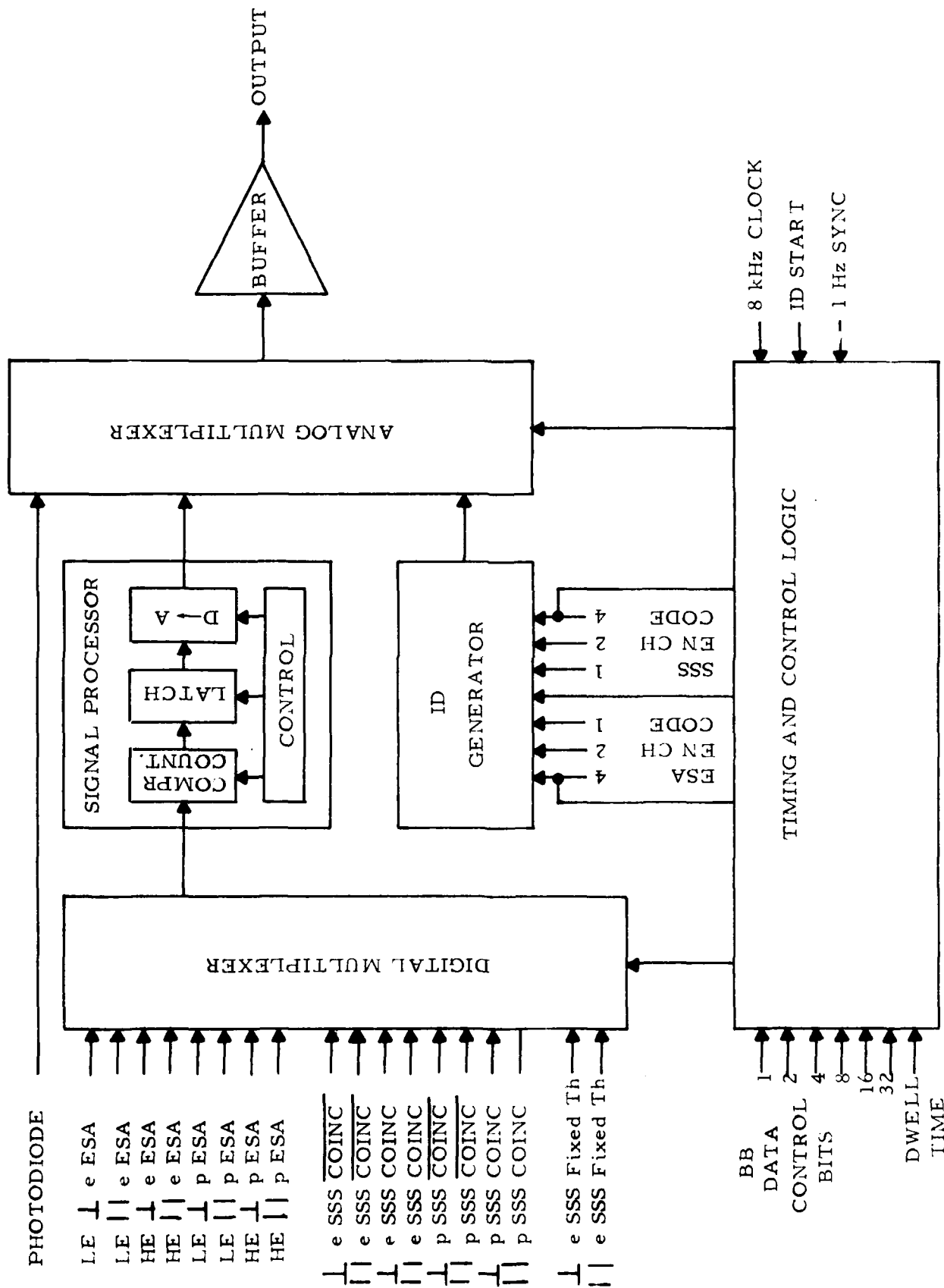
Figure 3.9 Broadband Data Multiplexer and Signal Processor Block Diagram
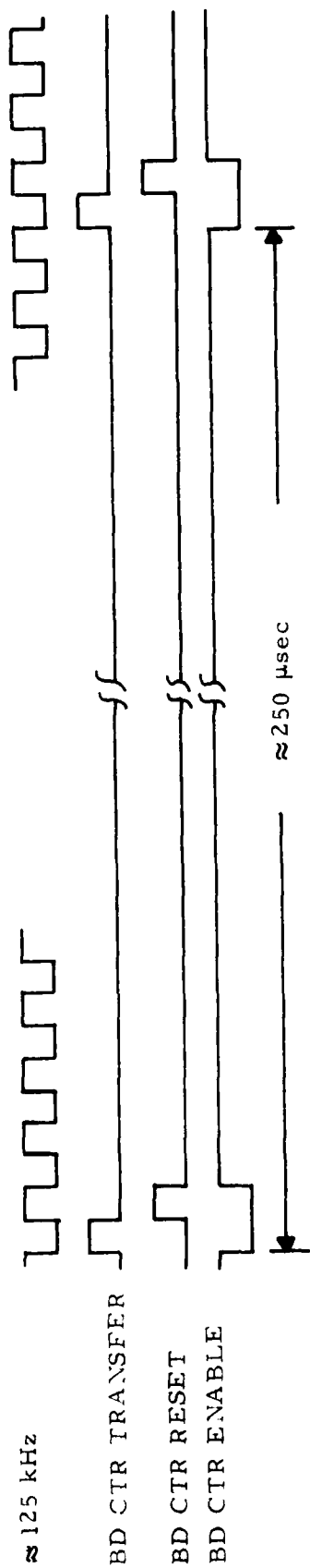
Figure 3.10 Broadband Data Signal Processor Timing Diagram
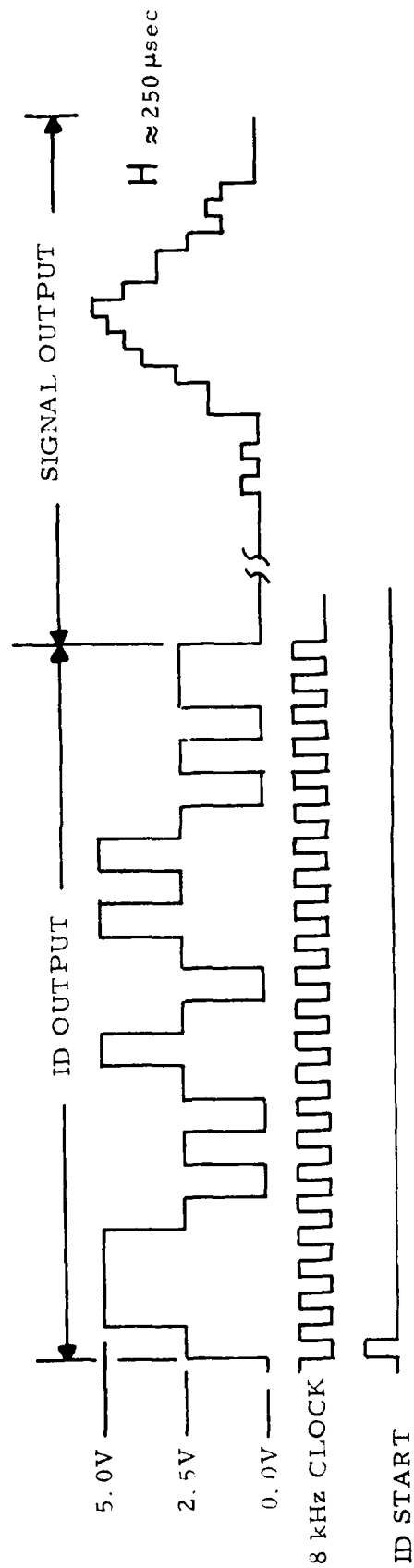
Figure 3.11 Typical Broadband Data Output.

Table 3.6

Broadband Data Output Voltage Level vs Input Counts

Input Counts	Counter State		Nominal Output V
	Exponent	Mantissa	
0	00	000	0.000
1	00	001	0.161
2	00	010	0.323
3	00	011	0.484
4	00	100	0.645
5	00	101	0.806
6	00	110	0.968
7	00	111	1.129
8,9	01	000	1.290
10,11	01	001	1.452
12,13	01	010	1.613
14,15	01	011	1.774
16,17	01	100	1.935
18,19	01	101	2.097
20,21	01	110	2.258
22,23	01	111	2.419
24-27	10	000	2.581
28-31	10	001	2.742
32-35	10	010	2.903
36-39	10	011	3.065
40-43	10	100	3.226
44-47	10	101	3.387
48-51	10	110	3.548
52-55	10	111	3.710
56-63	11	000	3.871
64-71	11	001	4.032
72-79	11	010	4.193
80-87	11	011	4.355
88-95	11	100	4.516
96-103	11	101	4.677
104-111	11	110	4.839
112-119	11	111	5.000

Table 3.7

Broadband Data Control Command Assignments

Control Bits						Channel Assignments		SCATHA COMMAND DESIGNATION
32	16	8	4	2	1			
0	0	0	0	0	0	Subcomm mode	1	6712
0	0	0	0	0	1	Photodiode		6649
0	0	0	0	1	0	Subcomm mode	2	6650
0	0	0	0	1	1		3	6651
0	0	0	1	0	0		4	6652
0	0	0	1	0	1		5	6653
0	0	0	1	1	0		6	6654
0	0	0	1	1	1		7	6655
0	0	1	0	0	0		8	6656
0	0	1	0	0	1		9	6657
0	0	1	0	1	0		10	6658
0	0	1	0	1	1		11	6659
0	0	1	1	0	0		12	6660
0	0	1	1	0	1		13	6661
0	0	1	1	1	0		14	6662
0	0	1	1	1	1		15	6663
0	1	0	0	0	0		16	6664
0	1	0	0	0	1	⊥ e SSS fixed threshold		6665
0	1	0	0	1	0	Subcomm mode	17	6666
0	1	0	0	1	1		18	6667
0	1	0	1	0	0		19	6668
0	1	0	1	0	1		20	6669
0	1	0	1	1	0		21	6670
0	1	0	1	1	1		22	6671
0	1	1	0	0	0		23	6672
0	1	1	0	0	1		24	6673
0	1	1	0	1	0		25	6674
0	1	1	0	1	1		26	6675
0	1	1	1	0	0		27	6676
0	1	1	1	0	1		28	6677
0	1	1	1	1	0		29	6678
0	1	1	1	1	1		30	6679
1	0	0	0	0	0		31	6680
1	0	0	0	0	1		32	6681
1	0	0	0	1	0	‖ e SSS fixed threshold		6682
1	0	0	0	1	1	Subcomm mode	33	6683
1	0	0	1	0	0		34	6684
1	0	0	1	0	1		35	6685
1	0	0	1	1	0		36	6686

Table 3.7 (cont'd)

						Type	Sym	e/p	Code	c	Index	Number
1	0	0	1	1	1						37	6687
1	0	1	0	0	0						38	6688
1	0	1	0	0	1						39	6689
1	0	1	0	1	0						40	6690
1	0	1	0	1	1						41	6691
1	0	1	1	0	0						42	6692
1	0	1	1	0	1						43	6693
1	0	1	1	1	0						44	6694
1	0	1	1	1	1						45	6695
1	1	0	0	0	0	LE	⊥	e	ESA			6696
1	1	0	0	0	1	LE	||	e	ESA			6697
1	1	0	0	1	0	HE	⊥	e	ESA			6698
1	1	0	0	1	1	HE	||	e	ESA			6699
1	1	0	1	0	0	LE	⊥	p	ESA			6700
1	1	0	1	0	1	LE	||	p	ESA			6701
1	1	0	1	1	0	HE	⊥	p	ESA			6702
1	1	0	1	1	1	HE	||	p	ESA			6703
1	1	1	0	0	0		⊥	e	SSS	c̄		6704
1	1	1	0	0	1		||	e	SSS	c̄		6705
1	1	1	0	1	0		⊥	e	SSS	c		6706
1	1	1	0	1	1		||	e	SSS	c		6707
1	1	1	1	0	0		⊥	p	SSS	c̄		6708
1	1	1	1	0	1		||	p	SSS	c̄		6709
1	1	1	1	1	0		⊥	p	SSS	c		6710
1	1	1	1	1	1		||	p	SSS	c		6711

assignments. The 45 subcommutated modes are delineated in Table 3.8. An additional magnitude command bit is used to select the subcommutated modes dwell time which can be either 1 or 8 complete energy sweeps if the selected unit is sweeping, or 0.2 sec or 102.4 sec if the selected unit is not sweeping. The switch to the next unit is initiated as the energy channel goes from 4 to 0 or at the beginning of a digital data accumulation interval.

The Broadband Data channel assignment and the energy channel of the unit to which it is assigned are specified by an 8 bit ID word which is generated every 200 msec - at the beginning of each data accumulation period. The ID word format is given in Table 3.9, and a typical broadband data output is shown in Figure 3.11. Note that each ID word is preceded by a 5.0 volt synchronization level and that a pseudo RZ format is used wherein the output goes to 2.5 volts between data bits. These two levels plus a zero volt logic output level (assuming at least one ID bit is zero) give a 3-point calibration of the entire BB data processing system.

The entire BB data multiplexer and signal processor is contained on a single plug-in printed circuit board.

3.6 ESA Power Control Circuitry

The ESA power control circuitry automatically turns off the Spiraltron electron multiplier bias and ESA deflection plate voltages during periods of UV or electron flux which exceed preset levels considered to be detrimental to the SEMs. A block diagram of this subsystem is shown in Figure 3.12.

A UV photodiode, with a field of view encompassing that of the $\perp$ e ESA, initiates an ESA shutdown when its output exceeds a prefixed threshold level corresponding to ≈50% of the level when looking directly at the sun. The e SSS fixed threshold pulse outputs are accumulated in 17 bit binary counters, while the e ESA pulse outputs are accumulated in 13 bit binary counters. An ESA shutdown is initiated if any of these counters overflows during a 200 msec data accumulation interval (this corresponds to a count rate in excess of 300 kHz for the SSSs or 20 kHz for the ESAs). If the shutdown is initiated by a SSS, power will remain off for approximately 1 second following the last 200 msec data accumulation interval during which an overflow occurs. If the shutdown is initiated by an ESA, power remains off for approximately 30 seconds (≈1/2 spacecraft revolution). These turn on delays prevent the power from cycling on and off (which might be detrimental to the SEMs and high voltage power supply) should the flux level quickly cycle above and below the threshold levels.

The ESA power control circuitry is enabled by ground command, via 2 magnitude command bits. One bit is used to enable ESA initiated shutdown, while the second bit is used to enable UV photodiode or SSS initiated shutdown.

The ESA power control circuitry is contained on a single plug-in printed circuit board along with the analog monitors discussed in Section 3.8.

Table 3.8A

Broadband Data Subcommutated Mode Frame Assignment

(Subcomm Mode 1)

Subcomm Mode	Frame #							
	1	2	3	4	5	6	7	8
1	LE ⊥ e ESA	LE ‖ e ESA	HE ⊥ e ESA	HE ‖ e ESA	LE ⊥ p ESA	LE ‖ p ESA	HE ⊥ p ESA	HE ‖ p ESA

Subcomm Mode	Frame #							
	9	10	11	12	13	14	15	16
1	⊥ e SSS c̄	‖ e SSS c̄	⊥ e SSS c	‖ e SSS c	⊥ p SSS c̄	‖ p SSS c̄	⊥ p SSS c	‖ p SSS c

43

Table 3.8B

(Subcomm modes 2-23)

Frame #

Subcomm. Mode	1	2	3	4	5	6	7	8
2	LE ⊥ e ESA	HE ⊥ e ESA	LE ⊥ p ESA	HE ⊥ p ESA	⊥ e SSS c	⊥ e SSS c	⊥ p SSS c	⊥ p SSS c
3	LE ‖ e ESA	HE ‖ e ESA	LE ‖ p ESA	HE ‖ p ESA	‖ e SSS c	‖ e SSS c	‖ p SSS c	‖ p SSS c
4	LE ⊥ e ESA	HE ‖ e ESA	HE ⊥ e ESA	HE ‖ e ESA	⊥ e SSS c	‖ e SSS c	⊥ e SSS c	‖ e SSS c
5	LE ⊥ p ESA	LE ‖ p ESA	HE ⊥ p ESA	HE ‖ p ESA	⊥ p SSS c	‖ p SSS c	⊥ p SSS c	‖ p SSS c
6	LE ⊥ e ESA	LE ‖ e ESA	LE ⊥ p ESA	LE ‖ p ESA	⊥ e SSS c	‖ e SSS c	⊥ p SSS c	‖ p SSS c
7	HE ⊥ e ESA	HE ‖ e ESA	HE ⊥ p ESA	HE ‖ p ESA				
8	LE ⊥ e ESA	HE ⊥ e ESA	⊥ e SSS c	⊥ e SSS c				
9	LE ‖ e ESA	HE ‖ e ESA	‖ e SSS c	‖ e SSS c				
10	LE ⊥ p ESA	HE ⊥ p ESA	⊥ p SSS c	⊥ p SSS c				
11	LE ‖ p ESA	HE ‖ p ESA	‖ p SSS c	‖ p SSS c				
12	LE ⊥ p ESA	LE ⊥ p ESA	⊥ e SSS c	⊥ p SSS c				
13	LE ‖ e ESA	LE ‖ p ESA	‖ e SSS c	‖ p SSS c				
14	HE ‖ p ESA	HE ‖ p ESA	⊥ e SSS c	⊥ p SSS c				
15	HE ‖ p ESA	HE ‖ p ESA	‖ e SSS c	‖ p SSS c				
16	LE ⊥ e ESA	LE ‖ e ESA	HE ⊥ e ESA	HE ‖ e ESA	LE ⊥ p ESA	LE ‖ p ESA	HE ⊥ p ESA	HE ‖ p ESA
17	LE ⊥ e ESA	HE ⊥ e ESA	LE ⊥ p ESA	HE ⊥ p ESA				
18	LE ‖ e ESA	HE ‖ e ESA	LE ‖ p ESA	HE ‖ p ESA				
19	LE ⊥ e ESA	LE ‖ e ESA	HE ⊥ e ESA	HE ‖ e ESA				
20	LE ⊥ p ESA	LE ‖ p ESA	HE ⊥ p ESA	HE ‖ p ESA				
21	LE ⊥ e ESA	LE ‖ e ESA	LE ⊥ p ESA	LE ‖ p ESA				
22	HE ⊥ e ESA	HE ‖ e ESA	HE ⊥ p ESA	HE ‖ p ESA				
23	LE ⊥ e ESA	HE ⊥ e ESA						

44

Table 3.8C

(Subcomm modes 24-45)

Frame #

Subcomm Mode	1	2	3	4	5	6	7	8
24	LE || e ESA	HE || e ESA						
25	LE ⊥ p ESA	HE ⊥ p ESA						
26	LE || p ESA	HE || p ESA						
27	LE ⊥ e ESA	LE ⊥ p ESA						
28	LE ||| e ESA	LE || e ESA						
29	HE ⊥ p ESA	HE ⊥ p ESA						
30	HE ||| p ESA	HE || p ESA						
31	⊥ e SSS c̄	|| e SSS c̄	⊥ e SSS c	|| e SSS c	⊥ p SSS c̄	|| p SSS c̄	⊥ p SSS c̄	||| p SSS c
32	⊥ e SSS c̄	⊥ e SSS c	⊥ p SSS c̄	⊥ p SSS c				
33	|| e SSS c̄	|| e SSS c	⊥ p SSS c̄	|| p SSS c				
34	⊥ e SSS c̄	|| e SSS c	⊥ e SSS c	|| e SSS c				
35	⊥ p SSS c̄	|| p SSS c	⊥ p SSS c̄	|| p SSS c				
36	⊥ e SSS c	|| e SSS c	⊥ p SSS c̄	|| p SSS c̄				
37	⊥ e SSS c̄	|| e SSS c	⊥ p SSS c	|| p SSS c				
38	⊥ e SSS c	|| e SSS c						
39	|| e SSS c̄	|| e SSS c						
40	⊥ p SSS c̄	⊥ p SSS c						
41	|| p SSS c̄	⊥ p SSS c						
42	|| e SSS c̄	|| p SSS c						
43	|| e SSS c̄	⊥ p SSS c						
44	⊥ e SSS c	⊥ p SSS c						
45	|| e SSS c	|| p SSS c						

45
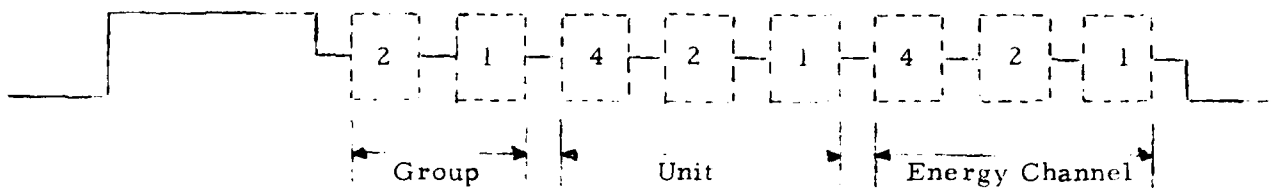
Table 3.9 - Broadband Data Identification Code Format

|	Broadband Data Identification Code Assignments				
Unit	Identification Code				
	Octal	Binary			
LE e ESA	00X	00	000	XXX	
LE e ESA	01X	00	001	XXX	
HE e ESA	02X	00	010	XXX	
HE e ESA	03X	00	011	XXX	
LE p ESA	04X	00	100	XXX	
LE p ESA	05X	00	101	XXX	
HE p ESA	06X	00	110	XXX	
HE p ESA	07X	00	111	XXX	
⊥ e SSS c̃	10X	01	000	XXX	
‖ e SSS c̃	11X	01	001	XXX	
⊥ e SSS c	12X	01	010	XXX	
‖ e SSS c̃	13X	01	011	XXX	
⊥ p SSS c̃	14X	01	100	XXX	
‖ p SSS c̃	15X	01	101	XXX	
⊥ p SSS c	16X	01	110	XXX	
‖ p SSS c	17X	01	111	XXX	
⊥ e SSS Th	24X or 26X	10	1X0	XXX	
‖ e SSS Th	34X or 36X	11	1X0	XXX	
Photodiode	25X or 27X or 35X or 37X	1X	1X1	XXX	
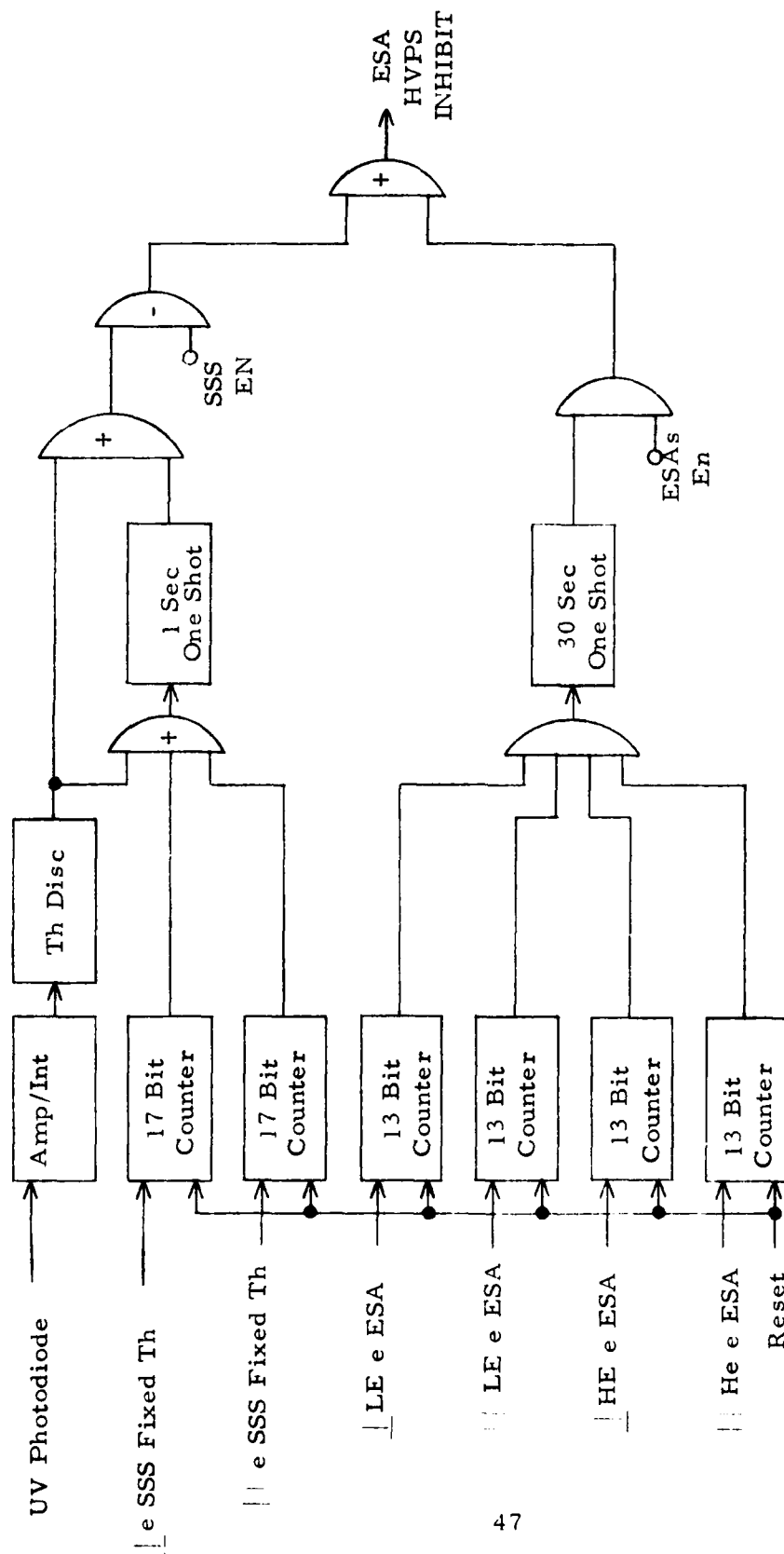
Figure 3.12. ESA Power Control Circuitry Block Diagram.

47

3.7 Magnitude Command Processor

A block diagram of the magnitude command interface circuitry is shown in Figure 3.13. This circuitry converts the 22 bit serial command received from the spacecraft into the parallel format required by the various instrument subsystems. The 22 bits are utilized as follows:

4 bits	-	ESA energy channel control
4 bits	-	SSS energy channel control
4 bits	-	SEM bias voltage control
6 bits	-	Broadband data channel assignment
1 bit	-	Broadband data subcomm dwell time
2 bits	-	ESA auto shutoff circuitry control

21

The remaining bit is used as a reset control bit. The control logic is such that a latch:

1) is updated if any of its data bits are set and the reset bit is not set

2) is cleared if any of its data bits are set and the reset bit is set

3) remains unchanged if all of its data bits are zero.

This scheme allows completely independent control of the various logical bit groups - the ESA energy channel control bits may be changed without affecting the SSS energy channel control bits, or any of the other control bits. This scheme also allows for simultaneous updating of 2 or more groups of control bits - the SSS and ESA energy channel control bits may be changed with a single magnitude command.

The magnitude command timing diagram is shown in Figure 3.14. The GATE, CLOCK, and DATA lines are supplied by the spacecraft. The data bits are presented on the DATA line 1/4 bit time following the leading (falling) edge of the CLOCK pulses and are serially transferred within the RSPD 1/4 bit time after that on the rising edge of the CLOCK pulses. The parallel transfer and latching takes place during the 1/4 bit time following the falling edge of the last (22nd) CLOCK pulse.

As mentioned previously, this circuitry is contained on the same plug-in printed circuit board as the digital data circuitry.

3.8 DC to DC Converter and Analog Monitors

This subsystem contains all DC to DC converters and high voltage power supplies necessary to generate the required instrument operating voltages, as listed in Table 3.10, as well as all analog voltage and temperature monitors necessary to ascertain proper instrument performance, as shown in Table 3.11.

The instrument operating voltages are divided into three groups, each of which can be turned on independently by real-time ground command. The
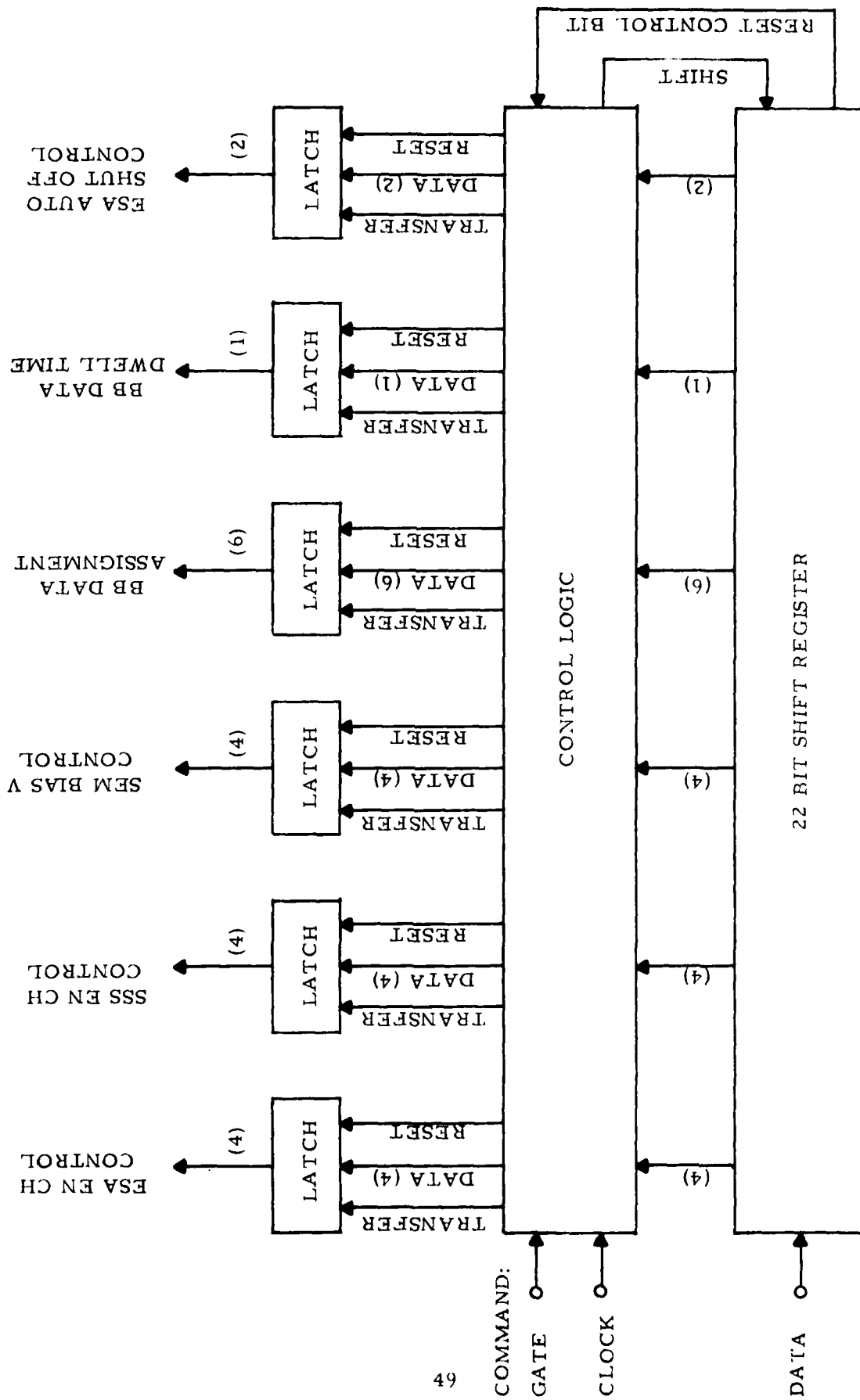
48

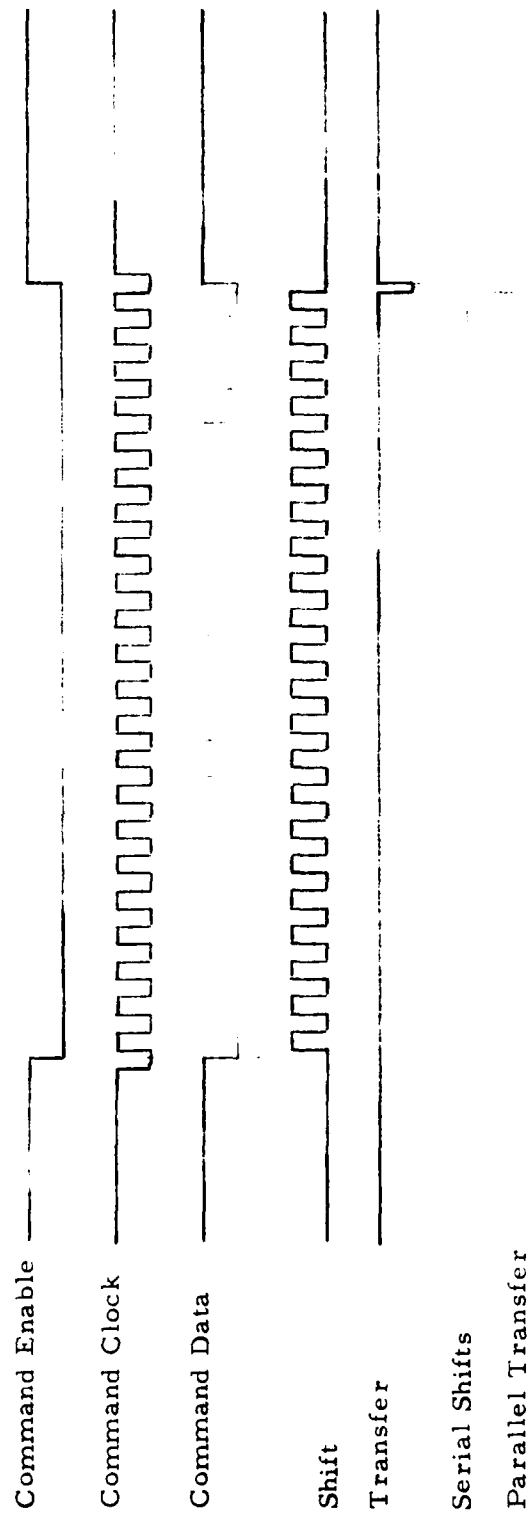Figure 3.13 Magnitude Command Circuitry Block Diagram

49

Command Enable

Command Clock

Command Data

Shift

Transfer

Serial Shifts

Parallel Transfer

Figure 3.14   Magnitude Command Timing Diagram

50

Table 3.10

Required Instrument Operating Voltages

Voltage	Group	Utilization
Sweep V A (5-100V)	A	Low Energy ESA Deflection
Sweep V B (150-3000V)	A	High Energy ESA Deflection
+3500V (nominal)	A	e ESA SEM Bias
+500V	A	e ESA SEM Bias
+2500V (nominal)	A	p ESA SEM Bias
-500V	A	p ESA SEM Bias
-30V	A	e ESA Secondary Suppression Grid
e SSD Bias V (≈+100V)	B	e SSD Detector Bias
+15V	C	Electronics Circuitry Operating Voltages
+10V	C	
-5V	C	
-10V	C	

Table 3.11

Analog Monitors

#	Function Monitored	MMC Designation	SCF Designation
1	+3500V (nominal	E4001	53500 V
2	+500V	E4002	5 + 500 V
3	+2500V (nominal)	E4003	52500 V
4	-500V	E4004	5 - 500 V
5	-30V	E4005	5 - 30 V
6	e SSD Bias V	E4006	5 ESB V
7	+15V	E4007	5 + 15 V
8	+10V	E4008	5 + 10 V
9	-5V	E4009	5 - 5 V
10	-10V	E4010	5 - 10 V
11	High Energy ESA Deflection V	E4011	5 HES V
12	Low Energy ESA Deflection V	E4012	5 LES V
13	$\perp$ p SSD Bias V	E4013	5 PER V
14	$\parallel$ p SSD Bias V	E4014	5 PAR V
15	DC to DC Converter Temp	E4015	5 CNV T
16	$\perp$ SSS Temp	E4016	5 PEST
17	$\parallel$ SSS Temp	E4017	5 PAST

first group (A) contains all of the ESA deflection and bias voltages and is controlled by the ESA power control circuitry as discussed in Section 3.6. Group B contains the solid state detector bias voltages, while group C contains all of the electronic circuitry operating voltages which are utilized by both the SSSs and ESAs. This scheme offers essentially independent control of the SSS and ESA portions of the instrument. Thus, should a failure occur in one, the other could still be operated. Separation of the ESA and SSS voltages also allows the ESAs to be shut off at excessively high flux levels while still obtaining SSS data.

As discussed previously, the two ESA sweep voltages are independently programmed by control voltages generated by the energy channel control circuitry, and the actual set of SEM bias voltages is selected from one of 16 possible sets by real-time ground command.

All of the RSPD's operating voltages, as well as three (3) subassembly temperatures, are monitored - as indicated in Table 3.11. The spacecraft integrator, Martin Maritta Corporation (MMC), designation, and the Satellite Control Facility numonic for these monitors are also indicated in that table.

The DC to DC Converter, which was designed and manufactured by SPACETAC Inc. under subcontract to Panametrics, is contained in a 2" x 4.5" x 5" subassembly which is shown in Figure 3.15. As mentioned previously, the analog monitors are contained on the same printed circuit board as the ESA power control circuitry. This board also contains the precision voltage regulator from which all analog control voltages are derived. The proton solid state detector bias voltages, which are also derived from this reference voltage, are generated on this board.
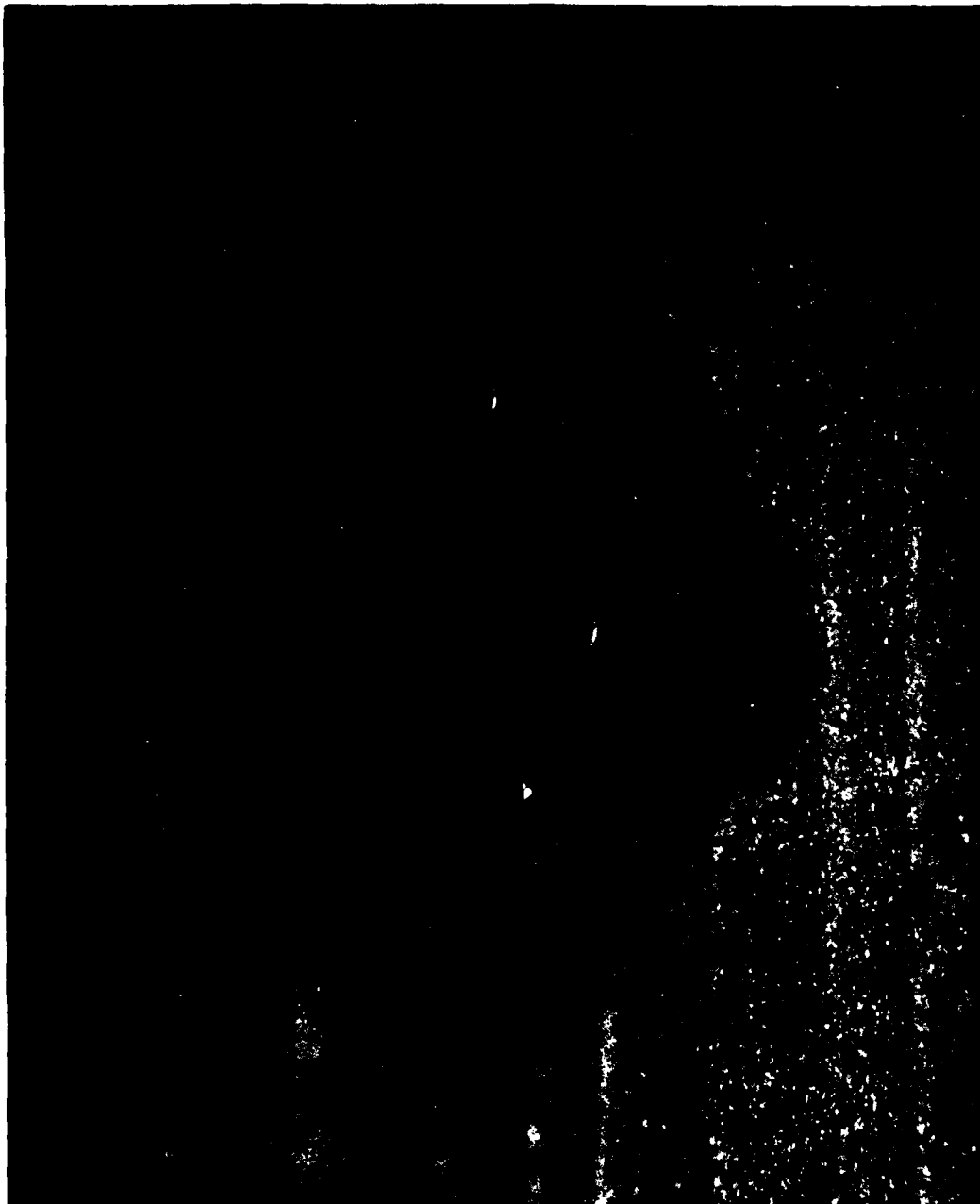
Figure 3.15 DC to DC Converter

4. INTERFACE REQUIREMENTS AND CHARACTERISTICS

The RSPD's interface requirements are detailed in Ref. 4. 1 - the instrument's interface control document which was prepared by the SCATHA satellite integrator Martin Marietta Corporation. The various electrical and mechanical characteristics and requirements are discussed briefly in the following sections.

4. 1 Electrical Interface

The RSPD's electrical interface control drawing is shown in Fig. 4. 1. This not only indicates actual interface pin connections but provides details of all I/O circuit types as well.

As mentioned in Section 3.8, the RSPD requires 3 power control commands. These are actually steady state inputs which are 28 ± 4 volts in the ON state and 0 ± 1 volt in the OFF state. The actual SCATHA satellite designation for these commands is given in Table 4.1 which also lists the single power off command. The actual power requirements for the various operating modes is given in Table 4.2. All of this operating power is provided by the LOW VOLTAGE ON command line, the other two are simply enabling inputs.

Table 4. 1

Power Control Commands	
Command	SCATHA Designation
Low Voltage On	6500
ESA On	6502
SSS On	6504
Power Off	6505

Table 4. 2

Power Requirements	
Mode	Power (watts)*
Low Voltage Only	3. 8
Low Voltage and SSS	4. 0
Low Voltage and ESA	4. 8
Low Voltage, SSS and ESA	5. 0

*The RSPD power requirement is essentially independent of input bus voltage.

55

Figure 4.1. RSPD Electrical Interface Control Drawing
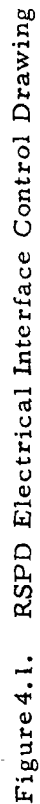
Details of the RSPD's magnitude command interface requirements and utilization has been discussed in the previous sections. SCATHA command designations for the various control bit groups are contained in the following tables:

ESA energy channel control bits - Table 3. 1
SSS energy channel control bits - Table 3. 2
SEM bias voltage control bits - Table 3. 3
BB data assignment bits - Table 3. 7

In addition, several commands have been defined which effect more than one control bit group. These are listed in Table 4. 3, as are the BB data dwell time and ESA power control commands designations.

Details of the RSPD's digital data circuitry and its spacecraft interface were discussed in Section 3. 4. The instrument's 208 bit series output consists of 19 logical bit groupings which are delineated in Table 4. 4. The Martin Marietta Corporation (MMC) designation and the Satellite Control Facility (SCF) numonic for each grouping is also shown.

Details of the RSPD's broadband data circuitry and its spacecraft interface are discussed in Section 3. 5. The actual BB data output circuit configuration is shown in Fig. 4. 1. Active filtering limits the bandwidth of the output signal to 4 kHz.

The RSPD's analog monitors, along with their SCF and MMC designations are listed in Table 3. 11. A typical analog monitor output circuit is shown in Fig. 4. 1. All monitors provide 0 to 5 volt levels to the spacecraft and are protected against over/under voltages.

4. 2 Mechanical Interface

The RSPD's outline drawing is shown in Fig. 4. 2, the Fields of View are better defined in Fig's. 4. 3 and 4. 4. The instrument is mounted on the satellite such that the fields of view are perpendicular and parallel to the spin axis, as shown in Fig. 4. 5.

The RSPD weighs 13. 0 lbs., its calculated moments of inertia are shown in Fig. 4. 2.

4. 3 Thermal Properties

The RSPD is designed to operate over the temperature range of -25° to $+30^\circ C$, with operation at the low end of this range being preferred - to keep the solid state detector noise levels low. Nonoperating, survival temperature limits are -35° to $+55^\circ C$.

Table 4.3

Miscellaneous Magnitude Commands	
Command	SCATHA Designation
Master Reset	6600
ESA and SSS Energy Channel Reset	6719
1 Consec. ESA & SSS Readout/En. Ch.	6720
2 Consec. ESA & SSS Readouts/En. Ch.	6721
4 Consec. ESA & SSS Readouts/En. Ch.	6722
8 Consec. ESA & SSS Readouts/En. Ch.	6723
16 Consec. ESA & SSS Readouts/En. Ch.	6724
32 Consec. ESA & SSS Readouts/En. Ch.	6725
64 Consec. ESA & SSS Readouts/En. Ch.	6726
128 Consec. ESA & SSS Readouts/En. Ch.	6727
256 Consec. ESA & SSS Readouts/En. Ch.	6728
512 Consec. ESA & SSS Readouts/En. Ch.	6729
1024 Consec. ESA & SSS Readouts/En. Ch.	6730
ESA and SSS Energy Channel 0	6731
ESA and SSS Energy Channel 1	6732
ESA and SSS Energy Channel 2	6733
ESA and SSS Energy Channel 3	6734
ESA and SSS Energy Channel 4	6735
Dwell Time A	6714
Dwell Time B	6713
ESA Auto Shutoff, A Enable	6715
ESA Auto Shutoff, B Enable	6716
ESA Auto Shutoff, A & B Enable	6717
ESA Auto Reset Disable	6718

Table 4.4

| Bit Numbers	Contents	MMC Designation	SCF Designation
1-4	SSS Ch # and Overflow Flag	E8001	5SSSEC
5-8	ESA Ch # and Overflow Flag	E8002	5ESAEC
9-20	LE ⌐ e ESA Counter	E4503	5LEPEE
21-32	LE ‖ e ESA Counter	E4504	5LEPAE
33-44	HE ⌐ e ESA Counter	E4505	5HEPEE
45-56	HE ‖ e ESA Counter	E4506	5HEPAE
57-68	LE ⌐ p ESA Counter	E4507	5LEPEP
69-80	LE ‖ p ESA Counter	E4508	5LEPAP
81-92	HE ⌐ p ESA Counter	E4509	5HEPEP
93-104	HE ‖ p ESA Counter	E4510	5HEPAP
105-116	⌐ e SSS Anti-Coincidence Counter	E4511	5PEEAC
117-128	‖ e SSS Anti-Coincidence Counter	E4512	5PAEAC
129-140	⌐ e SSS Coincidence Counter	E4513	5PEEC
141-152	‖ e SSS Coincidence Counter	E4514	5PAEC
153-164	⌐ p SSS Anti-Coincidence Counter	E4515	5PEPAC
165-176	‖ p SSS Anti-Coincidence Counter	E4516	5PAPAC
177-188	⌐ p SSS Coincidence Counter	E4517	5PEPC
189-200	‖ p SSS Coincidence Counter	E4518	5PAPC
201-208	⌐ e SSS Fixed Threshold Counter	E8019	5AUXC
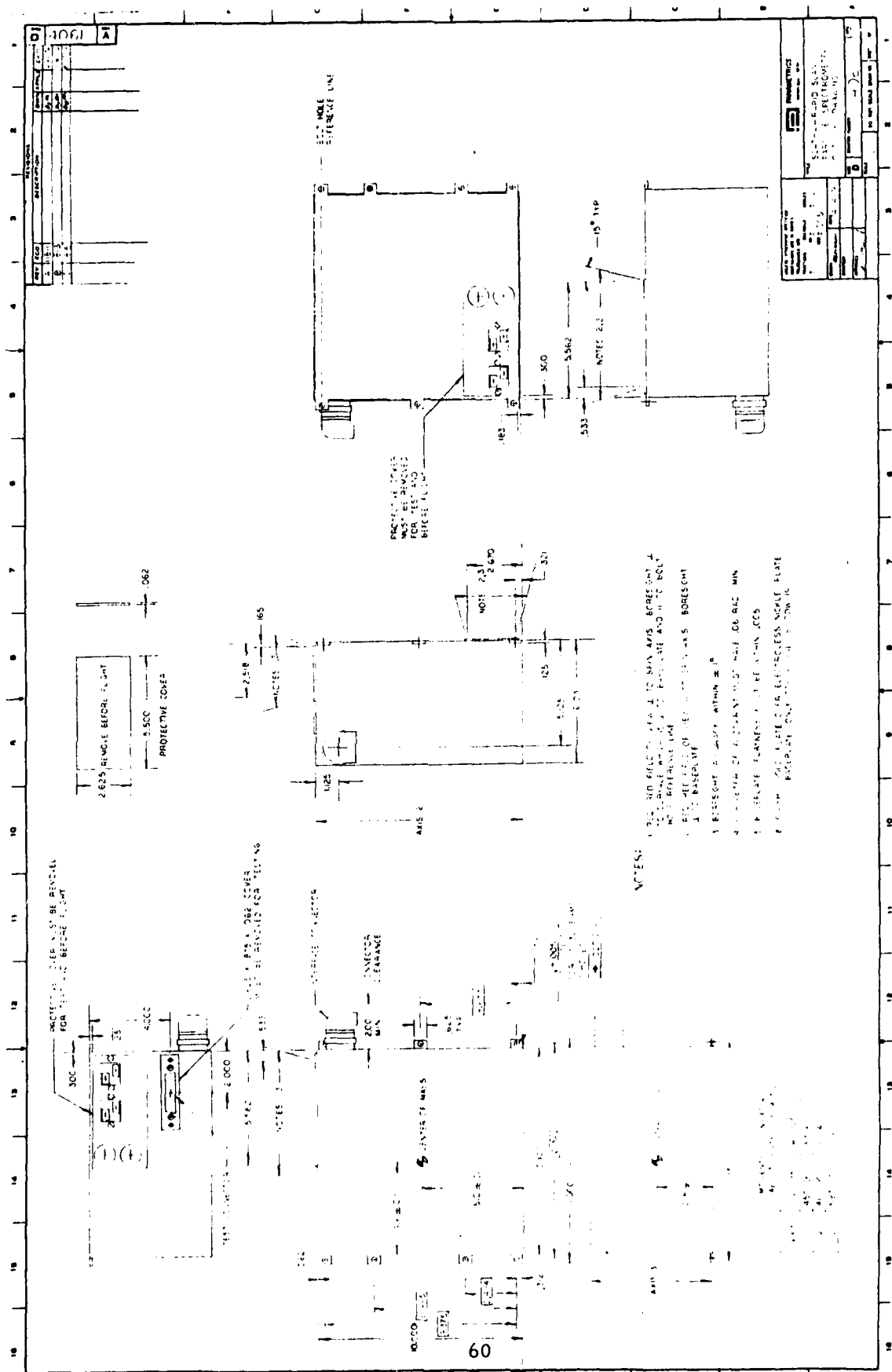
Figure 4.2. Outline Drawing

Figure 4.3. ⊥ Fields of View
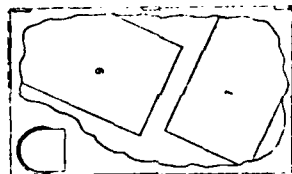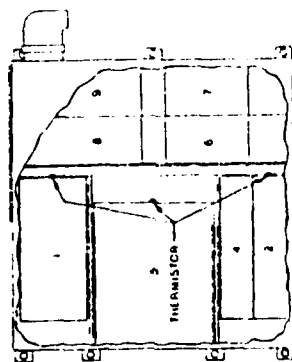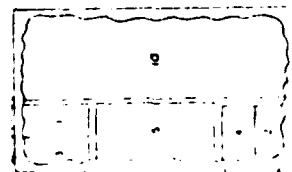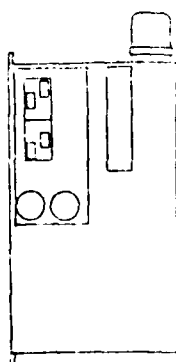
61

Figure 4.4. ‖ Fields of View
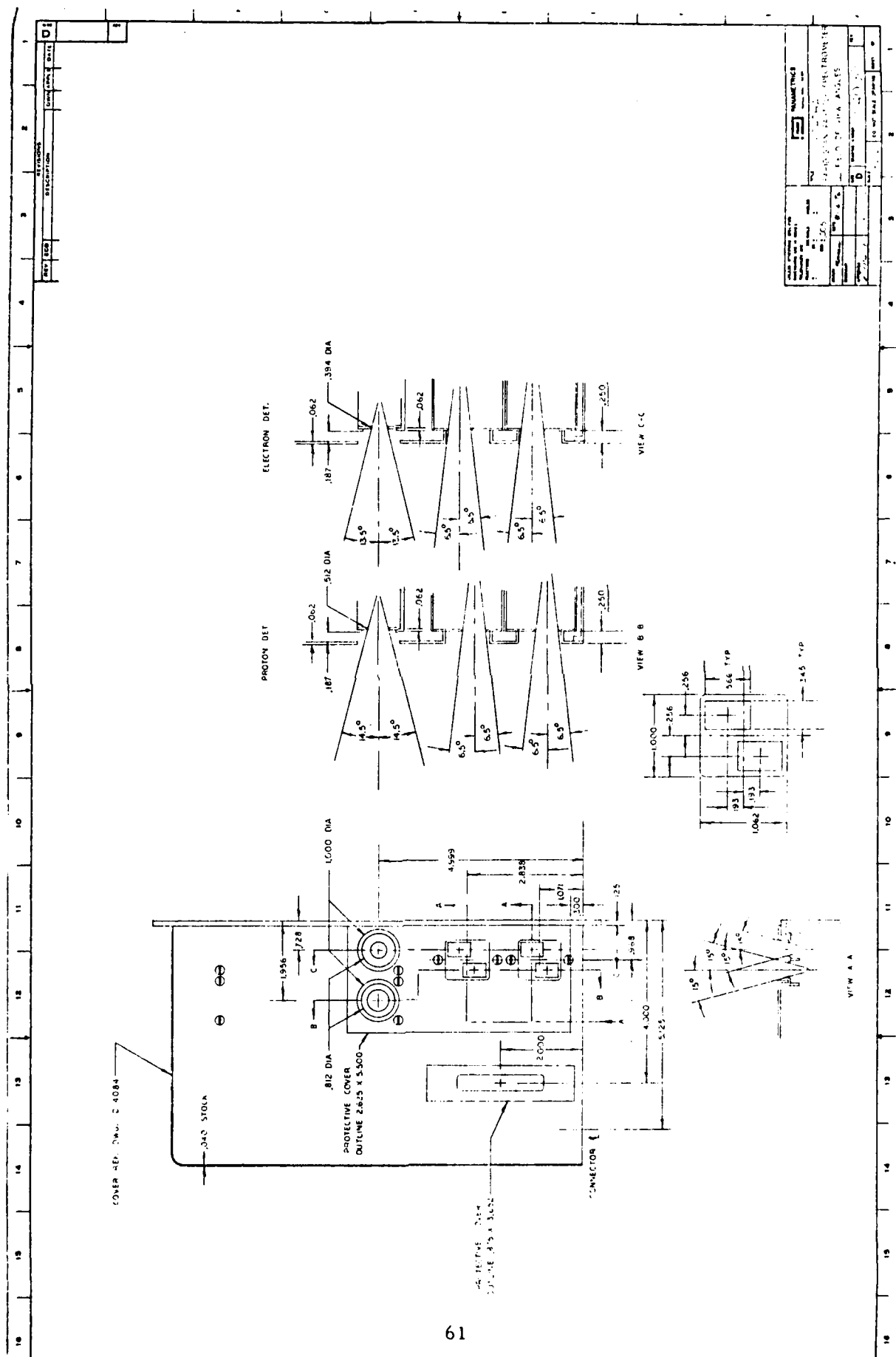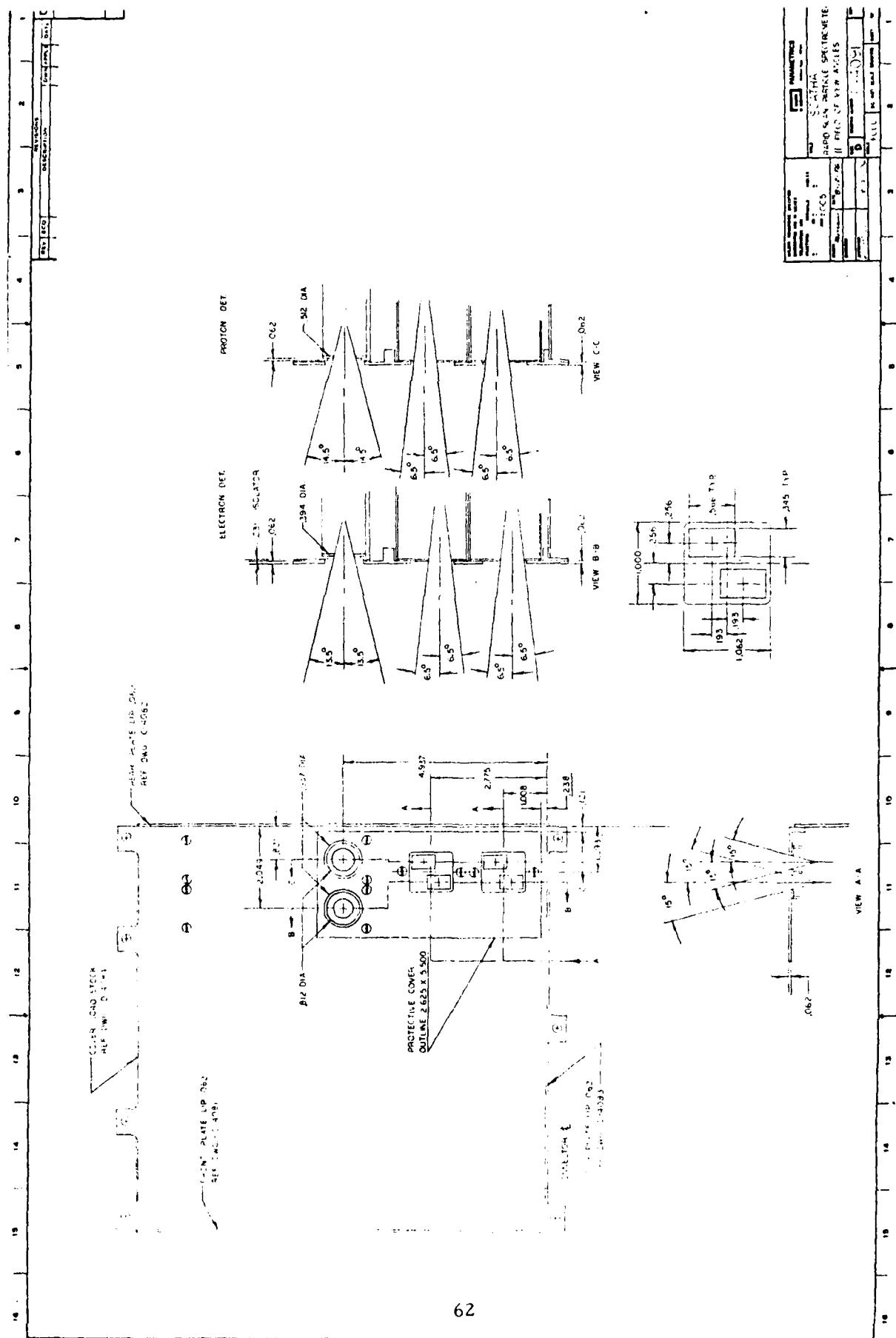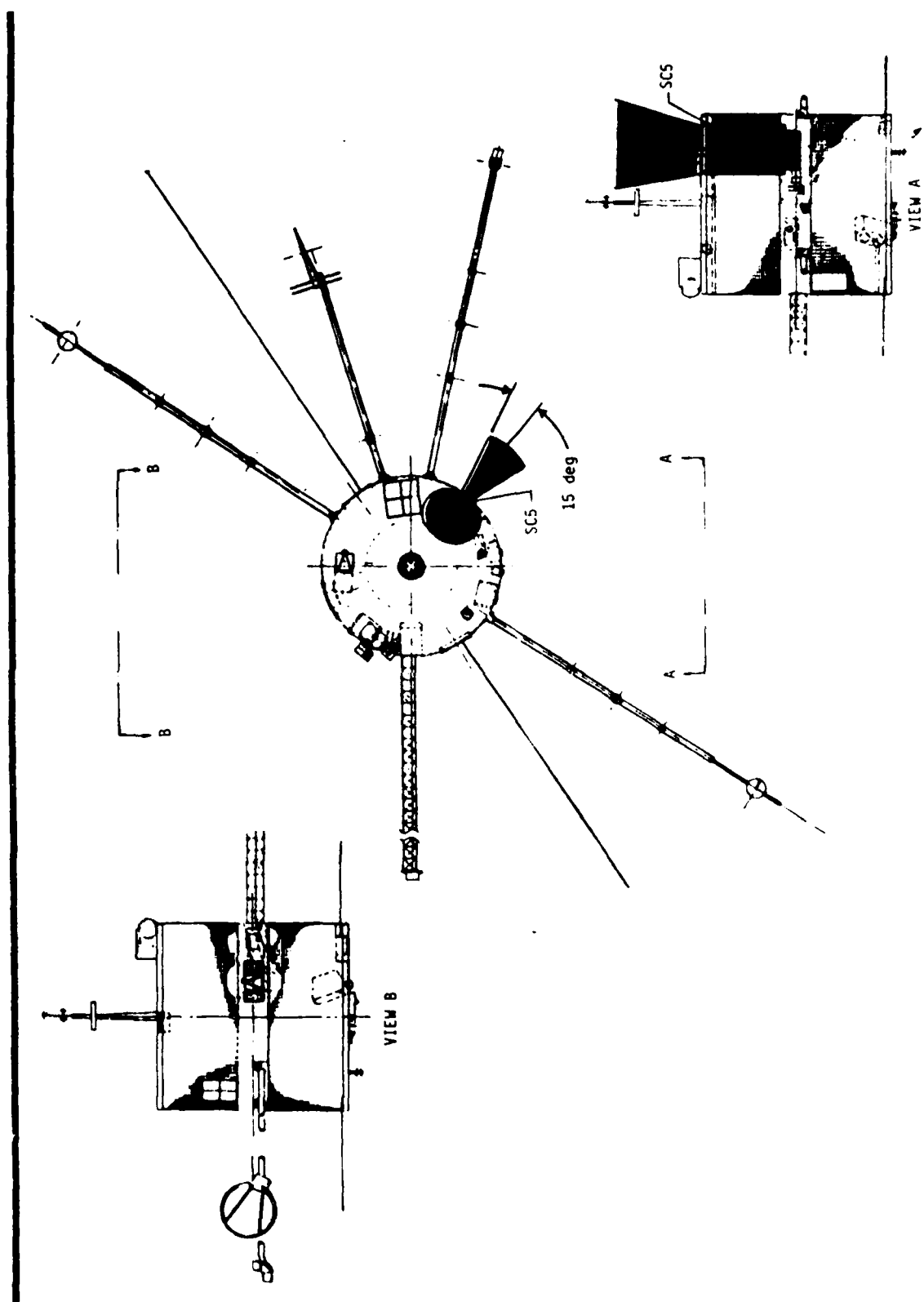
Figure 4.5. Satellite Mounting Configuration

63

The instrument's thermal model is shown in Fig. 4.6, which also shows the approvimate location of the three temperature sensors. This package is treated as a single mode by the satellite integrator, yielding the predicted on-orbit temperatures shown in Fig. 4.7. Fredicted temperatures are well within the desired range.
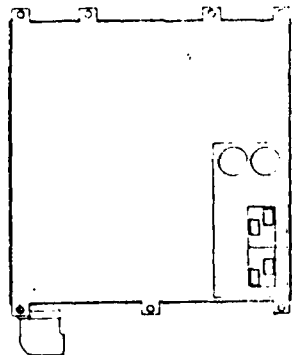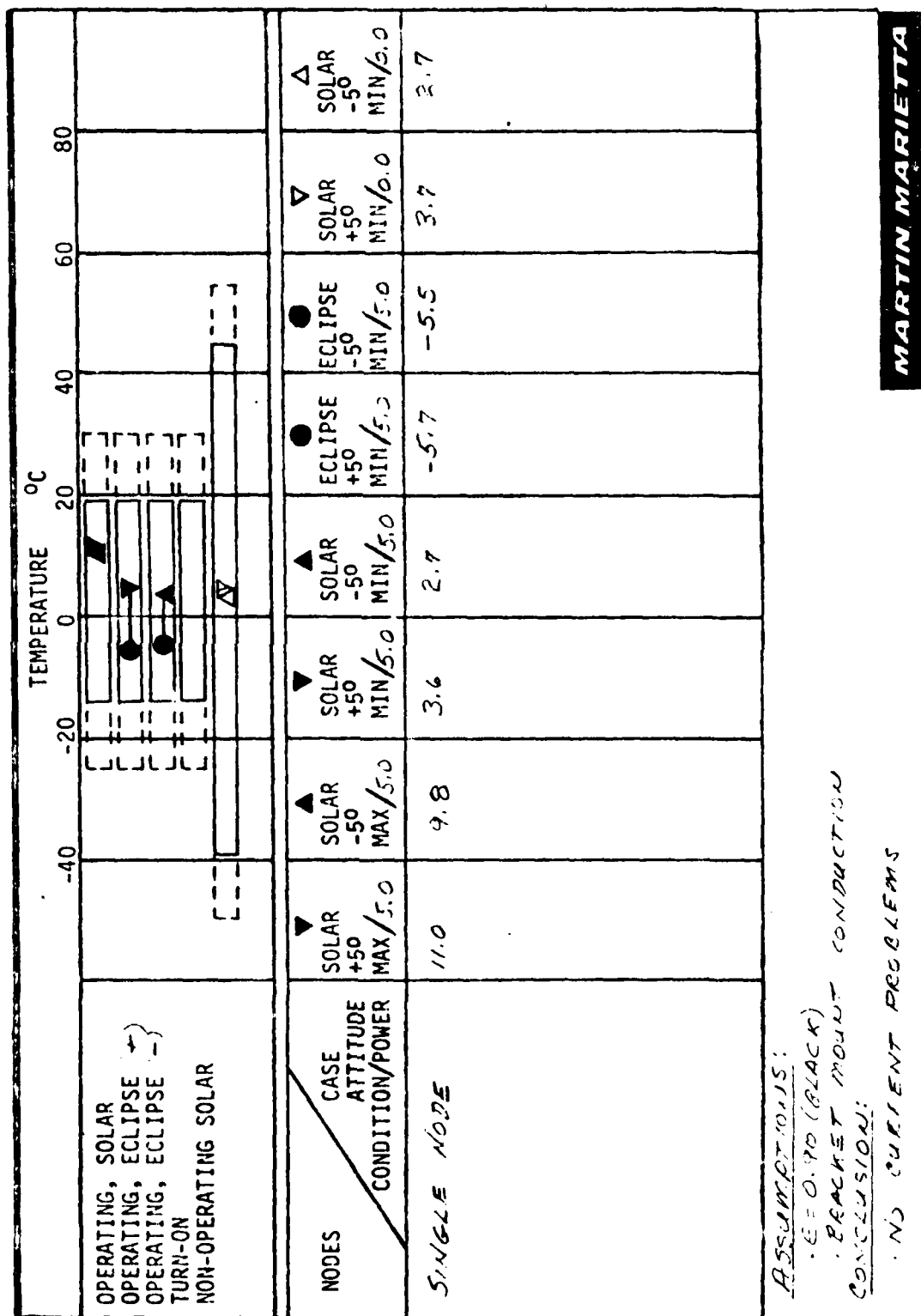
Figure 4.6 Thermal Model.

TEMPERATURE °C

OPERATING, SOLAR
OPERATING, ECLIPSE +
OPERATING, ECLIPSE -
TURN-ON
NON-OPERATING SOLAR

NODES CASE ATTITUDE CONDITION/POWER	SOLAR +50 MAX/5.0	SOLAR -50 MAX/5.0	SOLAR +50 MIN/5.0	SOLAR -50 MIN/5.0	ECLIPSE +50 MIN/5.0	ECLIPSE -50 MIN/5.0	SOLAR +50 MIN/6.0	SOLAR -50 MIN/6.0
SINGLE NODE	11.0	9.8	3.6	2.7	-5.7	-5.5	3.7	3.7

ASSUMPTIONS:
ε = 0.90 (BLACK)
BRACKET MOUNT CONDUCTION
CONCLUSION:
NO CURRENT PROBLEMS

MARTIN MARIETTA

PDR-2

Figure 4.7 On-Orbit Temperature Predictions.

5. TEST AND CALIBRATION

5.1 Ground Support Equipment

Two pieces of ground support equipment were designed and fabricated to allow independent testing of the RSPD - the spacecraft simulator, shown in Fig. 5.1 and the test pulse generator/test point monitor shown in Fig. 5.2.

The spacecraft simulator (Fig. 5.1) connects to the spacecraft interface connector on the RSPD and provides the following capabilities:

(1) An adjustable source of buss voltage (28 $\pm$ 4 volts DC) for the instrument's 3 power input lines, independent ON/OFF control and analog current meters are provided for each line, an analog voltage meter is also provided.

(2) A digital voltage meter (DVM) and selector switch for monitoring all of the RSPD's analog monitor outputs, external signals may also be monitored by the DVM via a panel mounted BNC connector.

(3) A complete simulation of the magnitude command input - the desired command bit pattern is entered in 22 toggle switches and serially transferred to the RSPD by depressing a push button.

(4) A complete simulation of the digital data circuitry control lines. The RSPD digital data is serially transferred to the spacecraft simulator where it is stored and displayed in an array of 208 light-emitting-diodes (LEDs).

(5) Provisions for varying the digital data accumulation time from the normal 200 msec to 1, 10 or 100 sec. A single cycle capability is also included whereby one set of data (208 bits) can be accumulated for 1, 10 or 100 sec, then transferred to the simulator and displayed for as long as desired.

(6) LED display of various spacecraft simulator signals are provided. A push button allows the testing of all LEDs.

Two cables have been fabricated for connecting the spacecraft simulator to the RSPD - one is used for normal testing at atmospheric pressure while the other is used for testing under vacuum.

The second piece of ground support equipment, the test pulse generator/ test point monitor (Fig. 5.2) connects to a test connector on the RSPD and provides the following capabilities:
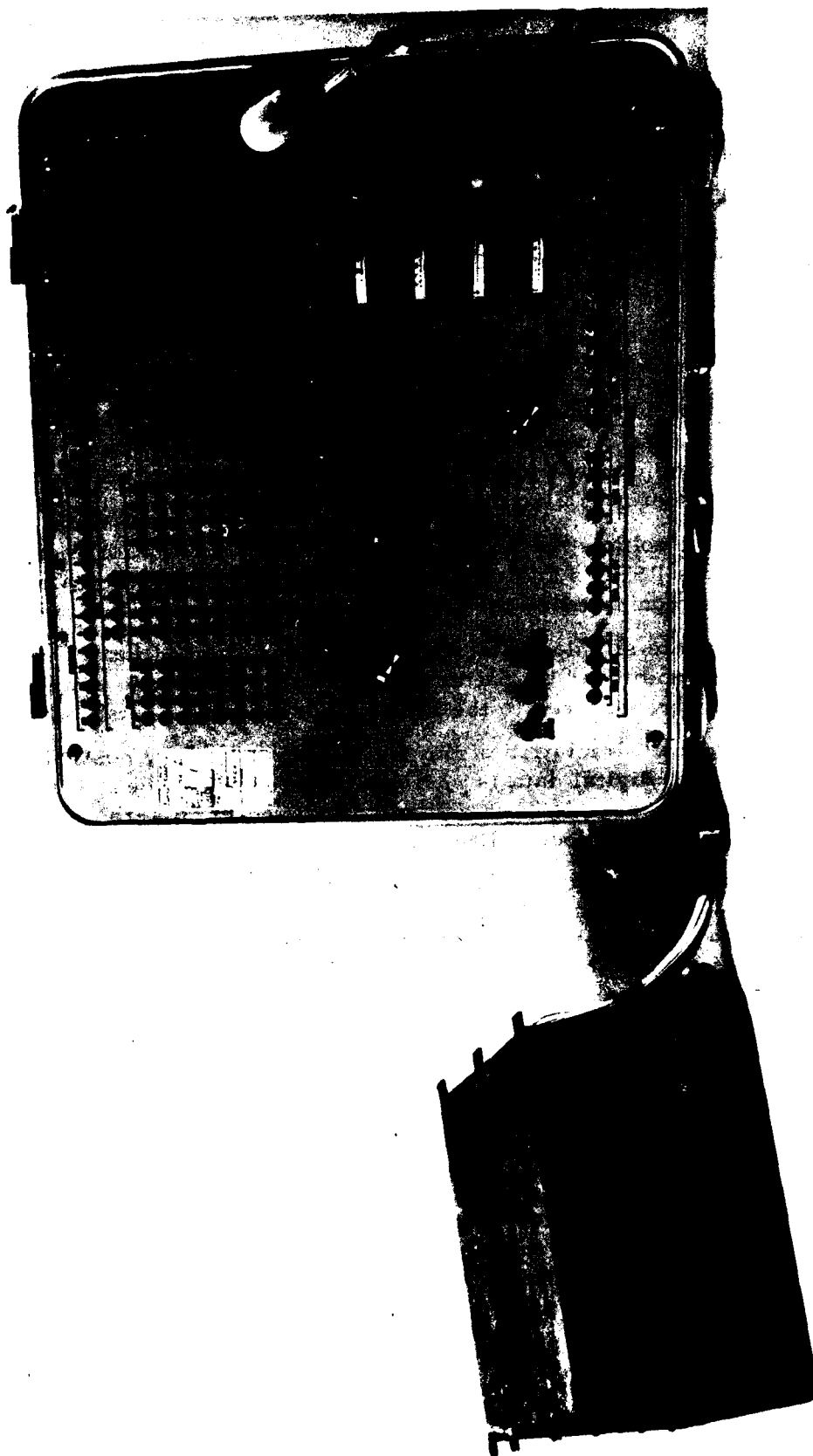
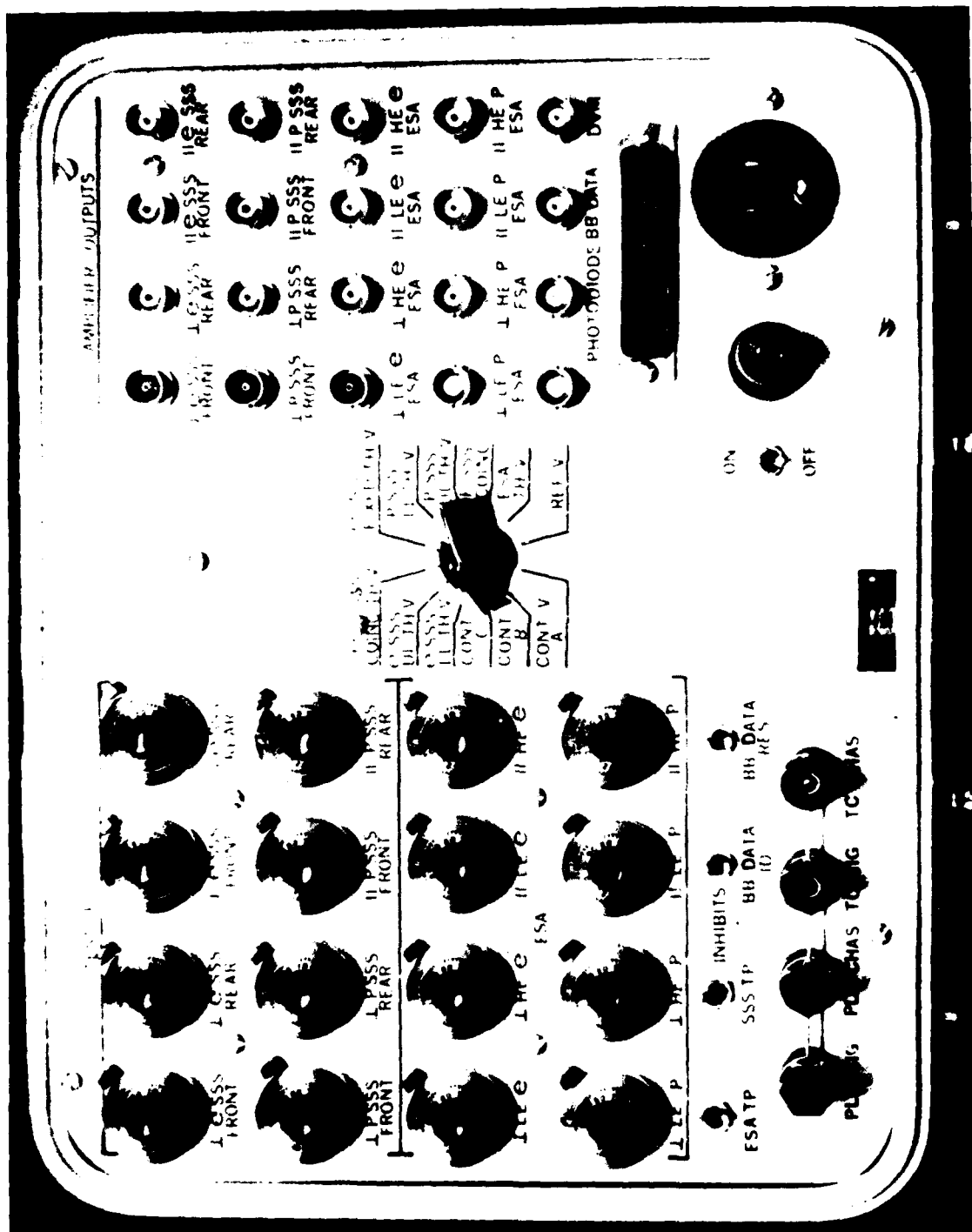Figure 5.1   RSPD Spacecraft Simulator

68

Figure 5.2 RSPD Test Pulse Generator/Test Point Monitor

(1) Sixteen independent, variable amplitude, test pulses which are applied to the SSS and ESA test pulse inputs. These allow independent stimulation of all amplification chains and the measurement of all threshold discriminator firing levels. Switches are provided for inhibiting the ESA and/or SSS test pulses.

(2) Sixteen panel mounted BNCs which are connected to the outputs of the final SSS and ESA amplification chains. This allows each of these outputs to be monitored by an oscilloscope or multi-channel pulse-height analyzer. BNCs are also provided for viewing the broadband data output and UV photodiode signals.

(3) A rotary switch which can route, via a BNC cable, one of several analog voltage test points to the spacecraft simulator DPM or any other suitable meter.

(4) Switches are provided for inhibiting the broadband data ID and/or resetting the broadband data counter. These prove very useful for certain tests.

A short ($\approx$ 12") cable must be used for connecting the test pulse generator/test point monitor to the RSPD; therefore, this unit may not be used for testing under vacuum. However, the RSPD test connector is located such that the test pulse generator/test point monitor may be used when the RSPD is on the satellite.

Both pieces of ground support equipment are completely self-contained. Each is packaged in a suitcase type aluminum carrying case and requires only a source of 110V AC power.

5. 2 Instrument Tests

Extensive breadboard testing of all major subsystems was carried out during the design of the RSPD, including temperature tests over the entire military temperature range (-50° to +125°C). Additional tests, carried out with engineering models of the ESA and SSS subassemblies, have been previously reported (Ref. 1. 8 and 1. 9). A great deal of analytical work was also done to ascertain that the RSPD would work properly in the anticipated radiation environment, with particular emphasis on the susceptability of the complementary metal oxide semiconductors (CMOS) logic circuitry used throughout the instrument - this also was reported in Ref. 1. 8.

The flight RSPD was subjected to a complete series of functional and environmental tests as follows:

        (1) baseline Functional Test
        (2) complete series of EMC tests
        (3) post EMC Functional Test

(4) complete series of thermal tests
(5) vibration and shock tests
(6) post vibration Functional Test
(7) vacuum test
(8) pre-delivery Functional Test

All of the indicated Functional Tests were carried out in accordance with a written procedure which runs approximately 4 hours and which provides complete verification of proper system performance.

The baseline functional test established the nominals to which all other test results were compared. EMC testing was carried out at Sanders Associates, Inc. in Nashua N. H This was a very extensive series of tests, carried out in accordance with the spacecraft electromagnetic compatibility test plan (Ref. 5. 1), test results are reported in Ref. 5. 2. The post EMC functional test verified that no malfunctions were induced by the various EMC tests.

Thermal testing consisted of the following sequence:

(1) functionat test at ambient temperature
(2) 20 hour non-operating soak at $-50^{\circ}C$
(3) functional test at $-25^{\circ}C$
(4) 20 hour non-operating soak at $+55^{\circ}C$
(5) functional test at $+30^{\circ}C$

The only failure during all of the instrument testing occurred during this sequence. The Δp SSS front detector, which is only about $5\,\mu m$ thick, was fractured during the non-operating soak at $-50^{\circ}C$. Following consultations with AFGL and MMC personnel, it was decided to change the non-operating soak temperature to $-35^{\circ}C$ which, considering the predicted on-orbit temperatures (Fig. 4. 7), seems much more realistic than $-50^{\circ}C$. The entire thermal test sequence was repeated, soaking at $-35^{\circ}C$ instead of $-50^{\circ}C$, following replacement of the Δp SSS front detector with absolutely no problems.

Shock and vibration tests, in accordance with the interface control document (Ref. 4. 1), were carried out at AFGL. The post vibration functional test verified that the RSPD had survived.

The vacuum test, carried out at Panametrics, consisted of a complete functional test under vacuum. This was somewhat of a formality as the RSPD had previously been operated under vacuum quite extensively during calibration.

The pre-delivery functional test was performed on November 29, 1978, and the instrument was ready for delivery to the spacecraft integrator (MMC)

at that time. However, MMC discovered that due to "an understandable misinterpretation of the ICD" the RSPD was not painted as they had expected. This situation was corrected, the pre-delivery performance repeated, and the unit hand carried to MMC on December 7, 1978.

Approximately midway through the acceptance functional test at MMC a malfunction was observed. The RSPD was returned to Panametrics, where it was found to be working perfectly. The "malfunction" which had been observed turned out to be caused by a peculiar characteristic of an oscilloscope used at MMC. The instrument was hand carried back to MMC, following one last pre-delivery test at Panametrics, and the acceptance test was successfully completed. A physical inspection, radiation survey and magnetic survey were also completed, by MMC personnel, prior to mounting the RSPD on the SCATHA satellite.

5.3 Spacecraft Tests

The RSPD was successfully integrated into the SCATHA satellite and underwent all of the spacecraft tests outlined in the System Test Plan (Ref. 5.3) including acoustic, shock and vibration, thermal vacuum and electromagnetic tests.

Three separate test sequences (combined efforts of Panametrics, AFGL and MMC personnel) were used throughout the spacecraft level tests to verify proper RSPD operation:

(1) The ALL MODES test is essentially the same as the instrument's functional test; it provides complete verification of proper system performance. The test pulse generator/test point monitor is connected to the RSPD during this test and extensive operator interaction is required. The test sequence runs approximately 4 hours.

(2) The NOMINAL MODES test is an abbreviated version of the all modes test requiring much less operator interaction. The test pulse generator/test point monitor is connected to the RSPD during this test sequence, which runs approximately 30 minutes.

(3) The MINIMUM MODES test is a totally automated, brief ($\approx$ 2 minute) test sequence which validates basic RSPD performance. The test pulse generator/test point monitor is not used for this test sequence.

Following the completion of the spacecraft test program the SCATHA satellite was successfully launched into near synchronous orbit on 30 January 1979.

5.4 Calibration

The several detector modules within the RSPD were individually calibrated by a number of methods. The procedures for the ESA s and the SSS s are different and will be described separately. Tests made with individual modules generally used radioactive sources, while the major ESA calibration at the Rice University facility were done with electron/proton beams (Ref. 1.11).

The ESA calibration was done in three sets of tests. The first test is to determine the proper operating voltages for the SEM detectors. This was done by testing each SEM with a tritium beta source, measuring the pulse output as a function of SEM bias voltage. Since all SEM s in a given RSPD unit operate from a common bias voltage source, these test results were used to select two groups of 8 SEM s, and an associated minimum bias voltage, for each RSPD (S/N 1 and S/N 2). The minimum bias voltage was used to set the bias voltage supply bias level 1, with the higher bias level steps then increasing from this level in fixed increments as described in Section 3.3.

The second set of ESA tests was also made with a tritium beta source, but with the fully assembled RSPD. The beta source (18.6 keV maximum electron energy) was scanned across each ESA aperture and counts taken in all ESA channels. This test verified proper channel operation by showing that only channels capable of detecting the tritium beta particles did indeed detect them, and that the angular fields of view were close to the desired ones. This test verified proton ESA operation only to the extent that they should not detect electrons. The last part of this test included use of a Kr lamp with emissions near 1200 Å to check that UV sensitivity was not excessive.

The third set of ESA tests was a detailed calibration of all ESA responses at the Rice University calibration facility. These tests provide detailed responses for each channel of each ESA for nearly 10 eV to 50 keV electrons and 100 eV to 30 keV protons. The results have been reduced and presented in detail in Ref. 1.11, for the flight unit RSPD (S/N1). The final calibration on the flight unit RSPD was done after the spacecraft (SCATHA) integration tests had all been completed. The flight RSPD was then hand-carried to Panametrics, Inc. for a final checkout and completion of the ___ at Rice University. During the calibration a failure was observed ___ Electron ESA, with the SEM apparently going into corona. Since ___ tron and proton ESA s are built as one module, they were ___ LE ESA from the backup unit, since it had been cali- ___ University some time earlier. Thus the repaired flight unit ___ brated in all ESA s, and after checkout was delivered to the ___ r installation on the SCATHA satellite prior to launch.

The final calibration at Rice University also included some UV sensitivity tests of the ESA s with a Kr lamp ($\simeq 1200 \text{Å}$ major output). These results indicated a somewhat greater UV sensitivity than measured earlier at Panametrics, Inc. , but still within the estimates made during the early design stage. The Rice measurements of UV sensitivity are in reasonable agreement with in-orbit observations of solar UV (see Section 6.3).

The SSS calibrations were done primarily during RSPD assembly to set the solid state detector gains and the thresholds. After the detector module and amplifier chains were completed, the gains of the 300 μm thick detectors (electron SSS front and rear, proton SSS rear) were set by irradiation with a Co-57 electron source (115/129 keV in 1. 0/0. 75 intensity ratio, average energy = 121 keV). The 121 keV average energy electrons were used to adjust the gains to within a few percent of the desired values, and to cross-calibrate a precision pulser which was then used to set the electronic thresholds.

The proton SSS front detectors cannot be calibrated with electron sources, since their extreme thinness (5-6 μm) results in them stopping electrons only to about 20 keV, which is in the noise. The thin detectors are calibrated with an Am-241 alpha source, with the 5. 48 MeV alpha particles losing only about 0. 9 MeV in the thin detectors. The actual energy loss was measured during the detector thickness measurement, and this was used to cross-calibrate a precision pulser when the amplifier gain was about a factor of two, too low. The pulser was then used to set the correct gains and the thresholds. This method was necessary since the desired amplifier chain gain results in the Am-241 ($\simeq 0. 9$ MeV) pulse being saturated, and thus useless for gain measurement.

After the final assembly of the RSPD the electron SSS s received a small amount of calibration in the Rice University electron beams (Ref. 1. 11). This was done only during the earliest tests, as later tests were done with a baffle in place to eliminate lower energy contaminating beams from the ESA s. The baffle also shielded the SSS s from the direct electron beam. A more detailed discussion of the electron SSS calibration is given in Ref. 1. 11.

6. INSTRUMENT OPERATIONS

6.1 Operating Constraints

Operation and handling of the RSPD is subject to the following constraints:

(1) The entrance apertures may not be touched, covered, or painted. Access to the protective covers closing these apertures is required for their removal during certain spacecraft level tests and prior to launch. The aperture covers are to be removed slowly and carefully and only when absolutely necessary.

(2) Access to the test connector is required during certain spacecraft level tests for attachment of the test pulse generator/test point monitor.

(3) The RSPD may be operated at atmospheric pressure and under high vacuum, but it must not be operated in the pressure region between one atmosphere and 10^{-5} Torr.

(4) The RSPD shall not be turned on until the space vehicle has been in final orbit for at least five days.

(5) The RSPD shall be commanded off prior to space vehicle thruster operation and shall remain off for a period of at least 15 minutes following thruster shutdown.

(6) The RSPD shall be commanded off during initial electron or ion gun operation until sufficient data on the effect of the beam systems indicates that the instrument may be safely operated.

6.2 General Operating Procedures

Operation of the RSPD is fairly straightforward. The normal configuration when using the spacecraft simulator is shown in Figure 6.1. Once the equipment is interconnected as shown and the spacecraft simulator and test pulse generator/test point monitor have been turned on and allowed to warm up, normal instrument operation would proceed as follows:

(1) Adjust the spacecraft simulator buss voltage (28 ± 4 volts) to the desired level.

(2) Depress the LOW VOLTAGE ON pushbutton.

(3) Place all MAGNITUDE COMMAND SWITCHES UP and depress the SEND MAGNITUDE COMMAND pushbutton; this places the RSPD in the master reset mode - the ESAs and SSSs cycling at 1 energy sweep per second, the SEM bias level at step 1, the BB data output in subcomm mode 1 with a dwell time of 1 energy sweep, and the ESA power control circuitry disabled.

(4) Depress the SSS ON pushbutton and the ESA ON pushbutton.

RAPID SCAN PARTICLE DETECTOR

Test Connector

TEST PULSE GENERATOR/TEST PULSE MONITOR

Interface Connector

SPACECRAFT SIMULATOR (Test Console)
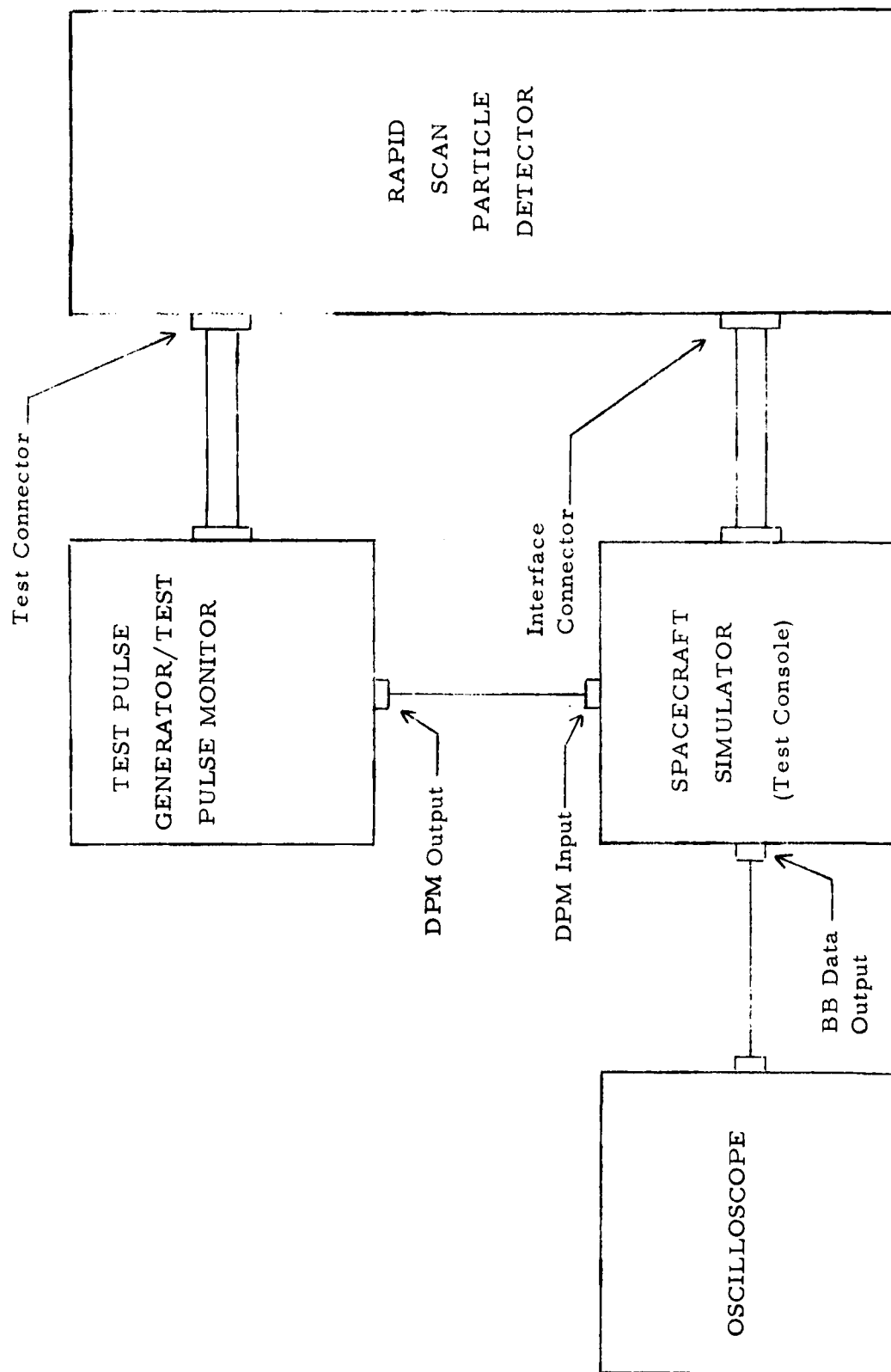
DPM Output

DPM Input

BB Data Output

OSCILLOSCOPE

Figure 6.1 Normal Operating Configuration

The RSPD is then completely on and functioning; the digital data may be monitored in the LEDs, and the analog monitor voltage levels may be measured with the DPM. The instrument's operating mode may be altered by appropriately configuring the 22 magnitude command switches and depressing the send magnitude command pushbutton. The magnitude command bit assignments are given in Tables 3.1, 3.2, 3.3, 3.7, and 4.3. The instrument is turned off by again depressing the ESA ON pushbutton, then the SSS ON pushbutton, and finally the LOW VOLTAGE ON pushbutton.

Normal operation of the RSPD, following its integration onto the SCATHA satellite, is essentially the same as above. To facilitate the turn-on sequence, the Satellite Control Facility (SCF) has defined a "block command" (B 6501) which consists of the following command sequence:

6500	Low Voltage On	
6600	Master Reset	
6502	ESA On	
6504	SSS On	

This block command turns the RSPD on and places it in the master reset mode. Any of the magnitude commands (Tables 3.1, 3.2, 3.3, 3.7, and 4.3) may now be sent to alter the instrument's operating mode, if desired. The RSPD is turned off by sending the POWER OFF (6505) command. This one command removes power from all three input lines. Further details of the instrument's in-orbit operating procedures are given in the following section.

6.3 Evaluation of In-Orbit Operation

The flight unit RSPD (S/N 1) was mounted in the SCATHA satellite (P78-2) and launched on 30 January 1979. The final orbit was achieved by 7 February 1979, with the orbital parameters as of that date being given in Table 6.1. The RSPD is called the SC5 payload on the SCATHA satellite, and remained off until after final orbit was achieved. The RSPD (SC5) was turned on for the first time on 9 February 1979, and checked out with an extensive command series. All components operated properly and the RSPD was left on with SEM bias level 1, except for turn off for attitude maneuvers. During the next two days some additional command testing was done, although time limitations for real-time passes did not allow all of the commands to be tested. Operation of the SEM's at the higher bias levels was first checked out after two days of operation, on 11 February.

During the first several days of operation the SEM gains in bias level 1 were observed to degrade with a time constant of a few days. On 16 February, about 175 hours after first turn-on, it was decided to operate the SEM's at bias level 8 since the LE electron ESAs were operating at about 25% detection efficiency in bias level 1. The normal operating mode was changed to include setting SEM bias level 8. At this time a bias level gain calibration sequence

77

Table 6.1

Final Orbit Parameters for the SCATHA Satellite
as of 7 February 1979

Perigee Altitude	14872 n. mi. = 27547 km
Apogee Altitude	23347 n. mi. = 43239 km
Inclination	7. 90 degrees
Right Ascension of Ascending Node	271. 4 degrees
Argument of Perigee	184. 8 degrees
Drift Rate	5. 13 degrees/day
Satellite SCATHA = P78-2	

was also introduced, making RSPD measurements for at least one spin period (>70 seconds) in each of bias levels 1, 4, 7, 10, 13, 16, and 8 (remaining in 8). This sequence was required to be performed at least once per week to allow SEM gain at bias level 8 (normal operating level) to be monitored and used for data analysis.

The SEM gains in bias level 1, relative to bias level 8, are plotted in Fig. 6.2 for the first 500 hours of operation. The time of change from bias level 1 to 8 for normal operation is indicated. The decrease in gain appears to continue for a few hundred hours, after which it levels off. The detailed gain (relative to bias level 8) vs. bias level variations are shown in Figs. 6.3 to 6.10, and show that the LE electron ESA s are significantly low in gain at bias level 8 after a few hundred hours. There seems to be some recovery in gain between 300 and 500 hours.

The SEM gain decrease is more pronounced for the $\perp$ ESA s, which view the sun once per satellite rotation. The measured UV sun pulse was clearly observed in all four $\perp$ ESA s, and gave peak count rates of 5-20 kHz. These count rates are in reasonable agreement with those expected, based on the Rice University UV sensitivity tests (Ref. 1.11). The solar UV pulse contributes a significant count accumulation to the SEM's in the perpendicular ESA's, and thus accounts for the more rapid gain degradation.

The SEM gain degradation resulted in the RSPD being turned off about 10 March and then being put into an SSS-only-on mode starting on 13 March to preserve the SEM gain for eclipse operations which were to begin on 16 March. On 17 March the ESA's were again turned on and a bias level check performed. It was found that after about one week off the SEM gains in bias level 1 were close to their original values. Over the next 24 hours the B. L. 1 (bias level 1) gains were observed to decay with a 1-2 day time constant for the perpendicular ESA s, and a several day time constant in the parallel ESA's, which do not view the sun. At this time the auto-shut-off B was enabled, using the photodiode to turn off the SEM bias voltage during the sun pulse and so reduce the effect of solar UV on the accumulated counts of the $\perp$ ESA s.
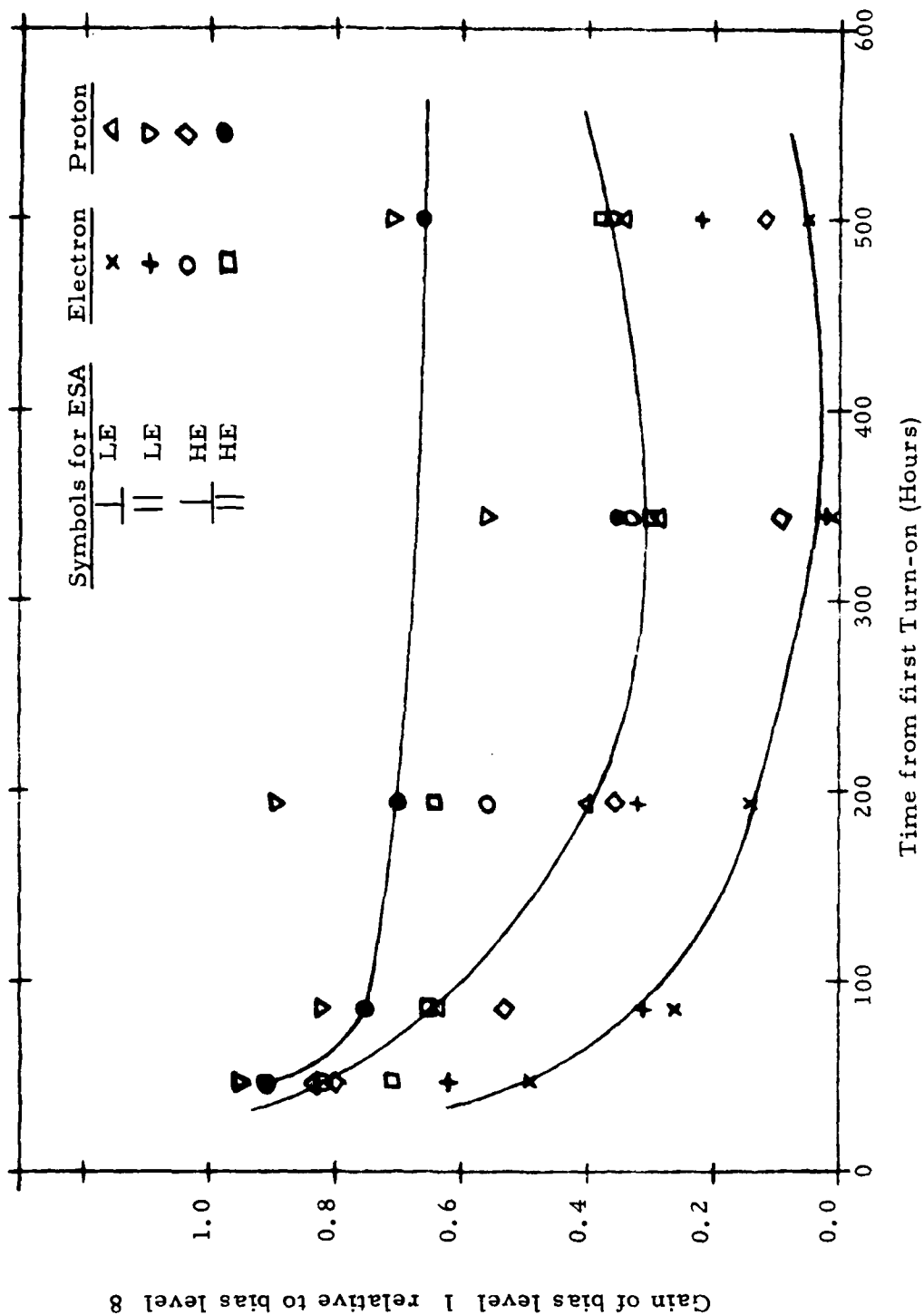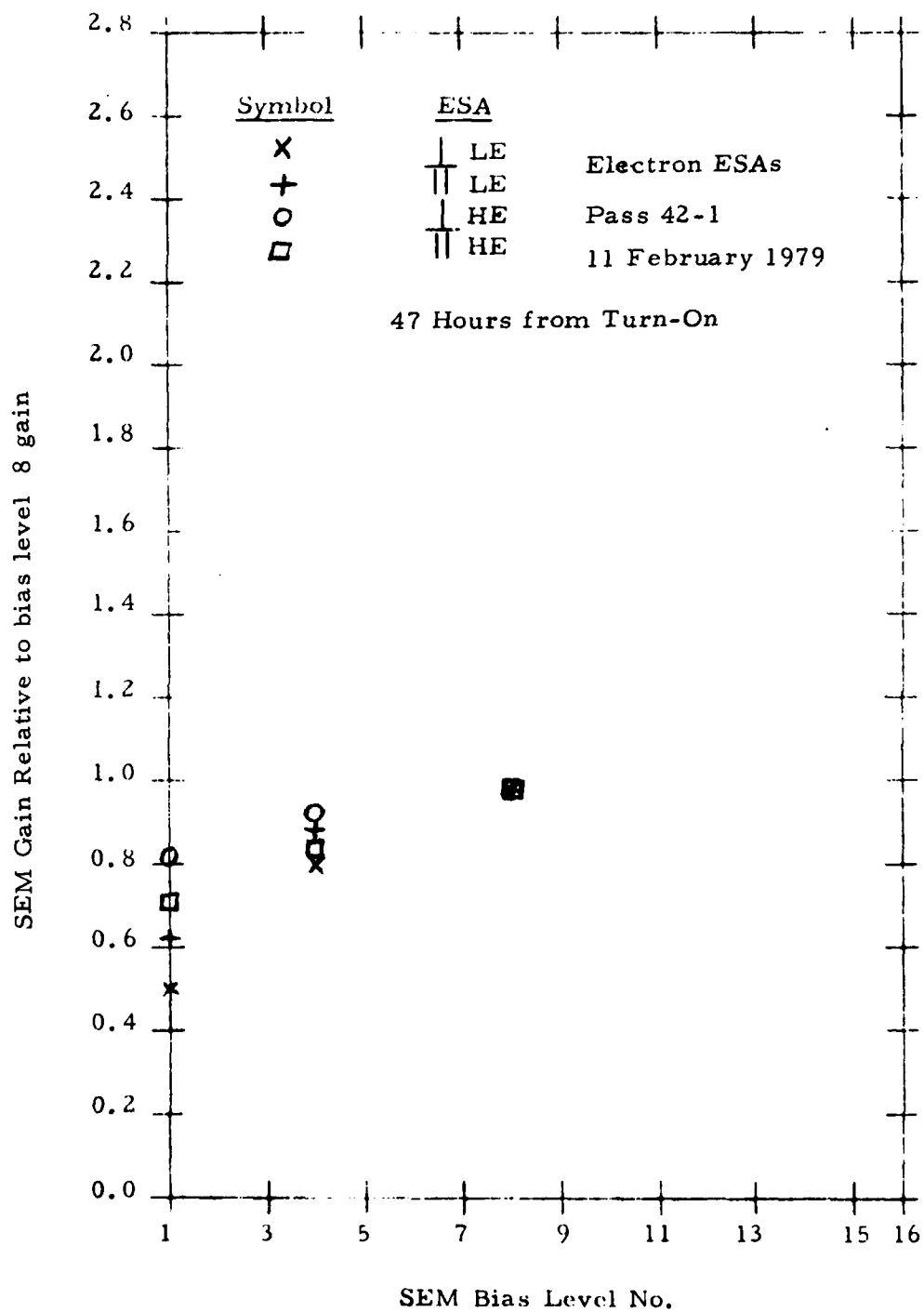
Figure 6.2 SEM Gains vs. Time After First Turn-On
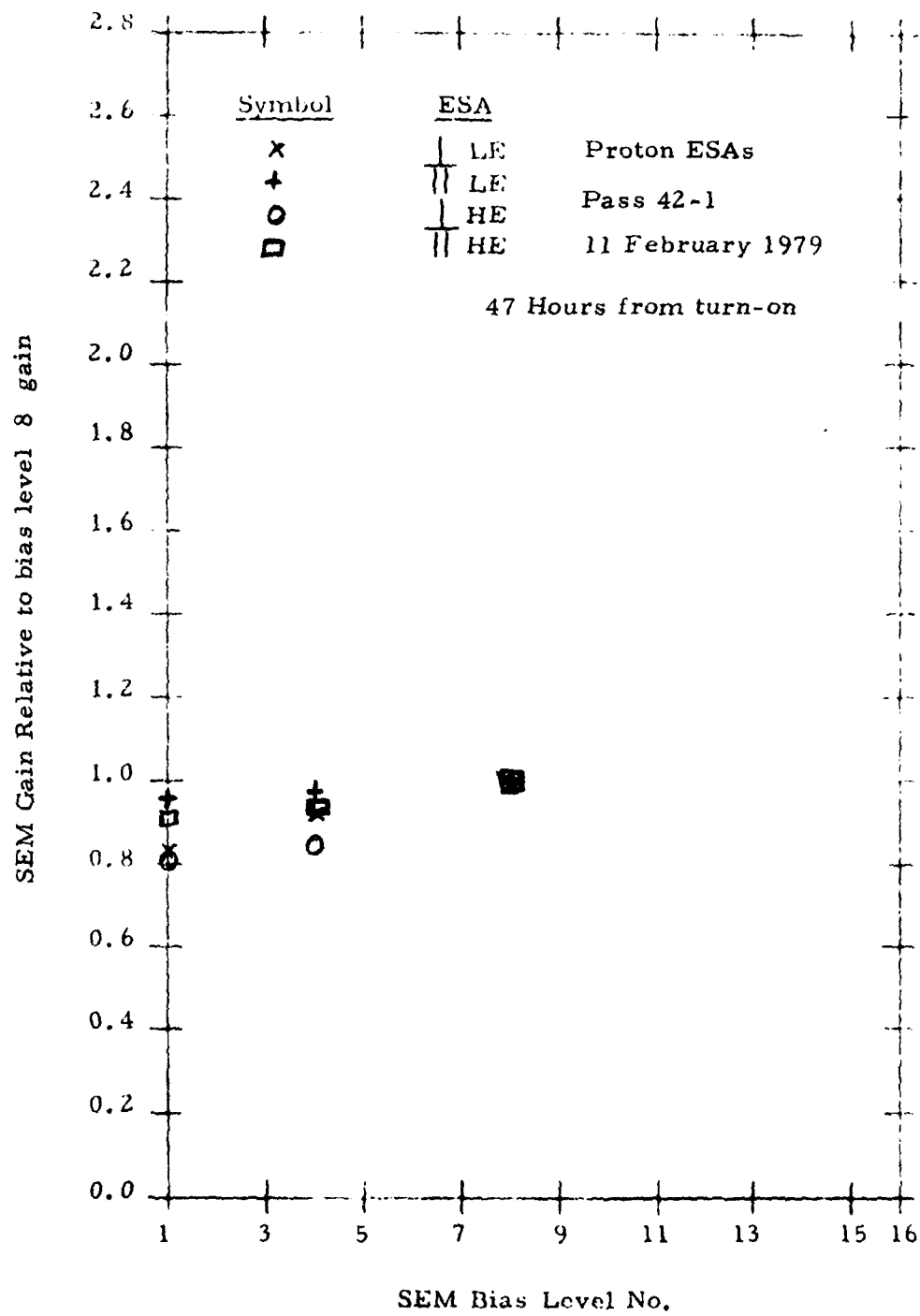
Figure 6.3 Electron ESA SEM Gains, 47 Hours
from Turn - On

80
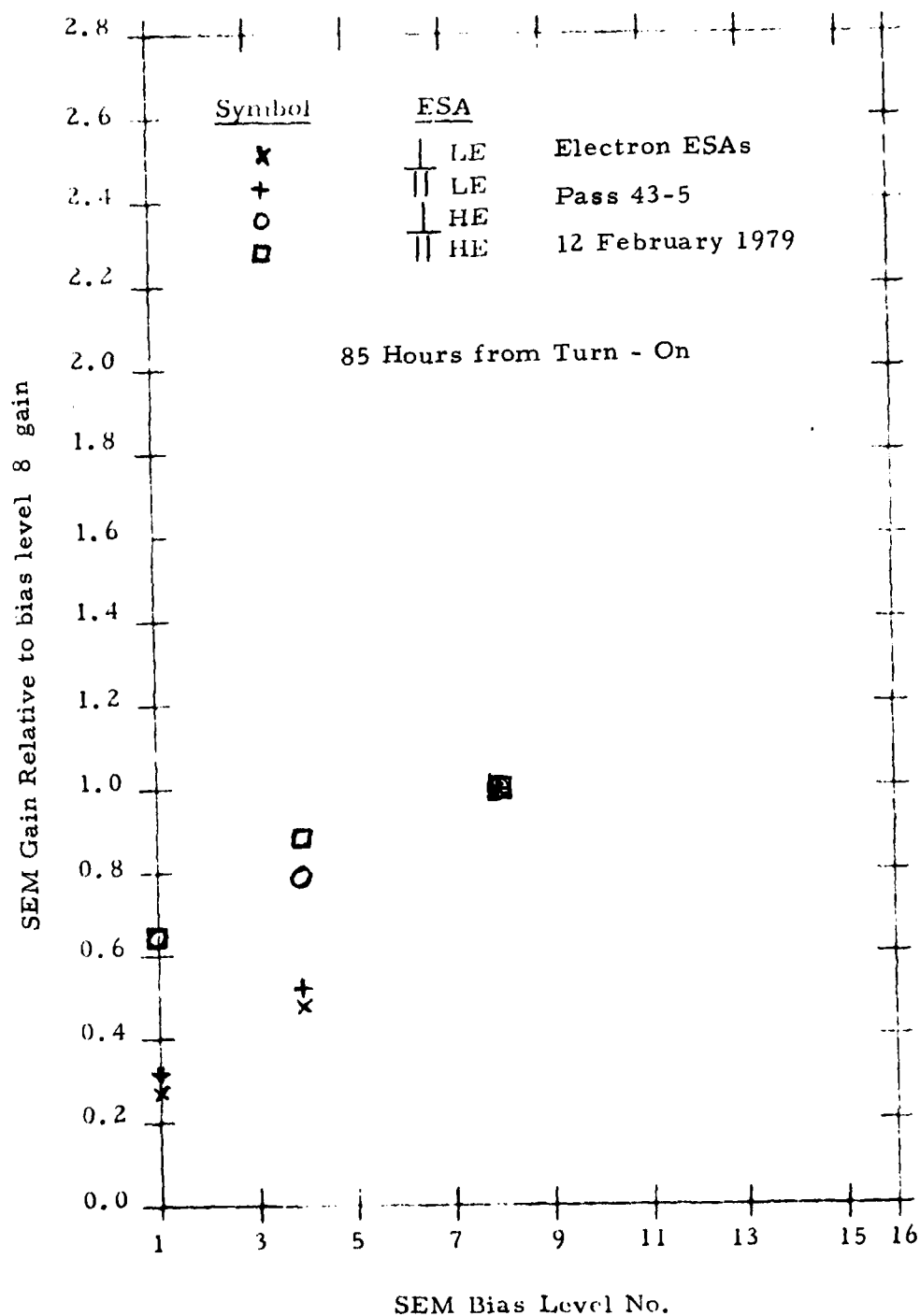
Figure 6.4 Proton ESA SEM Gains, 47 Hours
from Turn - On

81

Figure 6.5 Electron ESA SEM Gains, 85 Hours from
Turn - On

82

2.8

2.6

2.4

2.2

2.0

1.8

1.6

1.4

1.2

1.0

0.8

0.6

0.4

0.2

0.0

SEM Gain Relative to bias level 8 gain

Symbol ESA

x | LE
+ || LE
o | HE
□ || HE

Proton ESAs

Pass 43-5

12 February 1979

85 Hours from Turn - On

1   3   5   7   9   11   13   15 16
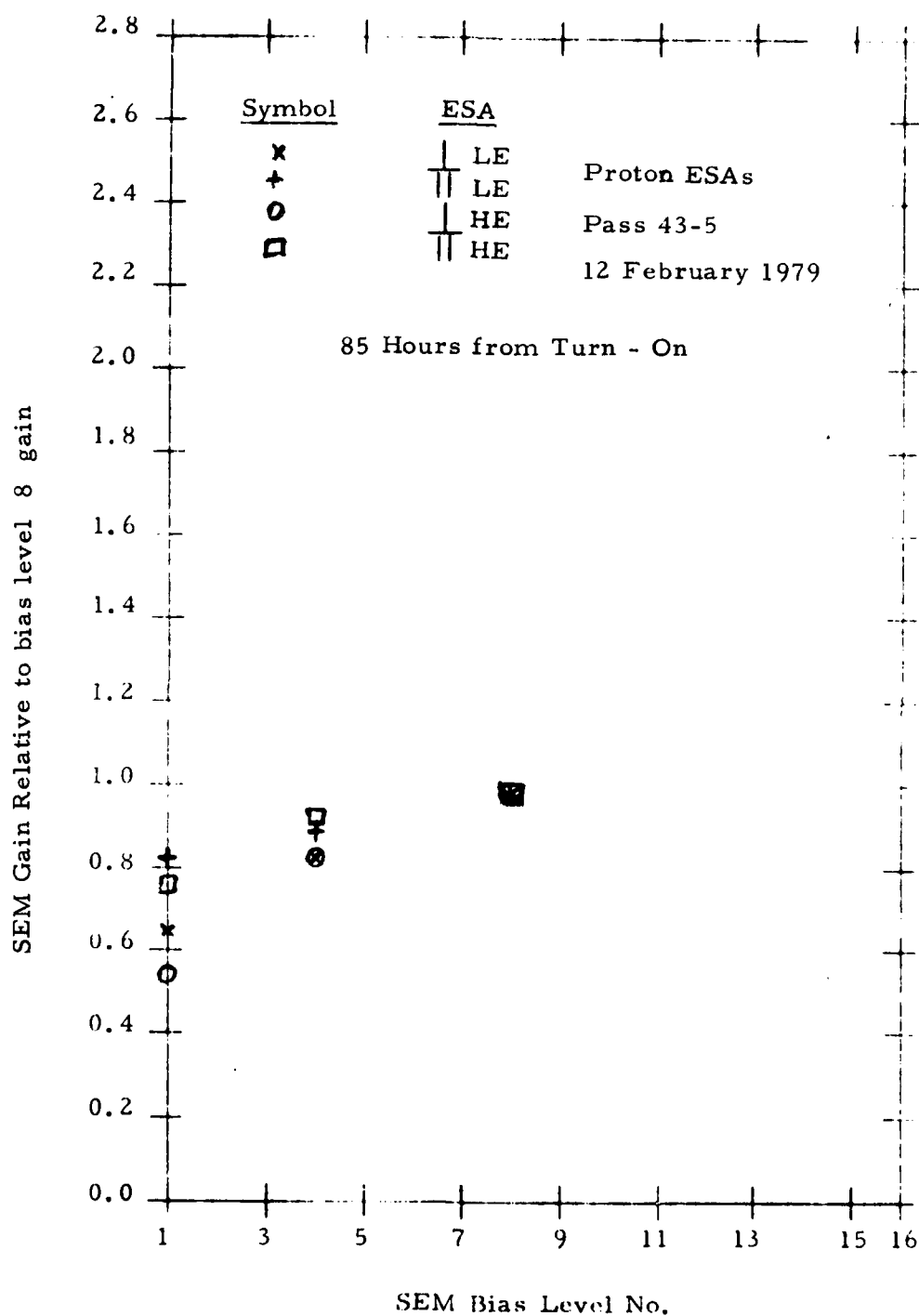
SEM Bias Level No.

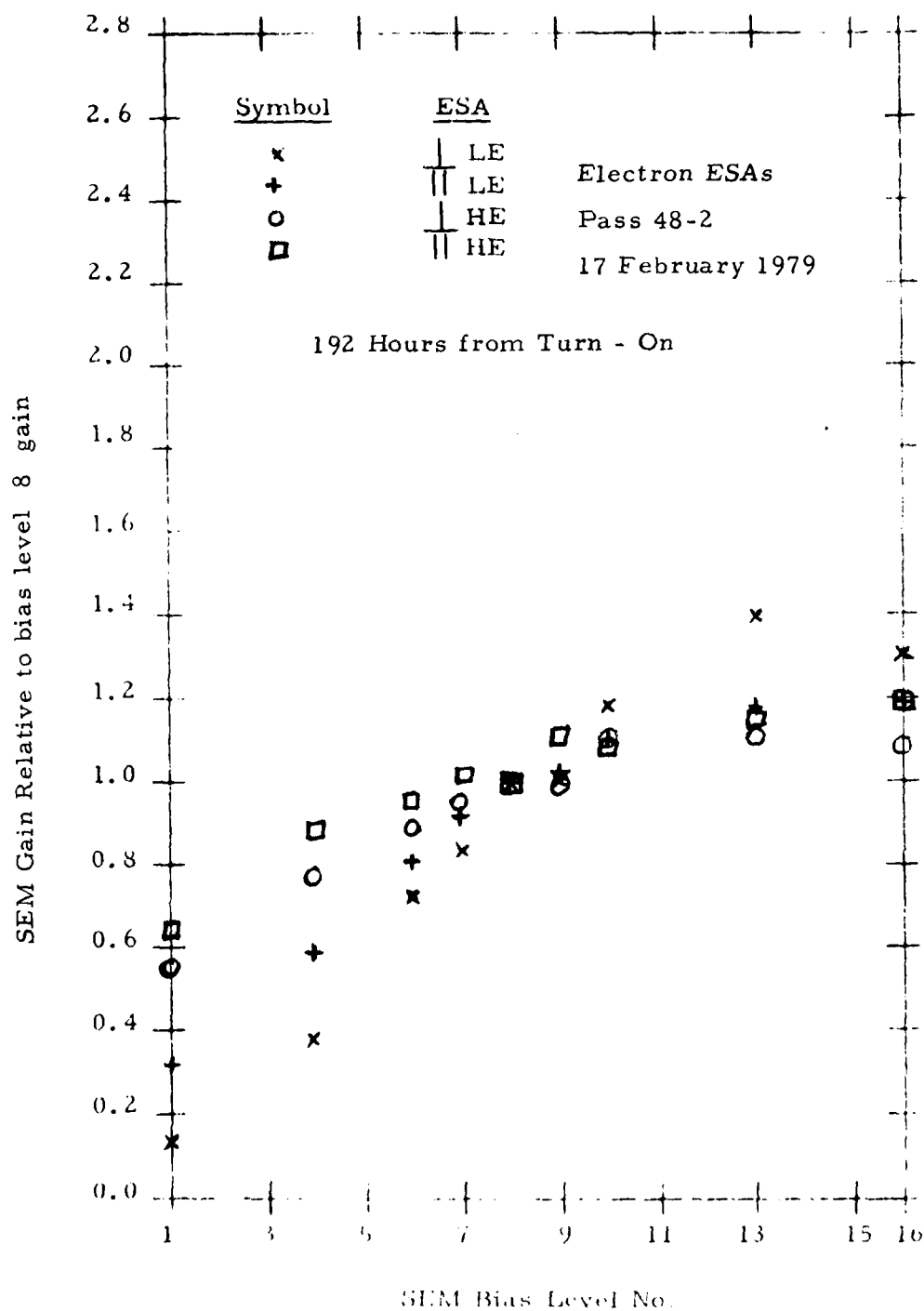Figure 6.6 Proton ESA SEM Gains, 85 Hours from
Turn - On

Figure 6. 7 Electron ESA SEM Gains, 192 Hours from
Turn - On

84

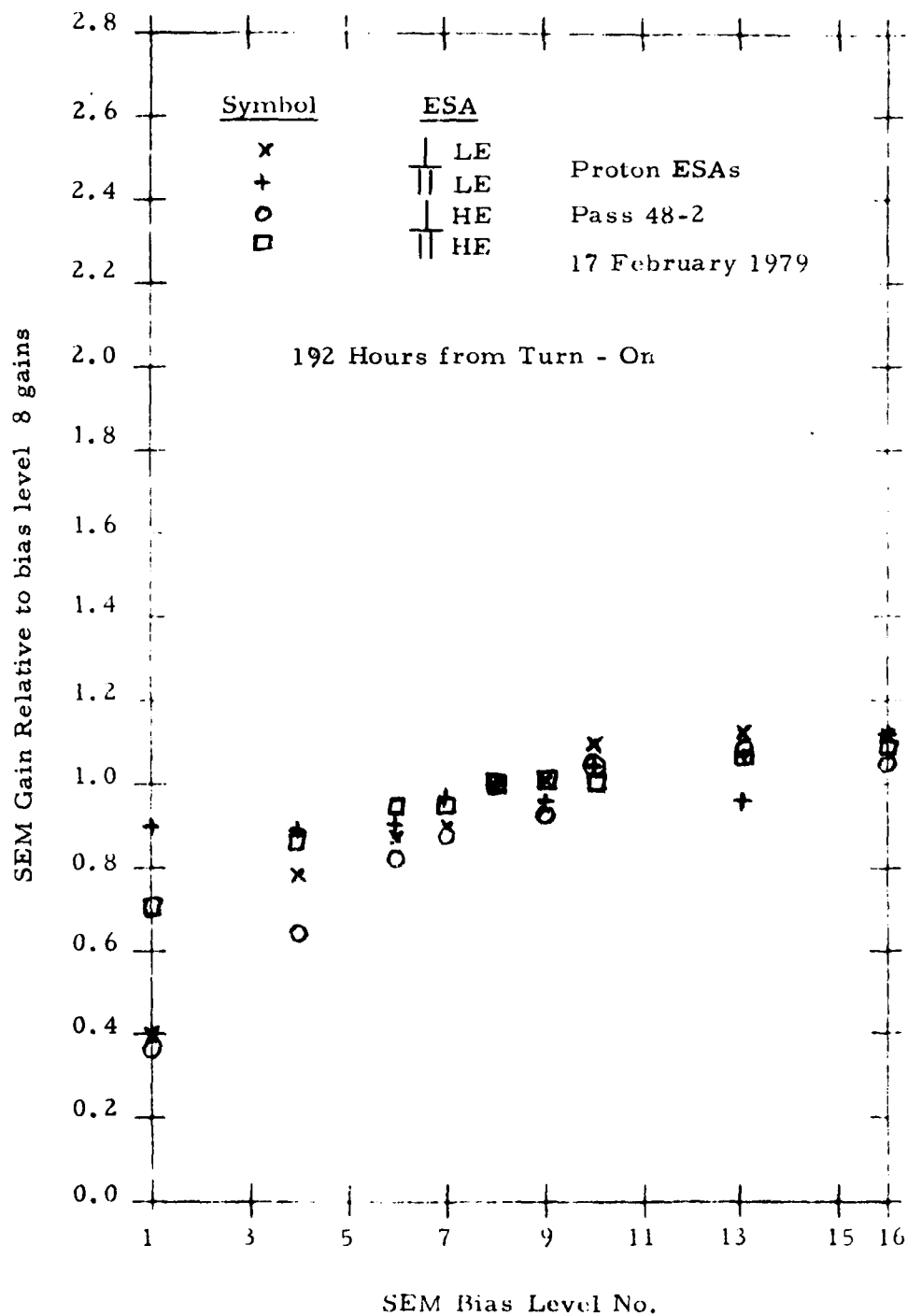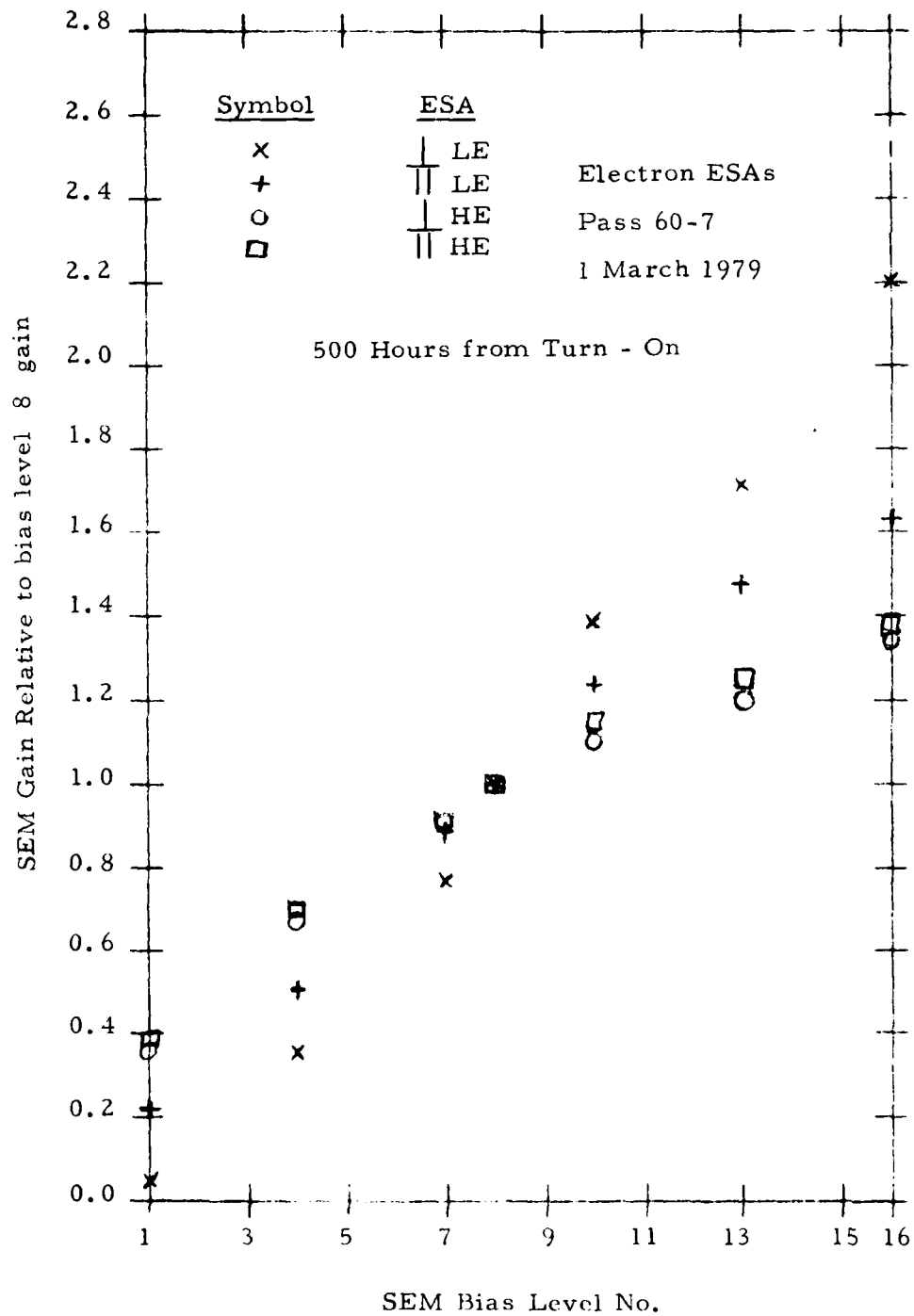Figure 6.8 Proton ESA SEM Gains, 192 Hours from
Turn - On

85

Figure 6:9 Electron ESA SEM Gains, 500 Hours from
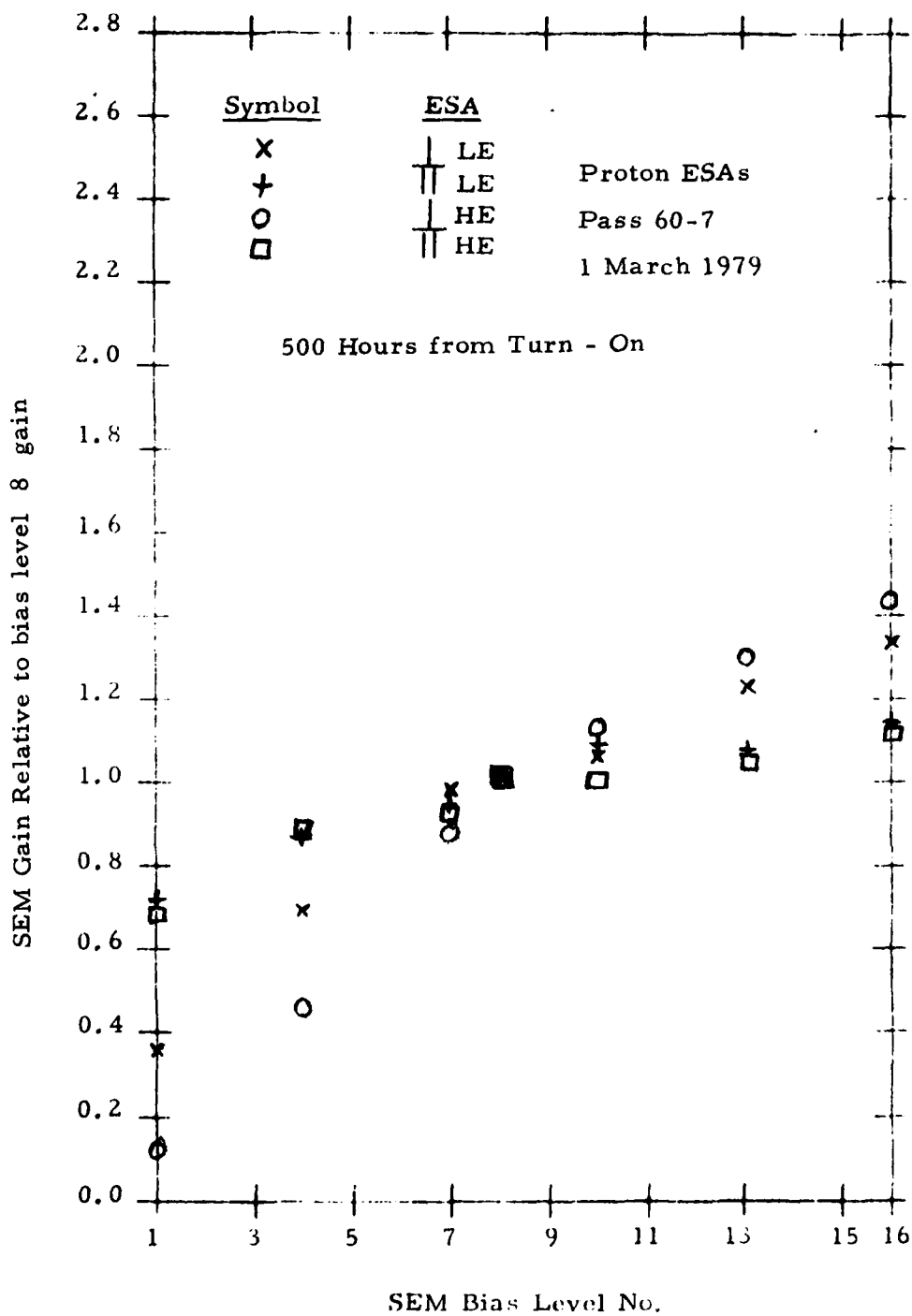Turn - On

86

Figure 6.10 Proton ESA SEM Gains, 500 Hours from
Turn - On

With the auto-off B enabled, the SEM gains still decayed with a several day time constant. Since the approximately 1 week off period had resulted in substantial recovery of SEM gain, it was decided to turn the ESA s on only about half of the time, which was to coincide with the eclipse time during eclipse season. This mode of operation was started on 19 March.

The start of electron/ion gun operations at the end of March resulted in the ESA s being turned on full time beginning on 30 March. Up to 30 March the SEM gain had been stable, but full-time operation resulted in more gain degradation. Thus, half-time operation was resumed at the end of 1 April. This mode of operation has been used since then and has resulted in substantially slower degradation of SEM gain. As of the beginning of September 1979, the two LE electron ESAs had the SEM gain at B. L. 8 degraded to somewhat less than 25%, while all other SEMs were better than 50%. Bias level calibrations have been run more than twice per week; therefore, substantial data exist to track the SEM gain variation with time.

At the beginning of September 1979 the RSPD is operating properly and should operate reliably with sufficient SEM gain for the entire September - October eclipse season. It is necessary to operate the ESAs on only half-time to prevent too rapid a gain degradation. On the basis of several months of operation, the SSSs should operate reliably for many years - to the point where radiation damage to satellite and RSPD electronics causes failure. The ESAs are partially degraded in SEM gain but should give reasonably useful operation for possibly another year. The exception may be the LE electron ESAs, which may be only marginally useful some months after the fall eclipse season.

The RSPD operation has resulted in much good data. Preliminary reduction has yielded good spectra. The flux levels have been observed to vary widely, particularly in the LE electron ESAs. Very intense LE electron fluxes have been observed quite frequently, especially in association with electron/ion gun operations; and this is probably the cause of the more rapid degradation of the LE electron ESA SEMs. Much detailed pitch angle data have been obtained, and a large amount of data have been obtained with the electron/ion gun operations.

The SEMs are expected to degrade slowly as their accumulated charge output approaches 1 coulomb. The RSPD SEMs have been operating in frequent high-flux environments, and this is the major cause of gain decrease. Some of the electron/ion gun operations also resulted in extremely high count rates in the SEMs and contributed to the gain decrease. It is recommended that during RSPD data analysis a summary be made of the total count output of each SEM, as the resulting gain vs. total count data would be very useful in evaluating overall SEM performance. Much of the observed degradation is most likely due to large accumulated count (hence, charge) output of the SEMs.

It should be emphasized that the bias level calibrations, being performed at least twice per week, provide sufficient data to allow compete spectral analysis of the ESA data even when the SEMs are operating at reduced gain. With such calibrations, even the most degraded SEMs (LE electron ESAs) are likely to yield good data for at least one year, and quite possibly more.

Some recent information on SEM gain stability (unpublished thus far) suggests that gain degradation results from the breakdown of hydrocarbons deposited on the SEM surface. The flight unit RSPD SEMs were the same as those used for the ESA calibration and thus had undergone considerable testing before flight. It is recommended that on future flights the SEMs be replaced with new, thoroughly cleaned (vacuum bake-out) SEMs as close to the launch date as possible. This is likely to significantly extend the useful life of the RSPD (or other space instrument) SEMs. Some reports suggest that sealing the SEMs (this actually requires that the entire detector housing be sealed) in dry nitrogen up to shortly before launch (1 day or less) (venting the unit in space would be better) results in extremely long SEM lifetime, possibly measured in decades.

The SSSs are expected to operate reliably for many years, so that spectral analysis above 60 keV should always be available. The 0.05 to 60 keV data from the ESAs should be completely usable for more than one year and partially usable for a number of years. Since the SCATHA satellite had an original design lifetime of 12 months, the RSPD was designed with ESA apertures which would give a reasonable expectation of reliable SEM gain for one year. It is presently expected that SCATHA operation will be extended to two years. The RSPD will give reliable data in all data channels for the one year of design, but there may be data loss in some channels (LE electron ESA) toward the end of the second, added, year. Overall, the RSPD is operating reliably on the SCATHA satellite and is fulfilling all design requirements.

7. SUMMARY AND CONCLUSIONS

The preceding sections have presented the design of an instrument which measures electrons and protons using electrostatic deflection and dE/dx measurements in silicon surface barrier detectors. This instrument's interface requirements, test and calibration, and actual operation have also been discussed.

Two identical instruments were fabricated. The first was successfully launched into near synchronous orbit on board the SCATHA satellite and is functioning normally. The second instrument is now in storage and could be flown on another satellite. Certain modifications would, of course, be necessary. These would depend upon the particular satellite on which it is flown but would involve, principally, changes in the instrument/satellite interface circuitry and replacement of the Spiraltron detectors.

The RSPD is an extremely versatile instrument. It measures electrons from 50 eV to 1 MeV and protons from 50 eV to 7 MeV. The command system allows essentially independent operation of the ESA and SSS portions of the instrument, thereby greatly increasing both the system's versatility and reliability. Its broadband data capability yields excellent time resolution. A summary of the RSPD's characteristics is given in Table 7.1.

Table 7.1
Summary of RSPD Characteristics

	Electrostatic Analyzers	Solid State Spectrometers
Particles Detected	Electrons and Protons	Electrons and Protons
Method of Energy Analysis	Electrostatic Deflection	Pulse Height Analysis of dE/dx Measurement
Detectors	Spiraltron Electron Multiplier	Silicon Surface Barrier $50mm^2$, 300μ e SSS Front $100mm^2$, 300μ e SSS Rear $25mm^2$, 5μ p SSS Front $100mm^2$, 300μ p SSS Rear
Energy Range (keV)		
- electrons	0.05-60	30-1000
- protons	0.05-60	70-7000
Energy Bins (keV)		
- electrons	0.05-0.12	30-45
	0.12-0.30	45-70
	0.30-0.70	70-120
	0.70-1.70	120-550
	1.70-4.20	170-265
	4.20-10.2	>950
	10.2-25	980-1100
	25-60	70-950
		$\perp / \parallel$
- protons	0.05-0.12	101-150
	0.12-0.30	150-225
	0.30-0.70	225-325
	0.70-1.70	325-450
	1.70-4.20	450-479/450-547
	4.20-10.2	-/547-598
	10.2-25	491-733/598-959
	25-60	733-1460/959-1870
		1460-3290/1870-4250
		3290-6750/4250-8610
Geometric Factor (cm^2-sr)		
- electrons	(low energy) 2.8×10^{-4} (high energy) 7.0×10^{-5}	3.55×10^{-3}
- protons	(low energy) 7.0×10^{-4} (high energy) 7.0×10^{-4}	6.68×10^{-3}
Counting Accuracy	Statistical	Statistical

91

Table 7.1 (cont'd)

	Electrostatic Analyzers	Solid State Spectrometers
In-Flight Calibration Means		
- electron	Test pulse generator and Sn^{119m}	Am-241
- proton	Test pulse generator	Am-241

Size	6"x10"x10"
Weight	13 lbs
Power Requirements	28±4 V DC, 5 W
Analog Monitor Output	
- Number	17
- Signal Level	0-5 volts
- Source Impedance	5 kΩ
- Sample Rate	any convenient rate
Digital Output Data	
- Number	1
- Format	200 bits serial
- Signal Level	TTL or CMOS compatible
- Source Impedance	TTL or CMOS compatible
- Sample Rate	5 times per second
Analog (BB) Output Data	
- Number	1
- Signal Level	0 to 5 volts
- Source Impedance	100Ω
- Format	Digital count ratemeter 250 μsec resolving time, internally subcommutated
Power Control Commands	

- Number	3 - Low Voltage ON/OFF
	   - ESA ON/OFF
	   - SSS ON/OFF

- Signal Level	ON - 28±4 Volts OFF - 1 ± 1 Volt
Magnitude Command	
- Number	1
- Format	22 bits serial
- Signal Level	TTL or CMOS compatible
- Input Impedance	TTL or CMOS compatible
- Composition	4 bits - ESA energy channel/sweep rate 4 bits - SSS energy channel/sweep rate 4 bits - SEM bias level 6 bits - BB data assignment 1 bit - BB data subcomm dwell time 2 bits - ESA auto shutoff 1 bit - reset

REFERENCES

1.1   De Forest, S. E. , "Spacecraft Charging at Synchronous Orbit",
       J. Geo Resh. 77, 651-659 (1972).

1.2   De Forest, S. E. and C. E. McIlwain, "Plasma Clouds in the Magneto-
       sphere," J. Geo. Resh. 76, 3587-3511 (1971).

1.3   Stevens, John R. and A. L. Vompola, "Description of the Space Test
       Program P78-2 Spacecraft and Payloads," SAMSO-TR-78-24, 31 October
       1978.

1.4   Pavel, Arthur L. , "SCATHA Satellite Instrumentation Report," AFGL-
       TR-76-0207, 10 September 1976.

1.5   Whalen, B. A. and I. B. McDarmid, "Temporal Behavior of Energetic
       Particle Precipitation during an Auroral Substorm," J. Geo. Resch.
       75, 123-132 (1970).

1.6   Paschmann, G. , R. G. Johnson, R. D. Sharp and E. G. Shelley,
       "Angular Distributions of Auroral Electrons in the Energy Range 0.8
       to 16 keV," J. Geo. Resch. 77, 6111-6120 (1972).

1.7   Frank, L. A. , "Initial Observations of Low Energy Electrons in the
       Earth's Magnetosphere with OGO 3," J. Geo. Resch. 72 185-195 (1967).

1.8   Hunerwadel, J. L. , P. R. Morel, F. A. Hanser, and B. Sellers,
       "Design of Instrumentation Suitable for the Investigation of Charge
       Buildup Phenomena at Synchronous Orbit," report AFCRL-TR-75-
       0365, July 1975. Scientific Report No. 1 for Contract No. F19628-
       74-C-0217. ADA015063.

1.9   Hunerwadel, J. L. , P. R. Morel, F. A. Hanser, and B. Sellers,
       "Design of Instrumentation Suitable for the Investigation of Charge
       Buildup Phenomena at Synchronous Orbit," report AFGL-TR-76-
       0263, July 1976. Scientific Report No. 2 for Contract No. F19628-
       74-C-0217.

1.10   Sellers, B. , F. A. Hanser, P. R. Morel, J. L. Hunerwadel, A. L. Pavel,
       L. Katz and P. L. Rothwell, "A High-Time Resolution Spectrometer
       for 0.05 to 500 keV Electrons and Protons" in Spacecraft Charging by
       Magnetospheric Plasmas, A. Rosen, Editor: Progress in Astronautics
       and Aeronautics, 47, AIAA, NY (1976).

1.11   Hanser, F. A. , D. A. Hardy, and B. Sellers, "Calibration of the Rapid
       Scan Particle Detector Mounted in the SCATHA Satellite," report AFGL-
       TR-79-0167, June 1979. Final Report for Contract No. F19628-77-C-
       0137.

REFERENCES (cont'd)

2.1   Archuleta, R. J. and S. E. De Forest, "Efficiency of Channel Electron Multipliers for Electrons of 1-50 keV," Rev. Sci. Instr. 42, 89-91 (1971).

2.2   Arnoldy, R. L. , R. O. Isaacson, D. F. Gats and L. W. Choy, "The Calibration of Electrostatic Analyzers and Channel Electron Multipliers Using Laboratory Simulated Omnidirectional Electron Beams," Rev. Sci. Instr. 44, 172-177 (1973).

2.3   Bordini, F. "Channel Electron Multiplier Efficiency for 10-1000 eV Electrons," Nucl. Instr. Meth. 97, 405-408 (1971).

2.4   Iglesias, G. E. and J. O. McGarity, "Channel Electron Multiplier Efficiency for Protons of 0. 2-10 keV," Rev. Sci. Instr. 42, 1728-1729 (1971).

2.5   Rothwell, P. R. , personal communication.

4.1   Martin Marietta Aerospace, "Rapid Scan Particle Detectors, SC5 Payload/Space Vehicle Interface Control Document Flight P78-2," CDRL Item A049 for Contract No. F04701-76-C-0116.

5.1   Martin Marietta Aerospace, "Electromagnetic Compatibility Test Plan, Space Test Program P78-2," CDRL Item A027 for Contract No. F04701--76-C-0116.

5.2   Sanders Associates, Inc. "Report of Electromagnetic Interference Test on Panametrics, Inc. SC5 Particle Detector," Report No. 2738.

5.3   Martin Marietta Aerospace, "Systems Test Plan, Space Test Program, Flight P78-2," CDRL Item A054 for Contract No. F04701-76-C-0116.